2038-5625

Italian Journal of Agrometeorology

Rivista Italiana di Agrometeorologia

n. 2 – 2023

Cover photo by Maurizio Borin

Italian Journal of Agrometeorology

n. 2 - 2023

Firenze University Press

The ***Italian Journal of Agrometeorology*** (***IJAm - Rivista Italiana di Agrometeorologia***) is the official periodical of the Italian Association of Agrometeorology (AIAM) and aims to publish original scientific contributions in English on agrometerology, as a science that studies the interactions of hydrological and meteorological factors with the agricultural and forest ecosystems, and with agriculture in its broadest sense (including livestock and fisheries).

SUBSCRIPTION INFORMATION
IJAm articles are freely available online, but print editions are available to paying subscribers. Subscription rates are in Eur and are applicable worldwide.
Annual Subscription: € 50,00 Single Issue: € 25,00

CONTACT INFORMATION
Please contact ordini@fupress.com, if you have any questions about your subscription or if you would like to place an order for the print edition. Information on payment methods will be provided after your initial correspondence.

Published by
Firenze University Press – University of Florence, Italy
Via Cittadella, 7 - 50144 Florence - Italy
http://www.fupress.com/ijam

Agrometeorology for sustainable water management in agroecosystems

This thematic issue wants to address the pressing need for improved irrigation management, enhanced crop water use efficiency, and better forecasting of the impact of climate change on precipitation and, consequently, on water availability for crops.
Through diverse contributions, we strive to provide the readers with essential tools and insights to adapt agricultural practices to emerging environmental challenges.

Guest editors:
Altobelli Filiberto, CREA Research Centre for Agricultural Policies and Bioeconomy, Rome
Dalla Marta Anna, Department of Agriculture, Food, Environment and Forestry -University of Firenze
Maucieri Carmelo, Department of Agronomy, Food, Natural resources, Animals and Environment-University of Padova

Acknowledgments

This thematic issue has been supported by the Agritech National Research Center and received funding from the European Union Next-GenerationEU (PIANO NAZIONALE DI RIPRESA E RESILIENZA (PNRR) – MISSIONE 4 COMPONENTE 2, INVESTIMENTO 1.4 – D.D. 1032 17/06/2022, CN00000022). This manuscript only reflects the authors' views and opinions, neither the European Union nor the European Commission can be considered responsible for them. Spoke 4, Work Package 4.2, Task 4.2.1 "Farm network setup (Living Labs): a network of farms representative of the different agricultural systems to apply innovative technologies for the sustainable management of crops, animals and forests" and Work Package 4.3, Task 4.3.3 "Risk management strategies and policies in the context of climate change".

Finanziato dall'Unione europea NextGenerationEU | Ministero dell'Università e della Ricerca | Italiadomani PIANO NAZIONALE DI RIPRESA E RESILIENZA | agritech National Research Center for Technology in Agriculture

Italian Journal of Agrometeorology
Rivista Italiana di Agrometeorologia

Firenze University Press
www.fupress.com/ijam

OPEN ACCESS

Citation: Borin, M. (2023). A wise irrigation to contribute to integrated water resource management. *Italian Journal of Agrometeorology* (2): 5-19. doi: 10.36253/ijam-2323

Received: September 25, 2023

Accepted: October 25, 2023

Published: January 20, 2024

Data Availability Statement: All relevant data are within the paper and its Supporting Information files.

Competing Interests: The Author(s) declare(s) no conflict of interest.

ORCID:

MB: 0000-0002-4074-2098

A wise irrigation to contribute to integrated water resource management

Maurizio Borin

Department of Agronomy, Food, Natural Resources, Animals and Environment – DAFNAE, University of Padua, Agripolis Campus, Viale dell'Università 16, Legnaro, PD, Italy
E-mail: maurizio.borin@unipd.it

Abstract. Irrigated agriculture accounts for about 20% of cultivated lands worldwide while currently generating an estimated 40% of crop production, and two-thirds of future gains in crop production are expected to come from irrigated lands. Therefore, irrigation is strategic to ensure food for the world's increasing population and slow down the pace of deforestation. Irrigated agriculture also accounts for more than 70% of global water withdrawals, and the way agriculture uses freshwater is crucial for ensuring availability for other activities and preserving water-related ecosystems. To give an agri-environmental interpretation of the water fluxes involved in irrigation, the total amount of water withdrawn from a source is called **white water** (W) and subdivided as follows: **gold water (G)** is the amount that is actually used by the crops. This fraction represents the ultimate goal of irrigation, which is to increase crop productivity and food availability. We can also consider this amount as the *irrigation water for crops*. The gold color means an income for the farm; **emerald water (E)** is the amount of water withdrawn for irrigation that does not reach the crops but provides ecosystem services, i.e., the benefits that people get from ecosystems. This amount of water is useful for the community and can be identified as *irrigation of the territory*; **red water (R)** is losses, i.e., the fraction of water that has to be reduced as much as possible if not eliminated. It is an economic, social and environmental cost; the red color is associated with the red traffic light that means STOP! The quantification of W has to be preceded by a careful evaluation of the benefits achievable with irrigation in relation to the environmental characteristics of the cultivation area. Strategic issues at this stage are the choice between full or deficit irrigation and the individuation of opportunities to exploration of opportunities to increase the availability of water resources by using non-conventional sources. The quantification of G and E fluxes is necessary to reduce losses, while strategies/techniques useful to reduce irrigation needs at the field level are key factors to allocate irrigation water within the framework of an integrated and sustainable management of water aimed at turning user conflicts into synergies. This implies multiple subjects and actors in a multi-disciplinary approach.

Keywords: irrigation efficiency, components of water fluxes, ecosystem services of irrigation.

"…let us not wait until the well is dry to understand the worth of water (Benjamin Franklin)"

1. IRRIGATION, A NECESSITY UNDER THREAT

Irrigated agriculture accounts for about 20% of cultivated lands worldwide, while generating an estimated 40% of crop production (FAO, 2015a, b; Turral et al., 2010). Yields are markedly higher and more stable with irrigation, also because farmers apply larger amounts of fertilizers and chemicals when they can fully meet the crop water requirements (Monjardino et al., 2013). Published estimates of the 2050 food demand vary hugely, but most of them agree with FAO projecting a 50-60% increase of the total global food demand between 2019 and 2050 (Falcon et al., 2022). Half or even two-thirds of future gains in crop production are expected to come from irrigated land (Kadiresan and Khanal, 2018), requiring a 10% increase of global water withdrawals (FAO, 2011; FAO, 2017) and calling for investments and interventions.

The role of irrigation is crucial with a view to a sustainable intensification of agriculture, but the need to "produce more with less" is underscored by the fact that the growing population has resulted in the freshwater resources available *per* person having declined by more than 20% in the last two decades. As the demand rises, freshwater becomes increasingly scarce, competition for it intensifies, and excessive water withdrawals threaten water-related ecosystems and the ecosystem services they provide (FAO, 2020). Globally, the world's freshwaters are distributed unevenly across space and time and subjected to contrasting driving forces between maintenance in the water bodies and withdrawals. On the one hand, living organisms, transportation, energy production and the many human activities associated with recreation (e.g., fishing, rowing, landscaping) require that water be maintained in lakes, basins, rivers, canals; on the other hand, agriculture, industry and households imply withdrawal and water body exploitation. This implies the issue of the equitability in water use, that is, the fair distribution of production factors among human beneficiaries based on their needs. Furthermore, the use of water for industry and domestic purposes most often does not imply any change of its physical status: water remains in its liquid phase. Water can be subjected to pollution. However, it can be re-used or returned to the water bodies very close to the withdrawal sites across space and time after appropriate treatment. Water used for irrigation is expected to be taken up and transpired by crops and dispersed into the atmosphere in the form of vapor; in this case, it enters the wider water cycle and is not reusable in the short term. Irrigated agriculture uses approximately 70% of the total amount of the freshwater withdrawn to supply the world's current food needs (Ingrao et al., 2023). The requirements are higher where water availability is low, as in dry areas and dry seasons. Industries and households are increasingly demanding water at the expense of agriculture, which is under pressure to release water to help meet these new needs. If agricultural production is to be sustainable, water resources must be used more efficiently while maintaining the goal of increasing productivity.

This scenario is complicated by the effects of climate change, which are already seriously disrupting rainfall patterns. Water scarcity is expected to increase with the modification of the distribution of rainfall patterns throughout the year, and so are water-related disasters. Increased drought frequency and subsequent water shortages in rainfed farmlands represent significant risks to livelihoods and food security, particularly of the most vulnerable populations in the least developed parts of the world (Kadiresan and Khanal, 2018). The amounts of water required to meet the future demand for food in a changing climate are estimated to be 40 to 100% higher than the needs in the absence of climate change (Turral et al., 2011).

At the world scale, the average irrigation efficiency is estimated to range between 40 and 50% (García-Tejero et al., 2011), and 41% of withdrawals are not compatible with sustaining ecosystem services (FAO, 2020). In Italy, total freshwater consumption ranges between 40 and 45 billion m^3 *per* year (ISTAT, 2019) (60% for agriculture, 25% for industry, and the remaining 15% for civil and domestic activities). It follows that the agricultural sector manages 24-27 billion m^3, the vast majority of which in irrigation systems. According to the 6th Census of Agriculture, irrigation is practiced by almost 40,000 Italian farms covering a total surface of about 2.5 million hectares (a little less than 20% of the national cultivated surface) and distributing 11.1 billion m^3 of water to their crops (Bellini, 2014). Northern Italy is the most hydro-driven agricultural system with the highest rate of irrigation investment on the land and the highest percentage of irrigated areas. Taking the distribution of the different irrigation methods into account (Figure 1) and their average values of field application efficiency (Brouwer et al., 1989), the overall application efficiency is estimated to be 50% at the farm level.

Irrigation systems need to be redesigned to reduce losses, alleviate the competitive pressure and tend toward an integrated water resource management.

2. PROPER USE OF WATER AND IRRIGATION EFFICIENCY

The first step to achieve a proper use of water is related to the evaluation of the benefits achievable with

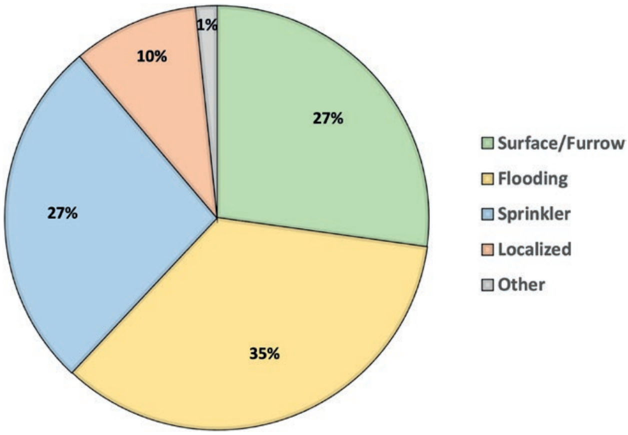

Figure 1. Distribution of the main categories of irrigation methods in Italy within the total irrigation volume (designed from ISTAT, 2014).

irrigation in relation to the environmental characteristics of the cultivation area. This implies that the transformation of a district from rainfed to irrigated has to be preceded by a suitability analysis of the land for irrigation to avoid the implementation of irrigation in unsuitable conditions. The assessment of land suitability for agriculture is a complex, multidisciplinary and multicriteria process which entails land topography, climate, water resources available for irrigation, soil capabilities and current management practices including land use and land cover (Seyedmohammadi et al., 2016; Aldababseh et al., 2018). The scientific literature is very rich of case studies regarding land suitability assessment for irrigation purposes, but their thorough analysis is out of the scope of this paper.

The traditional definition of irrigation efficiency given by Israelsen (1950) is "*the ratio of the irrigation water consumed by the crops of an irrigation farm or scheme to the water diverted from a river or other natural water source into the farm or scheme canal or canals*". It has evolved over time, and many different and sometimes conflicting definitions have been published (US Interagency Task Force, 1979). Despite variations and enhancements, the basic concept of irrigation efficiency implies that high efficiency reflects low losses; in other words, a high proportion of the water available at the head of a scheme is used to augment crop transpiration, and this is an appropriate engineering objective. Nevertheless, a more recent reflection on efficient irrigation (Perry, 2007) divides the water diverted to irrigation schemes into the following components:

The consumed fraction (essentially evapotranspiration (ET)) includes:

- beneficial consumption (for the intended purpose or another beneficial use such as environmental purposes);
- non-beneficial consumption such as weeds or consumption resulting from capillary rise during a fallow period.

The non-consumed fraction includes:

- recoverable flows (water flowing to drains and back into the river system for possible diversion downstream, and percolation to freshwater aquifers);
- non-recoverable flows (percolations to saline aquifers, outflow to drains that have no downstream diversions or direct outflow to the ocean).

This approach is relevant from a hydrological point of view because it fits in with the principle of continuity of mass. According to this interpretation, losses (the complement of efficiency) are composed of non-beneficial ET and the non-recoverable component of the non-consumed fraction. Nevertheless, once again the quantification of losses – and in turn irrigation efficiency – has to be calibrated according to the objectives. Strictly speaking, let us imagine a community of farmers and/or a related water authority obtaining authorization to withdraw water from a source (e.g., a lake, a river) and/or to build a dike to create a reservoir. They have to invest money, energy, professional skills, and gain best advantage from their investment. Consequently, they are interested in using water to increase crop productivity and the resulting farm income, so that they are only interested in the beneficial component of water consumption. They might be not interested in generating a recoverable flow, which is a more general type of "environmental demand" whose beneficiaries are the collectivity rather than the farmers. Then, the following questions arise: why do farmers and their water authority have to pay for this service? Who should pay?

3. AN AGRO-ENVIRONMENTAL VISION OF IRRIGATION WATER COMPONENTS

Following the concept of objectives and benefits associated with irrigation, the following theoretical approach can be proposed, figuring the world of irrigation in four components associated to colors (Figure 2):

- **White water (W)** is the total amount of water withdrawn from a source. The color suggests a white sheet, where a project is going to be written;
- **Gold water (G)** is the amount that is actually used by the crops. This fraction represents the ultimate goal of irrigation, enhanced productivity and food availability. We can also consider this amount as

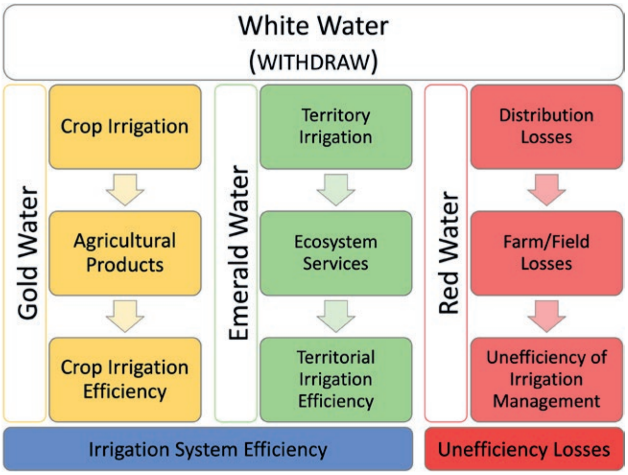

Figure 2. Classification of irrigation water according to the beneficiary.

the irrigation water for crops. The gold color means income for the farm;

- **Emerald water (E)** is the amount of water withdrawn for irrigation that does not reach the crops but provides ecosystem services. These are the benefits that people get from ecosystems (Millennium Ecosystem Assessment, 2005). They include provisioning services such as food and water; regulating services such as flood and disease control; cultural services such as spiritual, recreational, and cultural benefits; and supporting services such as nutrient cycling, that maintain the conditions for life on Earth. This amount of water is useful for the community and can be identified as irrigation of the territory. The emerald color suggests something precious, the gemstone symbol of hope, future, growth and renewal. Emerald is characterized by facets that represent the variability of ecosystem services attributable to the presence of water in irrigated territories;
- **Red water (R)** is losses, i.e., the fraction of water that has to be reduced as much as possible, if not eliminated. It is an economic, social and environmental cost. The red color is associated with the red traffic light that says STOP!

$$W = G + E + R.$$

According to the rationale inspiring the concept of irrigation efficiency:

- Gold Water Efficiency (GWE) = crop irrigation efficiency = G/W
- Emerald Water Efficiency (EWE) = E/W
- Irrigation System Efficiency (ISE) = (G+E)/W
- Inefficiency = R/W

The idea of associating water fluxes to colors calls to mind the methodology of evaluation of the water footprint (Hoekstra et al., 2011), but in this case it is only focused on the water used in the irrigation sector.

3.1. White water

Quantifying the correct amounts of the crop water needs is the first step when it comes to planning and managing the water resource under the pressure of contrasting interests, risks and uncertainties. Theoretically, the amount of white water can be easily identified and quantified from the field scale to the basin scale. FAO papers nos. 24 (Doorenbos and Pruitt, 1977), 33 (Doorenbos and Kassam, 1979), 56 (Allen et al., 1988), and 66 (Steduto et al., 2012) well describe the basics and the methodologies for determining the crop water requirements.

At the planning stage, the choice between full or deficit irrigation is a strategic issue, especially where water availability is particularly subjected to competition and limitations of use. The main objective of deficit irrigation is to increase the water use efficiency (WUE) of a crop by eliminating irrigation systems that have little impact on yield (FAO, 2002). The resulting yield reduction may be small compared with the benefits gained through diverting the saved water to irrigate other crops for which water would normally be insufficient under traditional irrigation practices. In other words, deficit irrigation serves a wider territory with the same amount of withdrawn water. This also implies socio-economic consequences such as a greater number of farms receiving water, higher skills to correctly manage water stress, adequate extension services for farmers, and/or available user-friendly systems or sensors for soil water measurements, together with flexible water prices (Rodrigues and Pereira, 2009). When looking for irrigation water sources, both quantity and quality have to be considered, and are related to each other. Relatively to the amount of water to be exploited, opportunities have to be explored and pursued to increase their availability. In this sense, the Italian territory needs deep rethinking of land reclamation, which is the result of a stratification of interventions and works performed over the centuries under changing objectives, priorities, technologies, policies, socio-economic and environmental conditions (Novello and McCann, 2017). The rationale of these interventions aims to quickly divert excess rainwater from the territory to guarantee its hydraulic safety. As a result, only 5% of rainfall is retained and used for irrigation in Italy at present (Coldiretti, 2021). The territory is also extremely fragile and vulnerable to severe climatic events. Therefore, it is urgent to plan and implement solutions combining the safety of the territory with the need to increase the number of water reservoirs. In this sense, the principles of the Varenne Agricole (Ministère de l'Agriculture et de la Souveraineté Alimentaire, 2022) can be an inspiring reference: store water during periods of high availability and make them available to crops during dry periods, and manage the water resources as close to the territory as possible.

The use for irrigation of marginal water resources such as drainage water, treated wastewater, of industrial and domestic origin, or desalinized water (Martínez-Alvarez et al., 2016) is an interesting option to widen the scope of water availability for irrigation and mitigate the demand for high-quality water. However, using these waters for irrigation may bring along various problems like toxicity to crops, damage to the soil quality, spreading of parasites, problems in irrigation systems and potential hazards to the environment and/or humans (Alcade Sanz and Gawlik, 2014). Theoretically, being able to use low-quality water for irrigation does not solely depend on its intrinsic characteristics, but also on its conditions of use (crop type, soil and climate conditions, or irrigation method) (Figure 3; Bortolini et al., 2018). Taking into consideration the water quality indicators, they can be categorized into three main groups, according to their effects on irrigation:

- Agronomic quality indicators: parameters causing toxicity effects on crops and/or degradation on soil fertility in the medium-long period. The most significative are: pH, giving general indications about the quality of the water resource; Electrical conductivity (EC), which is one of the major concerns with water used for irrigation; Sodium adsorption rate (SAR), expressing the toxicity effect on crops and degradation effects on soil fertility.
- Hygiene and health quality (Sanitary risk) indicators: parameters with no effect on crops yield but exerting dangerous effects on human health due to pathogens transmission, particularly when low quality water is used to irrigate fresh vegetables; some key indicators are: fecal indicator bacteria (*E. coli*), giving general indications about the quality of the water resource; Intestinal nematodos (Helminthes), very dangerous for human health.
- Management quality indicators: parameters as Total Suspended Solids (TSS), Bicarbonates (HCO_3), Sulphides, Mn, and Fe. They do not damage crops and

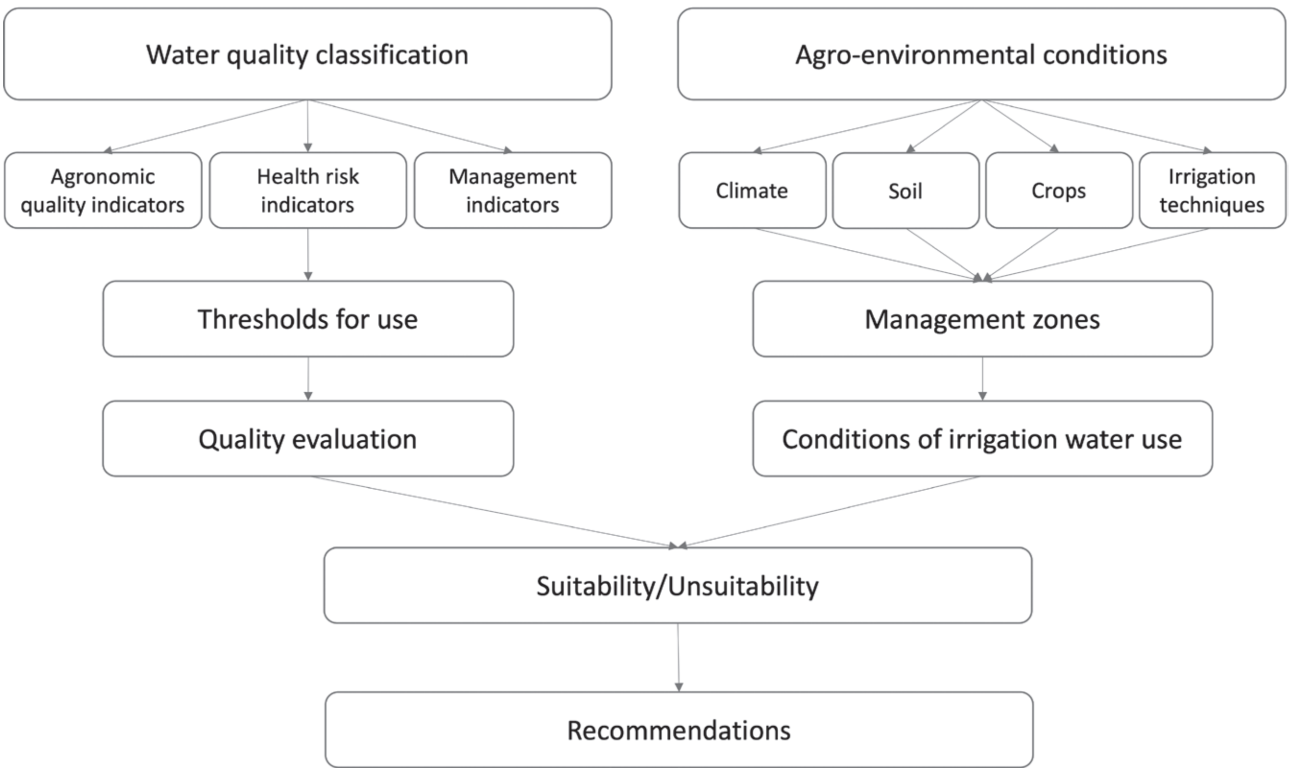

Figure 3. Scheme for a rational use of treated wastewater for crop irrigation.

soil, but cause negative effects in irrigation systems (especially clogging) resulting in a low distribution uniformity.

The use of low-quality water for irrigation deserves caution, attention and multi-criteria decision analysis (Paul et al., 2020), but can play a significant role in sustaining irrigation projects: at present almost 6 billion m^3 of treated wastewater are produced in Italy *per* year (more than half of the total irrigation volume applied to the crops), but their re-use in irrigation is infinitesimal (only 0.4% of the irrigated surface is supplied with these waters). When planning the valorization of marginal waters, matching production (which is continuous throughout the year) and water use (which is seasonal) has to be taken into account, and reservoirs have to be identified or created. Treated wastewater can be used in aquifer recharge schemes (Zheng et al., 2021) or temporarily stored in surface basins as multi-functional wetlands, which improve its quality (Smith, 2009).

3.2. Gold water

A wide availability of strategies and techniques can support the goal of reducing losses in the delivery and field distribution system, thus increasing the irrigation efficiency. The opportunities are offered by smart agriculture (Cesco et al., 2023) and advanced technologies, that are commonly known under the umbrella expression "smart irrigation" (Masseroni et al., 2020). These systems aim to adopt single or combined automation as well as information and communication technologies at the district and farm scales, besides customized and integrated model approaches at larger scales.

Without detailing this very large topic, some examples of technological innovation in the irrigation field are: i) mathematical models for the control of the main hydrological and agronomic variables; ii) the use of GIS environment for digital mapping of the territories and their geophysical and hydrological characteristics; iii) technologies for measuring quantifiable variables (flow rate, current speed levels) and water quality; iv) data transmission techniques; v) the observation of agricultural surfaces from remote sensors; and vi) the use of "smart" actuators that automate irrigation, known as the internet of things (IoT), which allow applying site-specific irrigation. Modernization or re-engineering of irrigation mostly include piped delivery systems, laser leveling of fields, conversion to pressurized systems for sprinklers, drips, or sub-surface drips.

Field irrigation systems with advanced technologies combined with good practices can increase efficiency and reduce water losses (Levidow et al., 2014; Tromboni et al., 2014). Precision agriculture methods are strategic for irrigation scheduling because they offer the potential to increase water use and economic efficiencies by optimally matching irrigation inputs to yields (Gobbo et al., 2019). In this context, unnecessary surface water runoff and water loss through evaporation is reduced. To this end, weather stations and IoT sensor networks provide information related to the soil moisture content, lower-soil moisture and evapotranspiration, while thermal aerial imagery data provide information on water availability.

Crop imagery remotely captured by cameras on board of satellites and other aerial platforms has opened the irrigation sector to the big data era. It provides timely updated spatial information on the crop status, and the opportunity to calculate vegetation indices such as NDVI, VHI, and others. Consequently, new and continuously updated tools are available to properly address irrigation scheduling and validate the results. The collected data are interpreted and analyzed at an appropriate scale and frequency, and this enables the delivery of innovative water management services in order to set the scene for the connection between water consumption and yield estimation during the growing season. The new technologies aim to: i) improve water supply efficiency at the farm level, as well as resilience to climate change; ii) plan irrigation based on the combination of physical and physiological parameters; iii) manage the effects of reducing irrigation regimes on crop yields; iv) test biostimulants – known and new ones – on crop use performance; v) manage irrigation with respect to the water salinization levels; and vi) optimize irrigation performance in terms of surface water ecological flow or groundwater levels. Thanks to these new technologies, the relationship between water stress levels and product quality parameters will be better controlled, and support for certification schemes for water savings based on new environmental labeling will be available.

GWE should be easily calculated because its two components can be measured.

3.3. Emerald water

The evaluation of the ecosystem services associated with the presence of water in irrigated territories is quite a recent topic, but the international literature has produced interesting contributions aiming to discriminate and describe positive and negative impacts (Avellán et al., 2018), highlight the need for stakeholders' involvement and payment systems (PES) (Jourdain and Vivithkeyoonvong, 2017; Ricart et al., 2019; Pérez-Blanco et al., 2022), and examine the advantages and disadvantages of saving water for irrigation to increase the environmental flow (e.g., Crossman et al., 2010; Estes et al., 2022).

Irrigation systems admittedly provide positive ecosystem services in all four categories: i) they contribute to provisioning, which includes food production (crops, fish and livestock), fodder, fuelwood, and pharmaceutical plant resources; ii) they support nature since irrigation systems host wildlife (birds, fish, biodiversity); iii) they regulate local climate, the water cycle, water purification and nutrient cycling; iv) they provide cultural services, since irrigation landscapes have a recreational value for many people, including urbanites, and a spiritual value especially in the rural communities managing ancient irrigation systems (Fleming et al., 2014; Raheem et al., 2015; Weerahewa et al., 2023). On the other hand, in some cases, human-built infrastructures related to irrigation can cause biodiversity losses and degrade ecosystem services (Avellán et al., 2018). In addition, in some cases the ecosystem services may become positive not immediately after the introduction of irrigation or the modification of the irrigation schemes: in fact, the environmental conditions are changed, a new climax has to be found and this takes time.

A same ecosystem service may be interpreted in contrasting ways, as exemplified in boxes 2 and 3.

Evaluating ecosystem services is complex because the processes can be difficult to measure, some services are non-material, and perception may differ among stakeholders and interests. Different economic approaches are available, but all of them are based on indirect estimations, not on measurements of the water volumes involved (Crossman et al., 2010; Estes et al., 2002; Pérez-Blanco and Sapino, 2022; Zucaro and Ruberto, 2019).

This short paragraph is not exhaustive, but it highlights how difficult it is to quantify the amount of emerald water necessary to support ESs and in turn EWE. This is a challenge for future research.

3.4. Red water

This fraction represents inefficiency. Therefore, it has to be reduced as much as possible. Nevertheless, Perry et al. (2017) warn on the risk of overestimating the beneficial effects of increasing irrigation efficiency by adopting modern technologies. According to their findings, the assumption that the saved water can be released into the environment or dedicated to other uses has not been confirmed in many projects in different parts of the world, particularly in the countries of the Near East and North Africa (NENA) region. The benefits of technology have to go along with physical control of the water resource by governments or other agencies responsible for sustainable use, followed by interventions to reduce allocations. Controlled access to water must precede the introduction of hi-tech, otherwise hi-tech might make the situation even worse: consumption *per* unit area increases, the irrigated area increases, and farmers will tend to pump more water from ever-deeper sources.

4. BENEFICIAL STRATEGIES FOR INCREASING GOLD WATER EFFICIENCY (GWE)

Field conservation practices typical of the rainfed agriculture can be useful to reduce irrigation needs at the field level and consequently cut down the amount of W. Indirectly, they enhance the GWE, since it is given by G/W. These practices can be aimed at increasing the water available to the plant roots or at ameliorating the productivity per unit of water consumed (Rockström and Barron, 2007).

4.1. Increasing the water available to the plant roots

Soil management strategies able to increase the soil organic matter content generally improve the soil structure and its water retention capacity. The effect is more visible in poor soils, where the enhancement of organic matter results in a field capacity higher than the wilting point, hence greater water availability for crops (Lal, 2020). Management options such as reduced soil tillage, organic biomass and amendment inputs, cover crops, crop rotation and others offer a wide choice of farming practices.

Controlled drainage is a rain-harvesting method aimed at retaining water in the soil. In areas with shallow groundwater, it aims to maintain the water table level at a desired depth by retaining an appropriate amount of drainage water in collecting ditches (Skaggs et al., 2012). The water table depth has to be regulated throughout the year with the aim of preserving as much water as possible without generating harmful conditions for crops and soil management purposes.

During the coldest and rainiest period, when rainfall exceeds the evapotranspiration rate (autumn and winter in northern Italy), controlled drainage can be used to avoid complete water outflow. However, special attention must be paid to prevent waterlogging (Gilliam and Skaggs, 1986) and allow agricultural soils to serve as temporary water storage units during heavy rainfall events to contribute to the hydraulic safety of the territory. In this sense, the management of controlled drainage at the field and district levels has to be accurate and integrated with land reclamation authorities and agrometeorological services providing reliable rainfall forecasting in terms of timing, amounts, and spatial distribution. If heavy rain is forecast and the water table is close to the soil surface, the drainage network has to be promptly discharged to offer empty porosity to store the forthcoming precipitation. Correctly managed controlled drainage has proved to allow saving up to 80% of the outflow volumes as compared to conventional drainage (Bonaiti and Borin, 2010; Tolomio and Borin, 2018), with subsequent advantages for crops (Tolomio and Borin, 2019).

4.2. Increasing productivity of water

When switching a territory from rainfed to irrigated, cropping systems usually evolve, and a wider choice of crops is possible. This can lead to an increased water demand and has to be carefully considered in the planning phase. To optimize irrigation, the cropping system has to be adapted in a different way: with a given amount of water allocated to an area (basin, district, farm), the target becomes the individuation of the crops and varieties allowing the best profit from water use. If water availability is a limiting factor, crops with lower water requirements can be adopted, like sorghum or sunflower (Giannini et al., 2022). Promising results are related to the availability of drought-tolerant maize varieties that yield more in drought-stressed environments with no penalty in non-stressed environments (Adee et al., 2016), and require less water to maximize grain yield as compared to the conventional hybrid (Mounce et al., 2015). Therefore, careful selection of hybrids can increase corn yield and WUE under water-limited conditions (Hao et al., 2015). The adequate choice of crop and variety has to be accompanied by all the other options permitting to increase the proportion of evapotranspiration flowing as productive transpiration as to obtain "more crop per drop". Adequate timing and spacing of sowing, weed and pest control, mulching, are only some examples of the wide range of the opportunities that can be adopted.

5. CONCLUDING REMARKS

Irrigation is indispensable to achieve the Zero hunger target of the 2030 UN Agenda because it is a powerful tool for sustainable intensification, and aims to produce more *per* surface unit.

Tackling the issue of ensuring more nutritious food for a growing population, the higher productivity of irrigated lands can slow down the pace of deforestation, hence "more irrigation, less deforestation". As meeting the future worldwide food needs has to be nutrition-sensitive, with diets often composed of relatively water-intensive foods (e.g., legumes, nuts, poultry and dairy products), the sustainable use of water resources will be ever more crucial (FAO, 2020).

Agriculture has an important role to play on the path to sustainability, as irrigated agriculture accounts for more than 70% of global water withdrawals worldwide. The way agriculture uses freshwater is crucial to ensure availability for other activities and preserve water-related ecosystems. Wise irrigation can contribute to allocate water within the framework of an integrated and sustainable management with a view to turning conflicts among users into synergies. This implies multiple subjects and actors in a multi-disciplinary approach.

The process leading to an integrated and sustainable water management can be figured out as the recipe of a delicious pie requiring ingredients and a MasterChef®.

The ingredients are:

– **Awareness**: everybody is aware of the drama of water scarcity and shortage and related disasters under the climate change scenario. In Europe, June 2022 was the third warmest on record globally and a sweltering heatwave contributed to record-breaking temperatures in many locations and had disastrous consequences on the agricultural sector (Devot et al., 2023). In Italy the combination of low rainfall and high temperatures has led to losses in agricultural production exceeding 6 billion euros (Coldiretti, 2022). The UN World Water Day, celebrated yearly on March 22nd, is only one of the many initiatives raising awareness and inspiring actions to tackle the water and sanitation crisis.
– **Urgency**: about 3.2 billion people, 1.4 billion of whom live in rural areas, are experiencing moderate to high levels of water stress, and 2.2 billion are living without. These huge figures underline how urgent it is to act, as stated by the UN SDG 6 Clean water and sanitation.
– **Technology**: never in human history have available technologies been abundant as today, and progress is continuously running and offering new solutions. Technologies in the irrigation sector offer a wide range of choices, from satellite imagery, automated control systems, precision irrigation methods to the simple smartphone app supporting farmers in the management of irrigation. Technology itself is not sufficient to reduce water consumptions by irrigated agriculture (Perry et al., 2017), adequate prepara-

tion and policy measures are required. On the other hand, technology provides an enormous stimulus for innovation and training, and adequate updating of operators for optimal use of water resources (ANBI, 2023).

– **Knowledge**: public and private researchers, technicians, institutions are issuing publications, reports, guidelines, and many other documents that continuously increase the wealth of knowledge available on the topic on water management in agriculture. FAO and WMO are leading bodies in spreading updated information on tendencies and figures at the world scale.
– **Skills:** knowledge and technology have to be combined to design the right solutions for the specific problems to be tackled. Dealing with irrigation within a sustainable water management framework, no unique solution is to be adopted uncritically in all conditions and environments. The problem is typically multi-disciplinary, and experts have to be able to read and recognize local situations and design tailored solutions: common issue, multiple answers.
– **Vision,** related to skills: the people involved in sustainable irrigation should be open-minded, able to work together with experts in different disciplines, willing to consider different solutions with respect to their own point of view. The projects have to be visionary, turned toward the future, rather than replicate already existing solutions.

The MasterChef® is represented by decision makers…, but the emerald is a symbol of hope, future, growth and renewal. Let us be optimistic!

ACKNOWLEDGMENTS

This study was carried out within the Agritech National Research Center and received funding from the European Union Next-GenerationEU (PIANO NAZIONALE DI RIPRESA E RESILIENZA (PNRR) – MISSIONE 4 COMPONENTE 2, INVESTIMENTO 1.4 – D.D. 1032 17/06/2022, CN00000022). This manuscript reflects only the authors' views and opinions, neither the European Union nor the European Commission can be considered responsible for them. Spoke 4, Work Package 4.2, Task 4.2.1 "Farm network setup (Living Labs): a network of farms representative of the different agricultural systems to apply innovative technologies for the sustainable management of crops, animals and forests" and Work Package 4.3, Task 4.3.3 "Risk management strategies and policies in the context of climate change".

REFERENCES

Adee, E., Roozeboom, K., Balboa, G. R., Schlegel, A., & Ciampitti, I. A. (2016). Drought-tolerant corn hybrids yield more in drought-stressed environments with no penalty in non-stressed environments. Frontiers in Plant Science, 7, 1534.

Aldababseh, A., Temimi, M., Maghelal, P., Branch, O., Wulfmeyer, V., 2018. Multi-criteria

evaluation of irrigated agriculture suitability to achieve food security in an arid environment.

Sustainability 10 (3), 803.

Alcalde, S., & Gawlik, B. (2014). Water Reuse in Europe-Relevant guidelines, needs for and barriers to innovation. EUR 26947. Luxembourg (Luxembourg): Publications Office of the European Union. JRC92582

Allen, R. G., Pereira, L. S., Raes, D., & Smith, M. (1998). Crop evapotranspiration-Guidelines for computing crop water requirements-FAO Irrigation and drainage paper 56. Fao, Rome, 300(9), D05109.

ANBI (2023). Consorzi di bonifica e sviluppo sostenibile. Itinerari e azioni per il raggiungimento degli Obiettivi dell'Agenda 2030. Ronzani Editore, ISBN: 979-12-5997-083-1

Avellán, T., Ardakanian, R., Perret, S. R., Ragab, R., Vlotman, W., Zainal, H., … & Gany, H. A. (2018). Considering resources beyond water: irrigation and drainage management in the context of the water–energy–food nexus. Irrigation and Drainage, 67(1), 12-21.

Bellini, G. (2014). 6° Censimento Generale dell'agricoltura. Utilizzo della risorsa idrica a fini irrigui in agricoltura'. Istituto Nazionale di Statistica (Istat), pp. 334. ISBN: 978-88-458-1805-9

Bonaiti, G., & Borin, M. (2010). Efficiency of controlled drainage and subirrigation in reducing nitrogen losses from agricultural fields. Agricultural Water Management, 98(2), 343-352.

Bortolini, L., Maucieri, C., & Borin, M. (2018). A tool for the evaluation of irrigation water quality in the arid and semi-arid regions. Agronomy, 8(2), 23.

Brouwer C., Prins K., &Heibloem M. (1989). Irrigation Water Management: Irrigation scheduling. Training manual n. 4, FAO, Rome

Cesco, S., Sambo, P., Borin, M., Basso, B., Orzes, G., & Mazzetto, F. (2023). Smart agriculture and digital twins: Applications and challenges in a vision of sustainability. European Journal of Agronomy, 146, 126809.

Coldiretti (2021). https://padova.coldiretti.it/news/acqua-coldiretti-veneto-puntare-sulle-risorse-del-pnnr-per-investire-sugli-invasi-salvan-il-veneto-trattiene-solo-il-5-della-pioggia/

Coldiretti (2022). https://www.agrifood.tech/sostenibilita/agricoltura-6-miliardi-di-danni-nellestate-2022-la-peggiore-siccita-da-500-anni/

Crossman, N. D., Connor, J. D., Bryan, B. A., Summers, D. M., & Ginnivan, J. (2010). Reconfiguring an irrigation landscape to improve provision of ecosystem services. Ecological economics, 69(5), 1031-1042.

Dal Ferro, N., & Borin, M. (2017). Environment, agro-system and quality of food production in Italy. Italian Journal of Agronomy, 12(2).

Devot, A., Royer, L., Caron Giauffret, E., Ayral, V., Deryng, D., Arvis, B., Giraud, L., Rouillard, J. (2023). Research for AGRI Committee – The impact of extreme climate events on agriculture production in the EU, European Parliament, Policy Department for Structural and Cohesion Policies, Brussels

Doorenbos, J., & Kassam, A. H. (1979). Yield response to water. FAO Irrigation and drainage paper 33, FAO, Rome, 203 pp.

Doorenbos, J., & Pruitt, W. O. (1977). Crop water requirements. FAO irrigation and drainage paper 24. Land and Water Development Division, FAO, Rome, 144 pp.

Estes Jr, M. G., Cruise, J., Ellenburg, W. L., Suhs, R., Cox, A., Runge, M., & Newby, A. (2022). Evaluating Ecosystem Services for the Expansion of Irrigation on Agricultural Land. Land, 11(12), 2316.

Falcon, W. P., Naylor, R. L., & Shankar, N. D. (2022). Rethinking global food demand for 2050. Population and Development Review, 48(4), 921-957.

FAO (2002). Deficit irrigation practices. FAO Water Reports 22, FAO, Rome. ISBN 92-5-104768-5, 101 pp.

FAO (2011). The state of the world's land and water resources for food and agriculture (SOLAW) – Managing systems at risk. Food and Agriculture Organization of the United Nations, Rome and Earthscan, London.

FAO (2015a). FAO Statistical Pocketbook 2015. Food and Agriculture Organization of the United Nations, Rome. ISBN 978-92-5-108802-9

FAO (2015b). AQUASTAT, FAO's global water information system. Rome. http://www.fao.org/nr/water/aquastat/data/query/index.html

FAO (2017). Water for Sustainable Food and Agriculture, a report produced for the G20 Presidency of Germany. Food and Agriculture Organization of the United Nations, Rome. ISBN 978-92-5-109977-3

FAO (2020). The State of Food and Agriculture 2020. Overcoming water challenges in agriculture. Rome. https://doi.org/10.4060/cb1447en

Finke, P., Hartwich, R., Dudal, R., Ibanez, J., Jamagne, M., King, D., Montanarella, L., & Yassoglou, N. (1998). Geo-referenced soil database for Europe. Manual of procedures, version 1.0. European Communities.

Fleming, W. M., Rivera, J. A., Miller, A., & Piccarello, M. (2014). Ecosystem services of traditional irrigation systems in northern New Mexico, USA. International Journal of Biodiversity Science, Ecosystem Services & Management, 10(4), 343-350.

García-Tejero, I.F., Durán-Zuazo, V.H., Muriel-Fernández, J.L., Rodríguez-Pleguezuelo, C.R. (2011). Water and Sustainable Agriculture. Springer, Dordrecht. https://doi.org/10.1007/978-94-007-2091-6

Giannini, V., Maucieri, C., Vamerali, T., Zanin, G., Schiavon, S., Pettenella, D. M., … & Borin, M. (2022). Sunflower: From Cortuso's Description (1585) to Current Agronomy, Uses and Perspectives. Agriculture, 12(12), 1978.

Gilliam, J. W., & Skaggs, R. W. (1986). Controlled agricultural drainage to maintain water quality. Journal of Irrigation and Drainage Engineering, 112(3), 254-263.

Gobbo, S., Lo Presti, S., Martello, M., Panunzi, L., Berti, A., & Morari, F. (2019). Integrating SEBAL with in-field crop water status measurement for precision irrigation applications—A case study. Remote Sensing, 11(17), 2069.

Hao, B., Xue, Q., Marek, T. H., Jessup, K. E., Becker, J., Hou, X., … & Howell, T. A. (2015). Water use and grain yield in drought-tolerant corn in the Texas High Plains. Agronomy Journal, 107(5), 1922-1930.

Hoekstra A.Y. Chapagain A.K., Aldaya M.M. & and Mekonnen M.M. (2011).The Water Footprint Assessment Manual: Setting the Global Standard. Earthscan Ed., Washington, DC, USA, ISBN: 978-1-84971-279-8. 203 p.

Ingrao, C., Strippoli, R., Lagioia, G., & Huisingh, D. (2023). Water scarcity in agriculture: An overview of causes, impacts and approaches for reducing the risks. Heliyon.

Israelsen, O.W. (1950). Irrigation Principles and Practices. John Wiley and Sons, Inc.: New York; 471 pp.

ISTAT (2019). Utilizzo e qualità della risorsa idrica in Italia. Istituto nazionale di statistica, Roma, pp. 104. ISBN 978-88-458-1976-6

Jourdain, D., & Vivithkeyoonvong, S. (2017). Valuation of ecosystem services provided by irrigated rice agriculture in Thailand: a choice experiment considering attribute nonattendance. Agricultural Economics, 48(5), 655-667.

Kadiresan, K., & Khanal, P. R. (2018). Rethinking irrigation for global food security. Irrigation and drainage, 67(1), 8-11.

Lal, R. (2020). Soil organic matter and water retention. Agronomy Journal, 112(5), 3265-3277.

Levidow, L., Zaccaria, D., Maia, R., Vivas, E., Todorovic, M., & Scardigno, A. (2014). Improving water-efficient irrigation: Prospects and difficulties of innovative practices. Agricultural Water Management, 146, 84-94.

Martínez-Alvarez, V., Martin-Gorriz, B., & Soto-García, M. (2016). Seawater desalination for crop irrigation—A review of current experiences and revealed key issues. Desalination, 381, 58-70.

Masseroni, D., Arbat, G., & de Lima, I. P. (2020). Managing and planning water resources for irrigation: Smart-irrigation systems for providing sustainable agriculture and maintaining ecosystem services. Water, 12(1), 263.

Ministère de l'Agriculture et de la Sovranité Alimentaire (2022). La varenne agricole Eau – Changement climatique. Conclusion du Varenne agricole de l'eau et de l'adaptation au changement climatique. 1er février 2022, Dossier de presse. https://agriculture.gouv.fr/dossier-de-presse-conclusions-du-varenne-agricole-de-leau-et-de-ladaptation-au-changement

Monjardino, M., McBeath, T. M., Brennan, L., & Llewellyn, R. S. (2013). Are farmers in low-rainfall cropping regions under-fertilising with nitrogen? A risk analysis. Agricultural Systems, 116, 37-51.

Mounce, R. B., O'Shaughnessy, S. A., Blaser, B. C., Colaizzi, P. D., & Evett, S. R. (2016). Crop response of drought-tolerant and conventional maize hybrids in a semiarid environment. Irrigation Science, 34, 231-244.

Novello, E., & McCann, J. C. (2017). The building of the Terra Firma: The Political Ecology of land reclamation in the Veneto from the sixteenth through the twenty-first century. Environmental History, 22, 460–485.

Paul, M., M Negahban-Azara, M., Shirmohammadia, A. & Montas, H. (2020). Assessment of agricultural land suitability for irrigation with reclaimed water using geospatial multi-criteria decision analysis. Agric. Water Man., 231, 105987

Pérez-Blanco, C. D., & Sapino, F. (2022). Economic sustainability of irrigation-dependent ecosystem services under growing water scarcity. Insights from the Reno River in Italy. Water Resources Research, 58(2), e2021WR030478.

Perry, C. (2007). Efficient irrigation; inefficient communication; flawed recommendations. Irrigation and Drainage: The Journal of the International Commission on Irrigation and Drainage, 56(4), 367-378.

Perry, C., Steduto, P., & Karajeh, F. (2017). Does improved irrigation technology save water? A review of the evidence. Food and Agriculture Organization of the United Nations, Cairo, 42.

Raheem, N., Archambault, S., Arellano, E., Gonzales, M., Kopp, D., Rivera, J., … & Dingwell, E. (2015). A framework for assessing ecosystem services in acequia irrigation communities of the Upper Río Grande watershed. Wiley Interdisciplinary Reviews: Water, 2(5), 559-575.

Ricart, S., Kirk, N., & Ribas, A. (2019). Ecosystem services and multifunctional agriculture: Unravelling informal stakeholders' perceptions and water governance in three European irrigation systems. Environmental Policy and Governance, 29(1), 23-34.

Rodrigues G.C. & Pereira L.S. (2009). Assessing economic impacts of deficit irrigation as related to water productivity and water costs. Biosyst. Eng., 103(4), 536-551.

Rockström, J. & Barron, J. (2007) Water productivity in rainfed systems: overview of challenges and analysis of opportunities in water scarcity prone savannahs. Irrig Sci 25:299–311.

Seyedmohammadi, J., Esmaeelnejad, L. & Ramezanpour, H., (2016). Land suitability assessment for optimum management of water consumption in precise agriculture. Model. Earth Syst. Environ. 2, 162.

Skaggs, R. W., Fausey, N. R., & Evans, R. O. (2012). Drainage water management. Journal of soil and water conservation, 67(6), 167A-172A.

Smith, B. R. (2009). Re-thinking wastewater landscapes: combining innovative strategies to address tomorrow's urban wastewater treatment challenges. Water Science and Technology, 60(6), 1465-1473.

Steduto, P., Hsiao, T. C., Fereres, E., & Raes, D. (2012). Crop yield response to water. FAO Irrigation and drainage paper 66, Food and Agriculture Organization of the United Nations, Rome, 505 pp.

Tolomio, M., & Borin, M. (2018). Water table management to save water and reduce nutrient losses from agricultural fields: 6 years of experience in North-Eastern Italy. Agricultural Water Management, 201, 1-10.

Tolomio, M., & Borin, M. (2019). Controlled drainage and crop production in a long-term experiment in North-Eastern Italy. Agricultural Water Management, 222, 21-29.

Tromboni, F., Bortolini, L., & Martello, M. (2014). The use of water in the agricultural sector: a procedure for the assessment of large-scale irrigation efficiency with GIS. Irrigation and Drainage, 63(4), 440-450.

Turral, H., Burke, J., & Faurès, J. M. (2011). Climate change, water and food security (No. 36). Food and agriculture organization of the United nations (FAO).

Turral, H., Svendsen, M., & Faures, J. M. (2010). Investing in irrigation: Reviewing the past and looking to the future. Agricultural Water Management, 97(4), 551-560.

US Interagency Task Force (1979). Irrigation Water Use and Management. US Gov't. Printing Office: Washington DC, USA; 143 pp.

Weerahewa, J., Timsina, J., Wickramasinghe, C., Mimasha, S., Dayananda, D., & Puspakumara, G. (2023). Ancient irrigation systems in Asia and Africa: Typologies, degradation and ecosystem services. Agricultural Systems, 205, 103580.

Zheng, Y., Ross, A., Villholth, K. G., & Dillon, P. (2021). Managing aquifer recharge: a showcase for resilience and sustainability. UNESCO, Paris.

Zucaro, R., & Ruberto, M. (2019). Evaluation of ecosystem services of irrigated agriculture: a policy option for a sustainable water management. Italian Review of Agricultural Economics, 74(3), 11-22.

BOX 1 – CLIMATE AND CLIMATE CHANGE IN ITALY

Italy is characterized by a wide variation of climatic conditions ranging from temperate to Mediterranean as a result of the interaction of a continental climate (northern and central-northern areas) with that of the Mediterranean basin (centre, south and islands) (Finke et al., 1998). This situation yields seven climatic regions described in Table 1 (Dal Ferro and Borin, 2017). The temperature trend shows increasing values, especially so since the 1990's (Figure 1).

Total rainfall is characterized by high variability across years, with a below-average period between 1985 and 1995. In the last 61 years, 2022, 2017 and 2001 have been the driest years, while 2010, 1976 and 1996 have been the wettest ones (Figure 2).

Increased lengths and frequencies of dry periods have been recorded in the last years, especially in the northern regions. The reduction of precipitations has clearly affected the aquifers, that have showed water retention values close to the historical minimum. In some Italian regions, a decrease of 60-70% in winter rainfall volumes has been recorded. In addition, winter snowfalls have also decreased, so that thawing and the overall water reservoirs have decreased too. Winter precipitations (both in the forms of rainfall and snow) almost completely infiltrate the rocks and soil and thus recharge groundwaters, also thanks to the low evapotranspiration rates. Thawing generally starts at the end of spring, and supplies surface water reservoirs before dry summers. Winter drought causes a deficit in the accumulation of water reserves, and its negative effects carry on into the irrigation season.

Table 1. Italian climatic regions.

Climatic regions	Annual temperature (°C)	Annual rainfall (mm)	Elevation range (m)	Wettest months	Driest months	Extension (%)
Alpine	2.8-10.7	838-1510	0-4000	Oct., May-Jun.	Jul.	17.7
Po Plain sub-continental	10.9-13.0	710-1030	0-600	Oct.	Jul.	17.5
Northern Apennines sub-continental	8.9-13.5	1000-1540	100-2000	Oct., Nov.	Jul.	13.4
Southern Apennines sub-continental	10.4-15.4	725-1160	0-2500	Jan.	Aug.	8.4
Coastal Mediterranean	11.7-16.4	735-1180	0-1300	Oct., Jan.	Jul.-Sept.	17.7
Semi-arid Mediterranean	13.9-18.5	560-1130	0-1700	Oct., Jan.	Jul.-Sept.	17.4
Arid Mediterranean	14.8-18.9	420-710	0-650	Nov.	May-Sept.	7.8

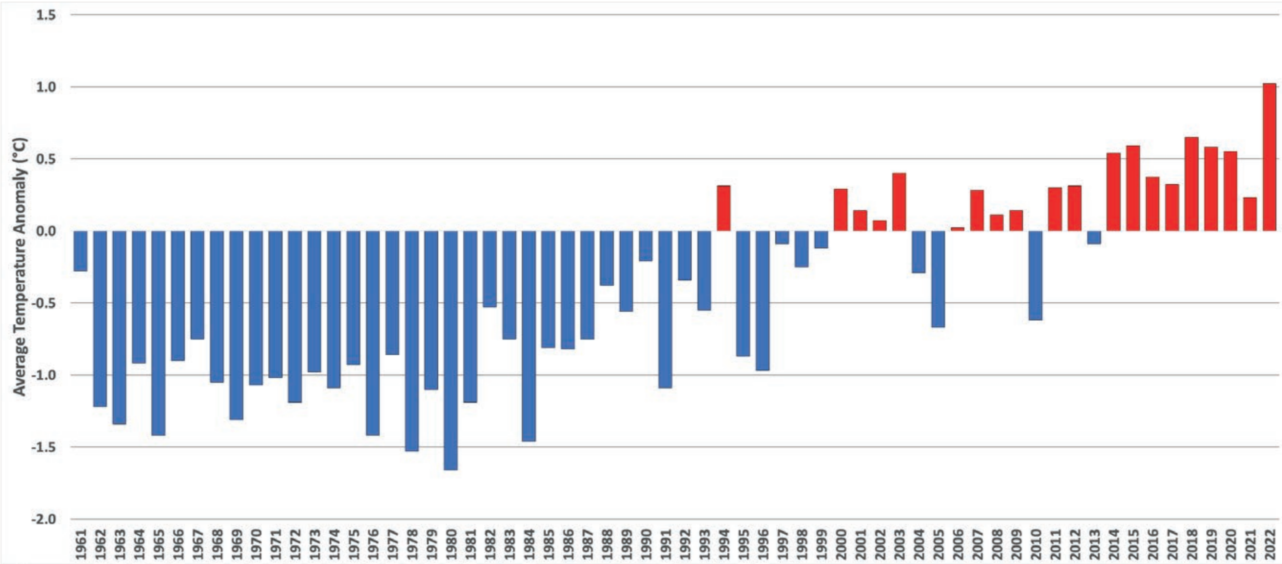

Figure 1. Time series of annual mean temperature anomalies (calculated from the normal value 1991-2020) during the 1961-2022 period. (Source: ISPRA https://www.isprambiente.gov.it/it/banche-dati/banche-dati-folder/clima-e-meteo/stato-variazioni-e-tendenze-del-clima-in-italia).

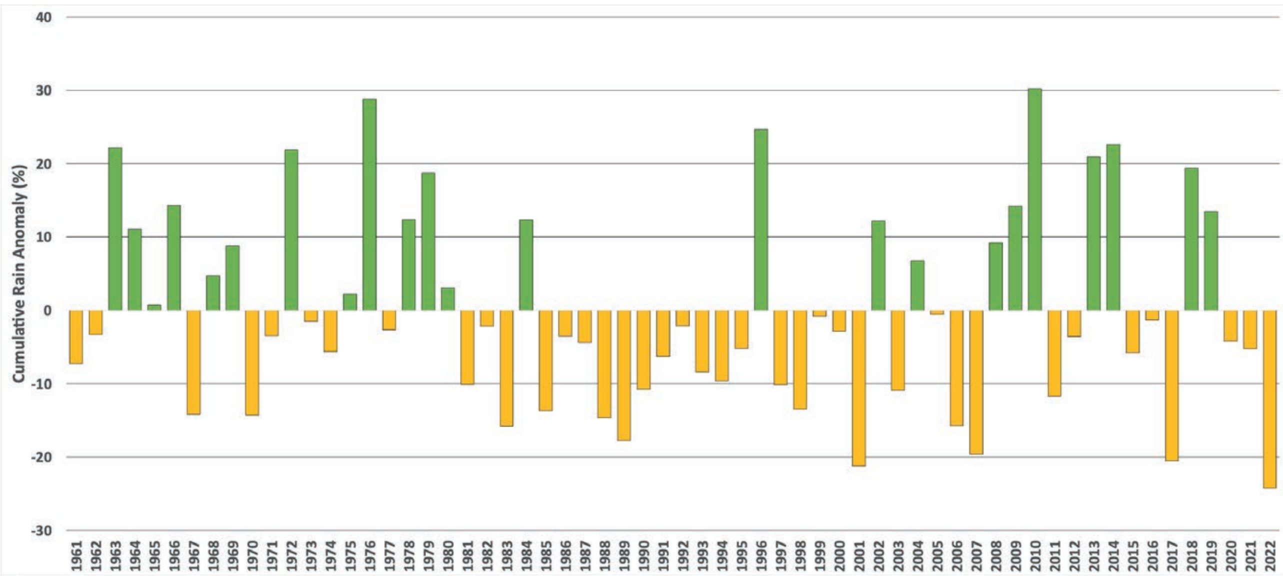

Figure 2. Time series of annual cumulative rainfall anomalies (calculated from the normal value 1991-2020) over the 1961-2022 period. (Source: ISPRA https://www.isprambiente.gov.it/it/banche-dati/banche-dati-folder/clima-e-meteo/stato-variazioni-e-tendenze-del-clima-in-italia).

BOX 2 – INEFFICIENT IRRIGATION AND AQUIFER RECHARGE: AN ECOSYSTEM SERVICE OR A DIS-SERVICE?

In the FAO Discussion Paper "Does improved irrigation technology save water? A review of the evidence", Perry et al. (2017) state that …*percolation from "inefficient" irrigation is often a major source of aquifer recharge*… and this can be interpreted as an ecosystem service. This statement contains the word "often", meaning that its validity is related to the majority of the case studies analyzed in the document but does not stand as a dogma. In other words, the role of aquifer recharge as a result of percolation from inefficient irrigation has to be defined in relation to local conditions.

In northern Italy, inefficient irrigation methods distribute 78% of the total irrigation volume; the value goes down to 31% if irrigation of rice (flooding) is excluded. Several water authorities and researchers are favorable to preserving surface and furrow irrigation, and highlight their contribution to groundwater recharge. Is this an ecosystem service or rather a dis-service? This brings about a few reflections:

1. Is it suitable to withdraw water from a river and decrease its flow during the most critical period of the year to use this water in an inefficient way?
2. Is it possible to manage aquifer recharge in other ways? The UNESCO report "Managing Aquifer Recharge: A Showcase for Resilience and Sustainability" (Zheng et al., 2021) presents 28 real-life examples of managed aquifer recharge (MAR) from around the world, and provides irrefutable evidence that water resources can be sustained, groundwater storage increased, environmental flows in streams enhanced, and seawater intrusion prevented, while passively "treating" water to improve its quality with natural processes. Different types of recharge methods are described, like in-channel modification, bank filtration, water spreading through infiltration basins, buried pipes, and recharge wells. The systems are functioning all over the year with different water sources, including treated waters. Special attention is paid to recovering water during the winter months. Therefore, alternative and sustainable solutions are available, a change of mindset is desirable.
3. (and not least) non-efficient irrigation and ensuing water percolation also cause non-point pollution, since nitrates and agrochemicals can be leached during irrigation.

The forested infiltration area (FIA) is a method for recharging groundwater aquifers by channeling surface waters during non-irrigation months (from September-October to April in northern Italy) to designated areas planted with various tree and/or shrub species (Figure 1). In addition to aquifer recharge, FIAs can offer ecosystem services such as renewable energy production, reduction of greenhouse gas emissions, landscape enhancement, or biodiversity increase.

These arguments suggest that in northern Italy the "dogma" stating that surface and furrow irrigation systems provide the ecosystem service of aquifer recharge has to be at least questioned.

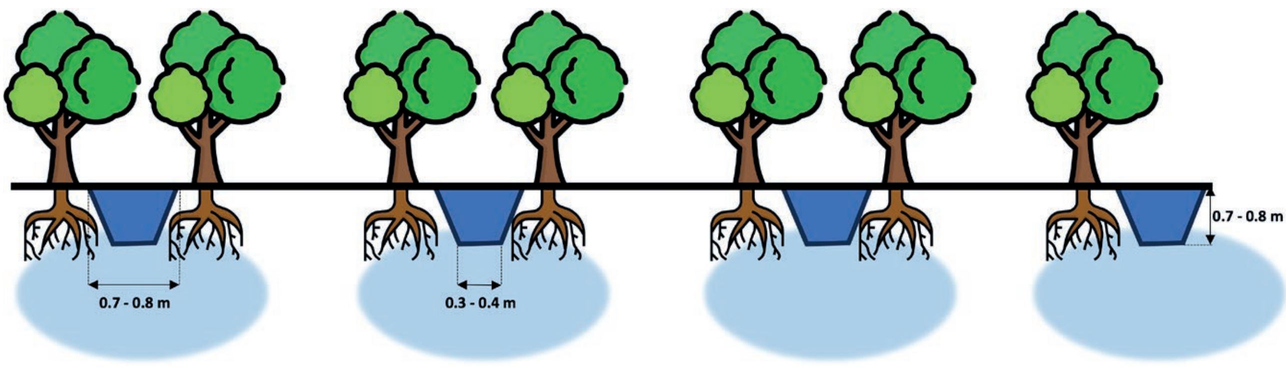

Figure 1. Scheme of a Forested Infiltration Area.

BOX 3 – IS THE DISTRIBUTION SYSTEM DELIVERING EMERALD OR RED WATER?

In Italy, around 150,000 out of more than 230,000 km of irrigation and drainage open-air canals and ditches are managed by the Reclamation and Irrigation Agencies (Consorzi di Bonifica) (www.anbi.it). This is a huge network, whose length is almost 4 times the Earth's circumference, that distributes water across the territory and stimulates life. On the other hand, only a fraction of the water delivered by such systems reaches the crops and is turned into gold water. A significant fraction is lost: does this provide ecosystem services or become red water?

Figure 1 shows an irrigation ditch distributing water withdrawn from Brenta River in northern Italy, in a typical historical system implemented in the medieval times. It is possible to assign this simple hydraulic element a list of ecosystem services, such as:

- Regulating services: microclimate regulation through shading, windbreaking, evapotranspiration, water cycle regulation, CO_2 sink in the riparian vegetation;
- Supporting services: supporting biodiversity as the stream itself and its hedgerows are ecological corridors; supporting life below water, pollinators, etc.;
- Provisioning services: wood, small fruits, fish, herbs;
- Cultural services: landscaping, visiting and relaxing, historical elements and infrastructures.

Substituting the open-air ditch with a pipeline would dramatically reduce water losses for sure , but is the change of landscape imaginable? Again, it is necessary to determine whether the ecosystem services appraised in this territory might cause dis-services in the lower part of the riverbed due to flux reduction and to quantify the amounts of water really necessary for the ecosystem services (emerald fraction) in order to avoid unnecessary losses.

Figure 1. Example of the ecosystem services of an irrigation ditch distributing water.

Italian Journal of
Agrometeorology
Rivista Italiana di Agrometeorologia

Firenze University Press
www.fupress.com/ijam

OPEN ACCESS

Citation: Toffanin, A., Maucieri, C., Rossi, G., Paulon, G., Trestini, S., & Borin, M. (2023). Does drip irrigation contribute to the economic sustainability of soybean production? *Italian Journal of Agrometeorology* (2): 21-31. doi: 10.36253/ijam-2318

Received: September 19, 2023

Accepted: November 25, 2023

Published: January 20, 2024

Data Availability Statement: All relevant data are within the paper and its Supporting Information files.

Competing Interests: The Author(s) declare(s) no conflict of interest.

ORCID:

AT: 0000-0001-9879-3149
CM: 0000-0003-4004-6612
ST: 0000-0002-9828-8262
MB: 0000-0002-4074-2098

Does drip irrigation contribute to the economic sustainability of soybean production?

Arianna Toffanin[1], Carmelo Maucieri[2,*], Giampaolo Rossi[1], Graziano Paulon[1], Samuele Trestini[3], Maurizio Borin[2]

[1] *Consorzio di Bonifica Veneto Orientale (CBVO) – Piazza Indipendenza 25, 30027 – San Donà di Piave (VE), Italy*
[2] *Department of Agronomy Food Natural resources Animals and Environment — DAFNAE, University of Padova, Agripolis Campus, Viale dell'Università 16, 35020 – Legnaro (PD), Italy*
[3] *Department of Land, Environment, Agriculture and Forestry — TESAF, University of Padova, Agripolis Campus, Viale dell'Università 16, 35020 – Legnaro (PD), Italy*
*Corresponding author. E-mail: carmelo.maucieri@unipd.it

Abstract. A two-year (2020, 2022) field experiment on soybean was conducted in northeaster Italy to evaluate the effect of irrigation (drip irrigation *vs*. rainfed), soil amendment (compost *vs*. digestate) and a cover crop (triticale *vs*. no cover crop) on grain yield and quality. Highly different rainfall amounts (627 mm and 258 mm in 2020 and 2022, respectively) and similar ET0 (578 mm and 581 mm in 2020 and 2022, respectively) were recorded during the growing seasons. Irrigation was managed using the web platform Irriframe suppling 51 mm in 2020 and 157 mm in 2022. Irrigation was the only experimental factor with significant effects on soybean grain yield and quality, except soil amendment on aboveground biomass production. In 2020, drip irrigation had no significant effect on grain yield (4.6 Mg ha^{-1} on average), while it increased it by 157% in 2022 compared to the rainfed control (1.0 Mg ha^{-1}). The grain protein content was reduced by irrigation (43.2 ± 1.3% and 42.6 ± 0.9% under rainfed and irrigation managements, respectively). No treatment effect was observed on the grain oil content. A positive effect of irrigation was observed on water use efficiency, with values ranging from 0.40 ± 0.19 kg m^{-3} to 0.71 ± 0.12 kg m^{-3}. The balance of the economic sustainability of drip irrigation was negative in both years: this irrigation method was not sustainable for soybean within the economic framework of the study area at the time. However, the results also confirmed that irrigation is a key agronomic technique to reduce production variability and dryland vulnerability of soybean.

Keywords: *Glycine max* L., drip irrigation, economic sustainability, soil organic amendment, cover crop, grain yield.

1. INTRODUCTION

Climate change is causing a shift in the distribution and quantity of precipitations, with an increase of the intensity and frequency of extreme events (droughts and floods). Variability in precipitations is occurring at both intraannual and inter-annual levels. This variability has a strong impact on the agricultural sector (Todorović et al., 2021; Ehsan et al., 2022), especially for herbaceous crops with a spring-summer cycle that are cultivated in areas where rainfall used to almost fully meet the crop's evapotranspiration demand. In this context, irrigation is now an indispensable agronomic technique to achieve sustainable yield levels (Tran et al., 2020).

The accessibility of water resources for human uses (household, industrial, agricultural, etc.) is highly dependent on their spatio-temporal distribution and the spatial water balance (Milly et al., 2005; Oki and Kanae, 2006; Konapala et al., 2020). As a result, ongoing climate change may severely reduce the volumes of available water, with a spectacular increase of competition among the various sectors of use (drinking, industrial, and agricultural). Considering that the agricultural sector is the largest user of the water resource (about 70% of all freshwater withdrawals; Wisser et al., 2008), greater efforts are required to reduce the volumes being used. This can be pursued at several scales – from the territorial to the farm scale – through efficient distribution networks managed by Reclamation Consortia at the territorial scale, and by adopting irrigation systems characterized by low irrigation volumes and high irrigation efficiency at the farm scale. Among irrigation systems, drip irrigation has also been proposed for open-field herbaceous crops. This technique offers a number of advantages over traditional irrigation systems (Lamm, 2002; Shahrokhnia and Zare, 2022), chief among them the supply of small volumes of water directly to the root zone of the crop, under the canopy. This minimizes evaporation losses from the soil and increases water use efficiency (WUE). Its adoption has to be supported by good economic results. At present, only few studies conducted in particular contexts have been published, and have given contrasting indications (Narayanamoorthy, 1997; Maisiri et al., 2005; Möller and Weatherhead, 2007; Khor and Feike, 2017). Therefore, the economic impact of drip irrigation should be further analyzed.

Soybean (*Glycine max* L.) is the fourth most widespread crop worldwide (FAOSTAT, 2021). It provides more than 25% of total proteins for human and animal feed, and its global production increased about 13-fold between 1961 and 2017 (Liu et al., 2020). It is a spring-summer crop characterized by high water requirements that can exceed 600 mm. It is frequently grown in rainfed conditions, but it also greatly benefits from irrigation, especially in light of climate change (Karges et al., 2022). In Italy, soybean is cultivated on about 324,000 ha, 40% of which in the Veneto Region, where this study was conducted (ISTAT, 2023).

The Living Labs (LL), a collaborative and user-centred open innovation approach (Beaudoin et al., 2022), has been applied to design the experiment. In the experimental area soybean is irrigated on about 16,000 ha, served by the Veneto Orientale Reclamation Consortium (CBVO). Farmers together with CBVO developed a strong interest on drip irrigation, to manage the open-field summer season herbaceous crops (corn and soybean), soil organic amendment and cover crop introduction in the crop rotation. In this frame an *On-Farm Experimentation* (OFE) has been set up to evaluate the effect of drip irrigation and its interaction with soil organic amendment and the use of cover crops (CC) on the yield, quality and economic performance of soybean.

2. MATERIALS AND METHODS

2.1. Experimental site

The on-farm experimentation was conducted at the "Podere Fiorentina" of the CBVO located in San Donà di Piave (45°38'13.10"N, 12°35'55.00"E, 1 m a.s.l.) during the 2020 and 2022 soybean growing seasons. The area falls into the Cfa climatic class (Köppen's classification), with rainfall mainly in spring and autumn, and frequent thunderstorms in hot and humid summers. Climate data collected by the Veneto Regional Agency for Environmental Protection (ARPAV) from 1992 to 2022 show an average annual rainfall of 966 mm and an average temperature of 13.7 °C (with average maximum and minimum temperatures of 19.1 °C and 8.9 °C, respectively); the mean ET0 is higher than rainfall from June to August.

2.2. Experimental layout

The experimental area covered 4.85 ha, and the layout included 8 plots of 0.3 to 0.9 ha (Figure 1). The studied variables were i) irrigation: drip irrigation (I) *vs.* no irrigation (R); ii) soil amendment: compost from pruning waste (C) *vs.* digestate solid fraction from anaerobic digestion of manure (D); iii) presence (CC - x *triticosecale*) or absence (No CC) of a CC during the winter period.

The soil was characterized by a sandy clay loam texture (USDA classification). Table 1 summarizes its main physical and hydrological characteristics obtained from 54 uniformly distributed sampling points in the experimental area. As showed by the low standard deviation, the soil profile was pretty uniform. We noted a low transversal variability and in view of this, the sub-plots (paragraph 2.3) were distributed along the longitudinal

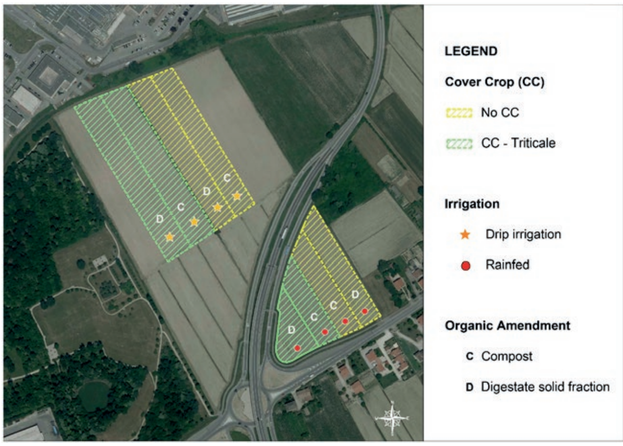

Figure 1. Experimental layout: eight plots with a combination of irrigation (drip irrigation *vs.* rainfed), cover crops (triticale *vs.* no CC), and organic amendments (compost *vs.* digestate solid fraction).

Table 1. Soil physical characteristics and hydrological properties (0-0.40 m depth) (average ± SD).

Variable	Value
Clay (%)	24.7 ± 3.4
Silt (%)	25.1 ± 2.3
Sand (%)	50.2 ± 5.4
Bulk density (Mg m^{-3})	1.26 ± 0.09
Field capacity (% v/v)	27.3 ± 2.1
Wilting point (% v/v)	8.3 ± 2.0

Table 2. Composition of compost and digestate solid fraction in each 2020 and 2022.

Year	Amendment	Quantity supplied (Mg ha^{-1})[1]	Dry Matter (% DM)	Organic Carbon (% DM)
2020	Compost	39.7	71.0	29.0
	Digestate	20.2	23.1	52.8
2022	Compost	43.1	55.4	31.0
	Digestate	21.6	20.2	52.8

[1] Fresh weight.

Figure 2. Installation and layout of drip lines.

transect of each main plot to represent all the spatial variability of the experimental site.

Soybean (Group 1) was sown on May 9th 2020 and May 11th 2022 with an interrow of 0.75 m, and harvested on October 19th 2020 and October 7th 2022. The organic amendments (together with the CC or weed biomass) were incorporated into the soil by plowing (0.30 m depth) carried out one week before sowing and followed by harrowing for seedbed preparation. The organic matrices were supplied yearly; their dry matter and OC content are reported in Table 2.

Soybean irrigation was carried out through surface drip irrigation by positioning one polyethylene drip line every two soybean rows (distance between two drip lines = 1.5 m) (Figure 2). The drip lines (16 mm diameter) had in-line drippers inserted along the pipe at 0.5 m spacing, with a discharge of 1.1 L h^{-1}. Irrigation was managed through the IRRIFRAME platform, which is a decision support system that integrates cloud data obtained from different sources (meteorological, farm and GIS data) in a water balance model set to simulate the soil water content at different soil depths. The irrigation volumes are reported in Table 3. Weeds were controlled chemically during the growing seasons.

2.3. Soybean sampling and analysis

Soybean was sampled at harvest from three permanent 4 m^2 sub-plots *per* plot by measuring total aerial biomass and grain yield. The sub-plots were distributed along a longitudinal transect at regular intervals from the field borders and between two consecutive fields; they were identified with the only purpose of sampling but were managed with the same field operation occurring in the relative field (Giannini et al., 2023). The dry matter content of the two fractions was determined in a thermoventilated oven at 65 °C. The oil and protein contents of soybean grains were determined by NIRS technology (Infratec-1241, Foss Analytical, Hillerød, Denmark).

The harvest index (HI) was calculated after grain yield and aerial biomass determination, using the following equation:

$$HI = \frac{Grain\ yield}{(Grain\ yield + Aboveground\ biomass)}$$

Water use efficiency (WUE) was calculated using the following equation:

$$WUE\ (kg\ mm^{-1}) = \frac{Grain\ yield}{(Rainfall + Irrigation)}$$

2.4. Meteorological data

Meteorological data and reference evapotranspiration (ET0), calculated by the FAO Penman Montieth equation (Allen et al., 1998), were acquired from the Noventa di Piave regional weather station belonging to ARPAV, located about 5 km from the experimental site. Considering the rain variability during the spring-summer season, the rain volume was measured with a rain gauge positioned within the experimental site.

The thermal sum was calculated as growing degree days (ΣGDD) for the whole growing season, using the following equation:

$$GDD = [(T_{max} + T_{min})/2\ ] - T_{base}$$

Where T_{base} is the temperature below which the growing process does not progress, set at 7 °C (Boote et al., 1998). GDD was set at 0 when $[(T_{max}+T_{min})/2]$ was lower than T_{base}. When T_{max} was higher than the optimal temperature (35 °C) (Boote et al., 1998), it was set at 35 °C.

2.5. Economic profitability of irrigation

The contribution of drip irrigation to economic sustainability was assessed using an approach of marginal profitability introduced by the innovation and by applying the following formula:

Irrigation marginal profitability (€ ha^{-1}) = Δ*revenue* – *Irrigation costs*

Where Δ*revenue* (€ ha^{-1}) was calculated as follows:

[*Grain yield with irrigation* (Mg ha^{-1}) – *Grain yield rainfed* (Mg ha^{-1})] * *Grain value* (€ Mg^{-1})

using a grain value of 385,00 € Mg^{-1} in 2020 and 610,50 € Mg^{-1} in 2022, as in the official price list of commodities exchange of Bologna.

The irrigation costs were calculated considering the depreciation costs of durable components [(pump 7,500.00 € and filter 8,000.00 € with a depreciation time of 10 years) + (other system components 4,000.00 € with a depreciation time of 5 years)], the direct costs for the purchase of irrigation equipment (drip lines) (350.00 € ha^{-1} in 2020; 740.00 € ha^{-1} in 2022) and fuel needed for the engine used to put the drip irrigation system under pressure (10.00 € ha^{-1} in 2020; 40.00 € ha^{-1} in 2022) as retrieved from a market survey, equipment and labor needed to set up and remove the irrigation system (115.00 € ha^{-1}), and the costs of labor during the irrigation season (0.25 h ha^{-1} equal to 2.50 € ha^{-1} for each irrigation event).

2.6. Statistical and data analysis

The variables were statistically analyzed by three-way ANOVA with irrigation, soil amendment and cover crop presence as experimental variables. Prior to the ANOVA, data were checked for normality by Shapiro-Wilk test and equal variance test. All statistical analyses were performed using R software (R Core Team, 2021) with the emmeans package for *post-hoc* comparisons (Lenth, 2021) at $p < 0.05$.

The variability of the effects of irrigation, costs and product prices observed during the two years was used to simulate different economic scenarios.

Table 3. Number of irrigation events and total volumes applied (mm) in 2020 and 2022.

Year	Number of irrigation events	Total irrigation volume (mm)	Irrigation season
2020	3	51	6 days (from July 24th to July 31st)
2022	20	157	51 days (from June 20th to August 10th)

3. RESULTS

3.1. Meteorological conditions and irrigation management

The two seasons showed a similar trend in air temperature, with maximum values recorded in July and August (Figure 3). However, different absolute values were measured. The monthly average temperature was higher in 2022 than in 2020, except in September (Table 4). As a consequence, the 2022 growing season was shorter (-8.5 %) than the first one (164 days) and it accumulated more GDD (+4.3 %) than the 2020 growing season (2,317 GDD) (Figure 4).

Evaluating the hydroclimatic balance of the experimental area for the last 31 years (1992-2022) in the May-

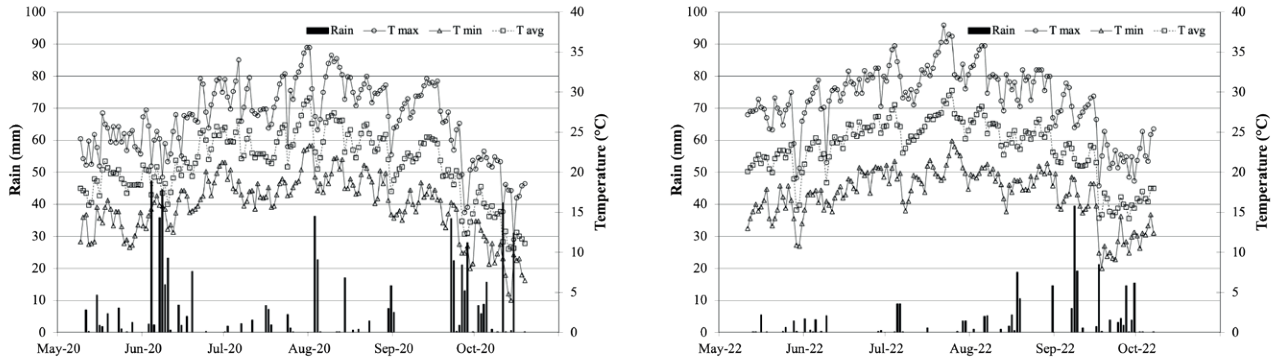

Figure 3. Rainfall and temperature trends recorded during the 2020 and 2022 growing seasons.

Table 4. Monthly average temperatures (°C) in 2020 and 2022 and delta temperature between the years.

Month	Temperature (°C)		D Temperature 2022-2020 (°C)
	2020	2022	
May	18.7	20.9	+2.2
June	21.1	24.2	+3.1
July	23.9	26.3	+2.4
August	24.3	25.1	+0.8
September	20.2	19.0	-1.2
October	13.7	17.1	+3.4

October timeframe (Figure 5), the rain volume exceeded ET0 only in 25.8% of the years, as in 2020. Among the negative values, the water deficit was lower than 350 mm only in 2003, as in 2022. The distribution of the annual water deficit was as follows: between 0 and -100 mm in 25.8% of the years, between -100 and -200 mm in 19.4% of the years, between -200 and -300 mm in 16.1% of the years, and between -300 and -400 mm in 12.9% of the years.

Different rain quantities and distributions between the two seasons were recorded from soybean sowing

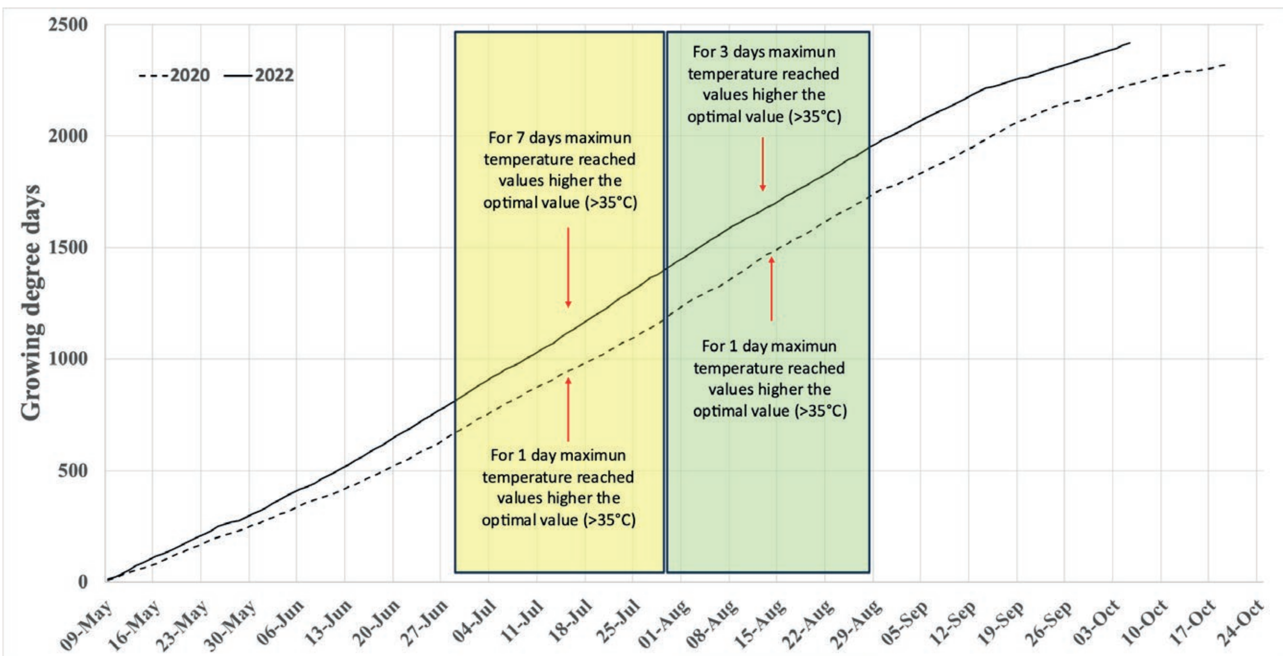

Figure 4. Accumulation of soybean growing degree days over the two growing seasons (dashed line, 2020; solid line, 2022). Yellow and green boxes indicate July and August, respectively.

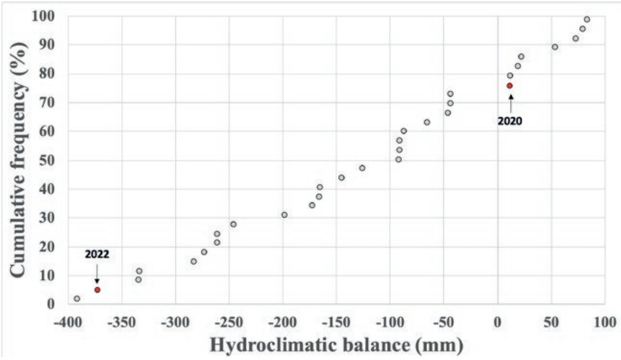

Figure 5. Cumulative frequency of the May-October hydroclimatic balance (mm) over the 1992-2022 period.

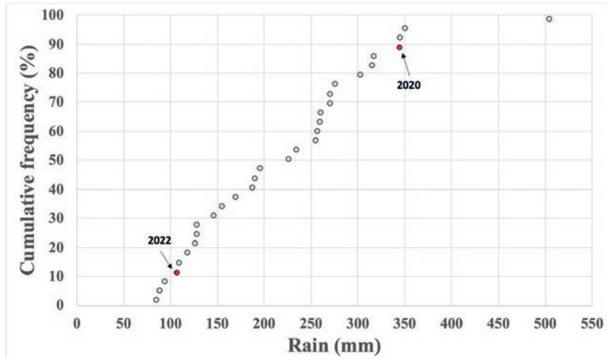

Figure 6. Cumulative frequency of June-August cumulative rainfall (mm) over the 1992-2022 period.

to harvesting (627 mm in 2020; 258 mm in 2022) (Figure 3). Conversely, similar ETmax values were calculated (372.3 mm in 2020; 381.0 mm in 2022) (Table 5). In addition to the low rainfall, the 2022 growing season was characterized by a non-optimal distribution for production purposes since 53.6% of cumulative rainfall (138.4 mm) were recorded in September. Rainy days with rain higher than 10 mm were 125% more frequent in 2020 than in 2022 (8 days).

Focusing on the irrigation season (June-August), 2020 and 2022 were the fourth wettest (344.4 mm) and the fourth driest (107.4 mm) year in the last 31 years, respectively (Figure 6). The opposite cumulative rainfall values in the two years reflect a long-lasting trend (1992-2022) showing cumulative rainfall between 100 and 200 mm in 38.7% of the years and between 250 and 350 mm in another 38.7%. In 2020, June rainfall was the highest (206.6 mm) recorded in the last 31 years, whereas only 15.8 mm were recorded in June 2022 (Table 5). July was a dry month in both years (34.0 mm rainfall in 2020; 27.4 mm in 2022; values usually exceeded with a probability of 77.4%). However, maximum temperatures greatly differed in July, and even in August (Figure 4): they were much higher in 2022 than in 2020, and rainfall was lower (-38.2%) (Table 5). Cumulatively (rain + irrigation), soybean received 678 mm *vs*. 412 mm during the growing seasons of 2020 and 2022, respectively. The irrigation volume represented 7.5% of the cumulative water supplied in 2020 *vs*. 37.4% in 2022.

3.2. Soybean yield and quality

Soybean grain yield was significantly affected by the year, irrigation, and their interaction (Table 6). Irrigation had no significant effect on grain yield in 2020 (mean 4.6 Mg ha^{-1}), while it increased it by 157% in 2022 compared to the rainfed treatment. The mean values across the two years showed a linear correlation between grain

Table 5. Rainfall, maximum crop evapotranspiration (ETmax)* and irrigation volumes in the 2020 and 2022 growing seasons.

Month	2020 growing season						2022 growing season					
	Rainfall (mm) (1)	Number of rainy days	Rainy days (> 10mm)	Irrigation (mm) (2)	ETmax (mm) (3)	Water balance (mm) (1+2-3)	Rainfall (mm) (1)	Number of rainy days	Rainy days (> 10mm)	Irrigation (mm) (2)	ETmax (mm) (3)	Water balance (mm) (1+2-3)
May	41.0	10	1	0	37.8	+2.9	12.0	8	0	0	37.4	-25.4
June	206.6	13	6	0	86.7	+119.9	15.8	8	0	30	89.5	-43.7
July	34.0	10	0	51	134.0	-49.0	27.4	8	0	79	141.5	-35.1
August	103.8	10	3	0	73.2	+30.6	64.2	10	3	34	79.4	+18.8
September	129.0	9	5	0	31.6	+97.4	138.4	15	5	0	28.7	+109.7
October	112.2	11	3	0	9.0	+103.2	0.6	3	0	0	4.4	-3.8
Σ	626.6	63	18	51	372.3	+305.0	258.4	52	8	154	381.0	+20.5

ETmax = Maximum possible water loss through evapotranspiration under ideal conditions without water limitations

Table 6. Soybean grain yield, straw production and water use efficiency (WUE) (average ± SD) under irrigated and rainfed conditions in 2020 and 2022. Different letters indicate significant differences (p<0.05).

Year	Irrigation	Grain (Mg ha-1)	Straw (Mg ha-1)	WUE (kg mm-1)
2020	Rainfed	4.5 ± 0.7 a	3.4 ± 0.7 ab	7.1 ± 1.2 a
	Drip irrigation	4.6 ± 0.5 a	2.9 ± 0.6 bc	6.8 ± 0.8 a
2022	Rainfed	1.0 0.5 c	2.5 ± 1.0 c	4.0 ± 1.9 c
	Drip irrigation	2.7 ± 0.5 b	4.1 1.0 a	6.4 ± 1.1 ab

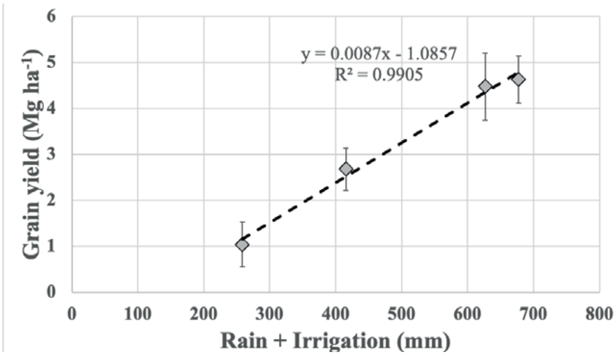

Figure 7. Correlation between water availability and soybean grain yield.

yield and total water availability during the growing cycle (Figure 7). A notable yield increase was observed from 258 to 627 mm of supplied water, with an increase in grain production of 10.7 kg ha^{-1} for each mm. The maximum grain yield was obtained in 2020, with a water volume supply ranging between 627 and 678 mm. CC and the soil amendment type did not have any significant effect on grain yield.

The soybean straw production significantly increased when the soil was amended with digestate solid fraction (+17.3%) compared to compost (2.98 ± 0.69 Mg ha^{-1}), and under irrigation (+20.1%) compared to rainfed (2.94 ± 0.76 Mg ha^{-1}). The 'year x irrigation management' interaction also influenced straw production, with a higher production under rainfed conditions in the rainier year and the opposite in the drier year (Table 6).

Considering the grain quality characteristics, only irrigation significantly influenced the protein content. It induced a reduction from 43.2 ± 1.3% to 42.6 ± 0.9%, while none of the factors under study influenced the oil content (mean 21.9 ± 0.7%).

3.3. Harvest index and water use efficiency

The HI was significantly higher in the wetter year (2020), with no difference between the two treatments (mean 0.59). The HI was lower in 2022 than in 2020, with a significantly higher value under the irrigated treatment (0.41) than under the rainfed one (0.28).

WUE was significantly influenced by the year, irrigation, and their interaction (Table 6). The highest values were obtained in the wetter year, with no significant difference between the irrigated and rainfed treatments (mean 7.0 kg grain mm^{-1}). In the less rainy year (2022), irrigation increased WUE by 60.1% compared to the rainfed treatment (4.0 kg grain mm^{-1}). WUE was not significantly different across the years under the irrigated treatment.

3.4 Irrigation and contribution to economic sustainability

The balance of drip irrigation economic sustainability was negative in both years (Table 7), showing that this irrigation method is not sustainable for soybean within the economic framework of the study area. In 2020, when the rainfall volume satisfied almost the entire crop water requirements (92.5%), the Drevenue due to the limited increase in grain production of the irrigated plots (+ 3.4%) was insufficient to cover the irrigation costs. In 2022, the irrigation provided 37.4% of the total water supplied during the growing season, and brought a grain yield increase of about 157%. Moreover, the grain price of soybean increased by 58.6% due to geopolitical reasons in 2022. However, for that same reason, the cost of annual irrigation equipment (drip tape) simultaneously increased by 111.4%. Both these aspects, together with the unusual meteorological conditions (especially maximum temperatures, Figure 4), caused a low absolute grain yield even under irrigated conditions and resulted in a negative balance in 2022.

An overall assessment of the contribution of drip irrigation to the economic sustainability of soybean production is presented in Table 8. Out of the twelve possible scenarios analyzed in this study, only one shows a clear economic benefit from drip irrigation, i.e., the scenario with low costs, high irrigation effects on yield increase and high market prices. The minimum price that would cover irrigation costs in that scenario is 430.00 € Mg^{-1}. Conversely, the minimum price of soybean that would cover irrigation costs under high effects of irrigation on the yield increase and high irrigation costs is 709.00 € Mg^{-1}. This is an exceptional scenario that occurred under conditions of severe supply difficulties, and therefore an unrealistic one under ordinary conditions to date.

Table 7. Balance of the economic sustainability (€ ha^{-1}) of the drip irrigation system.

Balance items		Growing season	
		2020	2022
*Revenue (€ ha^{-1}) = yield (Mg ha^{-1}) * price (€ Mg^{-1})*			
Irrigated treatment (drip irrigation)		1,780.94	1,634.11
Rainfed treatment		1,722.88	636.45
	Δrevenue	58.07	997.66
Irrigation costs (€ ha^{-1})			
Depreciation costs of durable components		235.00	235.00
Direct costs for irrigation equipment purchase		350.00	740.00
Equipment and labor needed to set up and remove the irrigation system		90.00	90.00
Costs of labor during the irrigation season		7.50	50.00
Fuel needed for the engine used to put the drip irrigation system in pressure		10.00	40.00
	Σcosts	692.50	1,155.00
Economic sustainability of irrigation (€ ha^{-1}) = DRevenue (€ ha^{-1}) - Irrigation costs (€ ha^{-1})		-634.43	-157.34

NB: Irrigation costs refer to an irrigation system serving 20 ha.

Table 8. Economic scenario analysis.

Grain Price	Irrigation Costs	Low Dyield	High Dyield
Low	Low	-634.43	-64.95
	High	-1,097.25	-527.45
High	Low	-600.93	+302.62
	High	-1,063.43	-157.34

NB: 2020 was characterized by a low price of soybean, low costs and a low Dyield; 2022 was characterized by a high price of soybean, high costs and a high Dyield.

4. DISCUSSION

Irrigation was the sole factor with significant effect on grain yield in relation to the amount and distribution of rainfall among the factors studied in the present work, except for the effect of soil amendments on aboveground biomass production. Irrigation increased grain yield only in the less rainy year (2022), with a recurrence time of 12.9%. This points to the need to plan for possible irrigation in relation to the course of rainfall throughout the year and confirms the results of a study conducted by Ray et al. (2015) aimed at globally estimating the contribution of weather conditions to the yield variability of major extensive field crops: weather conditions have a significant influence on soybean yield in 67% of the regions where it is grown.

Considering the inter-annual yield variation, a yield reduction was observed under both rainfed and irrigated treatments. However, the yield variation between the two years was lower under irrigation management, confirming that irrigation contributes to increase and stabilize yield over time (Grassini et al., 2014). The lower grain yield observed in the second year, even though irrigation was supplied, is attributable to heat stress because temperature exceeded the optimal maximum temperature for ten days in July and August. As recently observed by Jumrani and Bhatia (2019), the seed yield of soybean plants under drought stress at the reproductive stage decreased with the increase of day/night temperatures (30/22 °C -55%, 34/24 °C -59%, 38/24 °C -62% and 42/28 °C -65%) compared to the seed yield of well-watered plants. In our experiment, the irrigated treatment (where full crop water requirement was supplied) showed a yield decrease of 42.1% in 2022 (the year with higher temperature stress conditions) compared to 2020. In the same years, the seed yield decreased by 76.8% under rainfed conditions. Therefore, our data confirm that temperature stress further increases the detrimental effect of drought stress.

A positive correlation between grain yield and water availability during the flowering and grain filling stages has been observed by various authors (Brevedan and Egli, 2003; Chen and Wiatrak, 2010; Sobko et al., 2020). Our results confirm what is reported in these studies. In the less rainy year, rainfall was mainly concentrated in the late part of the crop cycle (August-September), and the soil water content maintained by irrigation between the flowering and grain filling stages increased the yield by 157%. Limited precipitation and a reduced soil water content have also been identified as main limiting factors for soybean seed yields (Gajić et al., 2018). Looking at the water requirements to maximize grain production, our data (from 627 to 678 mm) are within the range reported by Doorenbos and Kassam (1979) who estimated that the water requirement is between 450 mm and 700 mm for maximum production by soybean, depending on climate and the length of the growing period.

A positive effect of irrigation was also observed in terms of WUE, especially in the drier year. WUE values ranging from 0.69 ± 0.03 to 1.16 ± 0.06 kg m^{-3} were obtained by Anda et al. (2020) comparing two soybean genotypes. These authors observed that water stress during the reproductive stage improved WUE irrespective of the season and variety. In our study, WUE values ranged from 0.39 ± 0.18 to 0.86 ± 0.14 kg m^{-3} but with opposite trends, as higher values were obtained under higher rainfall conditions. This can be attributed to the particularly stressful conditions observed in the second year that significantly reduced grain yield despite irrigation.

The grain quality results of the present study disagree with Rotundo and Westgate (2009), who concluded from a meta-analysis that water stress reduces the protein and oil contents of soybean grains. In contrast, the increase in grain protein content under rainfed conditions is in agreement with the results of Candoğan and Yazgan (2016) and Kresović et al. (2017). Considering the grain oil content, our data are in line with the results of Pedersen and Lauer (2003) and Mertz-Henning et al. (2017), who did not observe any significant difference in soybean grain oil content between irrigated and rainfed management when comparing different genotypes under different environmental conditions.

The positive effects of irrigation on grain yield should also be considered in terms of the costs associated with irrigation in order to determine its overall and long-term profitability. Few studies have assessed the economic sustainability of drip irrigation. To the best of our knowledge, no study has been done on soybean, and available studies on other crops have reported contrasting results. The sustainability of irrigation certainly depends on the amount of seasonal rainfall and should be evaluated accordingly (Karges et al., 2022). With this in mind, the use of drip irrigation should be carefully evaluated because it has annual initial fixed costs (purchase and installation of drip lines). However, our data indicate that even in a very dry growing season (recurrence time of 12.9% in a 30 years period), drip irrigation it is not economically sustainable.

5. CONCLUSIONS

Among several experimental factors, the results of the present study show that irrigation is a key agronomic technique to reduce soybean yield variability and vulnerability to drought. However, the investment incurred for drip irrigation at the beginning of the crop cycle is not sustainable because of possible high rainfall volumes during the growing season (resulting in the irrigation system being unused) and/or the high uncertainty of annual costs and possible low grain yield due to other reasons.

Climate change is expected to further affect water availability in terms of quantity and distribution, with an increased number of drought stress events for crops. The simultaneous growth of the world population will result in serious food security uncertainties. In this context of an increased frequency of crop drought stress events, drip irrigation may be a key system to increase and stabilize soybean yield in order to pursue the goal of food security, but cost recovery should be assured. Based on the cost analysis, technological and/or agricultural policy solutions geared toward reducing the direct costs of this irrigation system are highly desirable.

ACKNOWLEDGMENTS

This study was carried out within the Agritech National Research Center and received funding from the European Union Next-GenerationEU (PIANO NAZIONALE DI RIPRESA E RESILIENZA (PNRR) – MISSIONE 4 COMPONENTE 2, INVESTIMENTO 1.4 – D.D. 1032 17/06/2022, CN00000022). This manuscript only reflects the authors' views and opinions, neither the European Union nor the European Commission can be considered responsible for them. Spoke 4, Work Package 4.2, Task 4.2.1 "Farm network setup (Living Labs): a network of farms representative of the different agricultural systems to apply innovative technologies for the sustainable management of crops, animals and forests" and Work Package 4.3, Task 4.3.3 "Risk management strategies and policies in the context of climate change".

REFERENCES

Anda, A., Soos, G., Menyhart, L., Kucserka, T., & Simon, B. (2020). Yield features of two soybean varieties under different water supplies and field conditions. Field crops research, 245, 107673.

Beaudoin, C., Joncoux, S., Jasmin, J.F., Berberi, A., McPhee, C., Schillo, R.S., Nguyen, V.M. (2022). A research agenda for evaluating living labs as an open innovation model for environmental and agricultural sustainability. Environmental Challenges, 7, 100505.

Boote, K.J., Jones, J.W., Hoogenboom, G., Pickering, N.B. (1998). The CROPGRO model for grain legumes. In: Tsuji, G.Y., Hoogenboom, G., Thornton, P.K. (eds) Understanding Options for Agricultural Production. Systems Approaches for Sustainable Agricultural Development, vol 7. Springer, Dordrecht.

Brevedan, R. E., & Egli, D. B. (2003). Short periods of water stress during seed filling, leaf senescence, and yield of soybean. Crop Science, 43(6), 2083-2088.

Candoğan, B. N., & Yazgan, S. (2016). Yield and quality response of soybean to full and deficit irrigation at different growth stages under sub-humid climatic conditions. Journal of Agricultural Sciences, 22(2), 129-144.

Chen, G., & Wiatrak, P. (2010). Soybean development and yield are influenced by planting date and environmental conditions in the southeastern coastal plain, United States. Agronomy Journal, 102(6), 1731-1737.

Doorenbos, J., & Kassam, A. H. (1979). Yield response to water. Irrigation and drainage paper, 33, 257.

Ehsan, N., Hoogenboom, G., Qamar, M. K., Wilkerson, C. J., Wajid, S. A., & Aziz, F. (2022). Climate change risk perception and adaptation to climate smart agriculture are required to increase wheat production for food security. Italian Journal of Agronomy, 17(4).

Gajić, B., Kresović, B., Tapanarova, A., Životić, L., & Todorović, M. (2018). Effect of irrigation regime on yield, harvest index and water productivity of soybean grown under different precipitation conditions in a temperate environment. Agricultural water management, 210, 224-231.

Grassini, P., Torrion, J. A., Cassman, K. G., Yang, H. S., & Specht, J. E. (2014). Drivers of spatial and temporal variation in soybean yield and irrigation requirements in the western US Corn Belt. Field Crops Research, 163, 32-46.

ISTAT (2023). http://dati.istat.it/Index.aspx?DataSetCode=DCSP_COLTIVAZIONI

Jumrani, K., & Bhatia, V. S. (2019). Interactive effect of temperature and water stress on physiological and biochemical processes in soybean. Physiology and Molecular Biology of Plants, 25(3), 667-681.

Karges, Bellingrath-Kimura, Watson, Stoddard, Halwani, Reckling, (2022). Agro-economic prospects for expanding soybean production beyond its current northerly limit in Europe. European Journal of Agronomy, 133:126415.

Khor, L. Y., & Feike, T. (2017). Economic sustainability of irrigation practices in arid cotton production. *Water Resources and Economics*, *20*, 40-52.

Konapala, Mishra, Wada, Mann, (2020). Climate change will affect global water availability through compounding changes in seasonal precipitation and evaporation. Nature communications, 11(1):3044.

Kresović, B., Gajić, B., Tapanarova, A., Pejić, B., Dugalić, G., & Sredojević, Z. (2017). Impact of deficit irrigation on yield and chemical properties of soybean seeds in temperate climate. Contemporary Agriculture, 66(1-2), 14-20.

Lamm, F.R. (2002, December). Advantages and disadvantages of subsurface drip irrigation. In International Meeting on Advances in Drip/Micro Irrigation, Puerto de La Cruz, Tenerife, Canary Islands (pp. 1-13).

Lenth, R.V., 2021. Emmeans: Estimated Marginal Means, Aka Least-squares Means. R Package Version 1.5.5-1.

Liu, Zhang, Feng, Tian, (2020). Toward a "green revolution" for soybean. Molecular plant, 13(5):688-697.

Maisiri, N., Senzanje, A., Rockstrom, J., & Twomlow, S. J. (2005). On farm evaluation of the effect of low cost drip irrigation on water and crop productivity compared to conventional surface irrigation system. *Physics and Chemistry of the Earth, parts A/B/C*, *30*(11-16), 783-791.

Mertz-Henning, L. M., Ferreira, L. C., Henning, F. A., Mandarino, J. M., Santos, E. D., Oliveira, M. C., … & Neumaier, N. (2017). Effect of water deficit-induced at vegetative and reproductive stages on protein and oil content in soybean grains. Agronomy, 8(1), 3.

Milly, Dunne, Vecchia, (2005). Global pattern of trends in streamflow and water availability in a changing climate. Nature, 438(7066):347-350.

Möller, M., & Weatherhead, E. K. (2007). Evaluating drip irrigation in commercial tea production in Tanzania. *Irrigation and Drainage Systems*, *21*, 17-34.

Narayanamoorthy, A. (1997). Economic viability of drip irrigation: An empirical analysis from Maharashtra. Indian Journal of Agricultural Economics, 52(4), 728-739.

Oki, Kanae, (2006). Global hydrological cycles and world water resources. science, 313(5790):1068-1072.

Pedersen, P., & Lauer, J. G. (2003). Soybean agronomic response to management systems in the upper Midwest. *Agronomy Journal*, *95*(5), 1146-1151.

R Core Team. (2021). R: A language and environment for statistical computing. R Foundation for Statistical Computing.

Ray, Gerber, MacDonald, West, (2015). Climate variation explains a third of global crop yield variability. Nature Communications, 6(1):5989.

Rotundo, Westgate, (2009). Meta-analysis of environmental effects on soybean seed composition. Field Crops Research, 110(2):147-156.

Shahrokhnia, M. A., & Zare, E. (2022). Technical and economic study of irrigation scheduling devices on

corn water productivity in a semi-arid region. Italian Journal of Agrometeorology, (1), 13-22.
Sobko, Stahl, Hahn, Zikeli, Claupein, Gruber, (2020). Environmental effects on soybean (*Glycine max* (L.) Merr) production in central and South Germany. Agronomy, 10(12):1847.
Todorović, S. Z., Ivanović, S. M., & Bogdanov, N. L. (2021). The influence of extreme weather events on farm economic performance–a case study from Serbia. Italian Journal of Agrometeorology, 2021(1), 51-62.
Tran, A. T. M., Eitzinger, J., & Manschadi, A. M. (2020). Response of maize yield under changing climate and production conditions in Vietnam. Italian Journal of Agrometeorology, (1), 73-84.
Wisser, D., Frolking, S., Douglas, E. M., Fekete, B. M., Vörösmarty, C. J., & Schumann, A. H. (2008). Global irrigation water demand: Variability and uncertainties arising from agricultural and climate data sets. Geophysical Research Letters, 35(24).

Italian Journal of Agrometeorology
Rivista Italiana di Agrometeorologia

Firenze University Press
www.fupress.com/ijam

OPEN ACCESS

Citation: Correa Matos do Amaral, M.A., Batista de Souza, J.M., Viana da Silva, L., de Oliveira Costa, J., de Freitas Sia, E., Ileno de Sousa, E. G., Araújo Sá, D.G., Tavares Correa, G.K., Ferreira Castro, K.C., & Guerreiro Martorano, L. (2023). Agronomic performance and energy potential of cassava varieties under Amazonian edaphoclimatic conditions. *Italian Journal of Agrometeorology* (2): 33-40. doi: 10.36253/ijam-2290

Received: August 22, 2023

Accepted: November 10, 2023

Published: January 20, 2024

Data Availability Statement: All relevant data are within the paper and its Supporting Information files.

Competing Interests: The Author(s) declare(s) no conflict of interest.

Agronomic performance and energy potential of cassava varieties under Amazonian edaphoclimatic conditions

Marcos Antonio Correa Matos do Amaral[1,*], João Marcos Batista de Souza[1], Leonardo Viana da Silva[1], Jéfferson de Oliveira Costa[2], Eliandra de Freitas Sia[3], Ellen Gabrielle Ileno de Sousa[3], Diogo Guilherme Araújo Sá[3], Greyce Kelly Tavares Correa[1], Kelly Christina Ferreira Castro[3], Lucieta Guerreiro Martorano[4]

[1] *Federal University of West Para/UFOPA, Juruti campus, 68170-000 Juruti, PA, Brazil*
[2] *Minas Gerais Agricultural Research Agency/EPAMIG, Experimental Field of Gorutuba, 39525-000 Nova Porteirinha, MG, Brazil*
[3] *Federal University of West Para/UFOPA, Institute of Biodiversity and Forests, 68040-255 Santarém, PA, Brazil*
[4] *Brazilian Agricultural Research Corporation/EMBRAPA, EMBRAPA Eastern Amazon, 68020-640 Santarém, PA, Brazil*
*Corresponding author. E-mail: marcos.amaral@ufopa.edu.br

Abstract. Cassava is a crop that stands out in the Amazon region of Brazil, due to its regional scope and substantial production at the national level. However, the average yield of cassava in Amazonian environments is still considered low. The introduction of new varieties and the development of appropriate techniques for the cultivation of cassava under the edaphoclimatic conditions of the Amazon can improve its yield in the region. The objective of this research was to evaluate the agronomic performance and energy potential of six cassava varieties (BRS Mari, BRS Poti, BRS Formosa, Manivão, Jurará and Coraci) cultivated under Amazonian edaphoclimatic conditions. The study was conducted in Juruti, PA, Brazil and a randomized block design was used, with six blocks and six treatments (varieties), totaling 36 experimental units. The agronomic performance was evaluated based on the emergence index (EI), survival index (SI), plant height (PH), stem diameter (SD), above-ground biomass (Yab), yield of storage roots (Ysr), and harvest index (HI). The energy potential was evaluated based on reducing sugars (RS) and total soluble sugars (TSS). All studied varieties presented satisfactory agronomic performances. The Jurará and Coraci varieties stood out in terms of EI and SI, with average values above 0.9. The Manivão variety showed the highest average values of PH and SD, 2.7 and 0.023 m, respectively, at the end of the evaluation period. The BRS Mari variety had the highest RS content among the studied varieties, while the BRS Formosa variety had the highest TSS, with average values of 2.91 and 2.66%, respectively. All varieties showed an HI above 50%, a Ysr amplitude between 15 and 26 $Mg \cdot ha^{-1}$, and a Yab between 8 and 21 $Mg \cdot ha^{-1}$, indicating good adaptation to Amazonian edaphoclimatic conditions.

Keywords: adaptability, Amazonian environments, bioenergy, *Manihot esculenta* Crantz, yield.

HIGHLIGHTS

1) The Jurará and Coraci varieties stood out in the emergence and survival indices.

2) The cassava varieties evaluated showed a harvest index >50%.

3) The BRS Mari variety had the highest reducing sugar content, while the BRS Formosa variety had the highest total soluble sugar content.

4) The BRS Mari variety had the highest storage root yield with an average of 26 $Mg{\cdot}ha^{-1}$.

5) The above-ground biomass yield ranged from 8 to 21 $Mg{\cdot}ha^{-1}$.

1. INTRODUCTION

Cassava (*Manihot esculenta* Crantz) is the main food source for more than 800 million people, making it the sixth most important crop globally after wheat, rice, maize, potatoes and barley. World production is estimated at around 315 million tons. Globally, about 63% of cassava is produced in Africa, 28% in Asia and 9% in the Americas. Brazil is the fourth largest producer of cassava in the world, with Nigeria in first place due to its own consumption, followed by Thailand and Indonesia, which export almost all production in the form of starch, pellets and various derivatives to Europe and Asia (FAOSTAT, 2023).

Cassava is used to produce a wide range of products, including starch, starch products, bioethanol and animal feed. The plant is considered one of the crops with the greatest potential to fill the world's food supply gap in the coming years. In addition, cassava can be grown with minimal labor on marginal lands with inconsistent rainfall under low intensity management. In Brazil, cassava performs well in low-fertility soils and in a variety of climates. It has become one of the most popular items in the Brazilian diet since the beginning of colonization. The main cassava product is flour, which can be used by all individuals in the population in various ways, from the simplest everyday dishes to the most sophisticated and refined national cuisine, playing a key role in building cultural identity. It is one of the staple items of the diet of virtually the entire Brazilian population, and arguably the most important food crop, especially for low-income communities (Alves-Pereira et al., 2011; Fiorda et al., 2013; Figueiredo et al., 2014; Somavilla et al., 2022).

The Amazon region that includes the Pará State stands out as one of the largest producers in the national ranking, and 96% of the cassava produced there comes from family farming, which is necessary to guarantee a subsistence living for the families involved in production. However, the average yield of the cassava crop in Amazonian environments is still considered low, less than 15 $Mg{\cdot}ha^{-1}$. Cassava is one crop that has a very high productive potential, which can reach up to 90 $Mg{\cdot}ha^{-1}$. The technological level of the local producers is still very low and relatively common practices of soil correction and fertilization are rarely followed. The genetic makeup of the cultivar used often does not reach the productive potential of the region, and the farmers engage in monoculture on a small scale (Silva et al., 2012; Rosa et al., 2014; Filgueiras and Homma, 2016; Brito et al., 2019; Lima et al., 2020).

Some of the factors that contribute to the low yield of the cassava crop are the use of genetic material with low productive potential, inadequate soil management, and lack of effective pest control, as well as prevention of disease and invasive plant takeover. One of the best ways to increase the yield is to choose improved varieties that are productive, resistant to pathogen attacks, and that allow for proper soil management. Therefore, knowing the cassava varieties with the best agronomic performance in a particular region contributes to a better crop yield (Kizito et al., 2007; Farias Neto et al., 2013; Streck et al., 2014; Adiele et al., 2021).

The introduction of new varieties and the development of appropriate techniques for the cultivation of cassava under the edaphoclimatic conditions of each mesoregion constitute the challenges that have to be overcome to improve productivity and quality. The goal is to change farming practices so cassava cultivation stops being just a subsistence crop and becomes a profitable business venture. Such a farm would be capable of supplying not only local demands, but also those of other regions, in addition to generating jobs in the labor market and enhancing the quality of life of the workers. Cassava varieties differ in productivity, both forage and roots, which will allow selection, according to the desired purpose. The regional evaluation of new varieties is necessary since, in the case of cassava, the interaction between the genotype and the environment is very pronounced. Genetic materials already known in other regions are used, which reduces the average time to obtain varieties that meet the specific needs of farmers, as well as cassava processing industries.

Thus, the objective of this research was to evaluate the agronomic performance and energy potential of six cassava varieties, BRS Mari, BRS Poti, BRS Formosa, Manivão, Jurará and Coraci, cultivated under Amazonian edaphoclimatic conditions.

2. MATERIAL AND METHODS

2.1. Location and characterization of the experimental area

The experiments were conducted in Juruti, PA, Brazil, in an agricultural production area located in Esperança community (coordinates 02°19'52"S, 55°58'40"W and 36 m altitude), from December 2021 to November de 2022. The climate in the region, according to the Köppen classification, is of the Am type a monsoon area, characterized by intense rain and very hot weather. The average annual temperature is 26.9 °C, with the highest monthly average temperatures in September and October. Rainfall occurs during all months of the year, but monthly precipitation is highest from December to May. The driest months are August and September, when evapotranspiration was greater than the average monthly rainfall recorded over the last 30 years (Fig. 1A).

Considering the normal climatological characteristics of the region, there is a water surplus from January until the second ten days of June. Thereafter, there is a water deficit until the third ten days of December (Fig. 1B). For a soil with an available water capacity (AWC) of 100 mm, it appears that the soil water storage (SWS) was maximal from the second ten-day period of January to the first ten-day period of June. From then on, the SWS decreased until the first ten days of December, when the normal storage level was restored (Fig. 1C).

The area has a relatively flat, well-drained topography. The soil in the area is of the deep dystrophic yellow latosol type, with a pH of 4.5 and organic matter around 2 dag·dm^{-3}. The chemical characteristics of the soil in the experimental area in the layers from 0 to 0.20 m and from 0.20 to 0.40 m can be seen in Table 1.

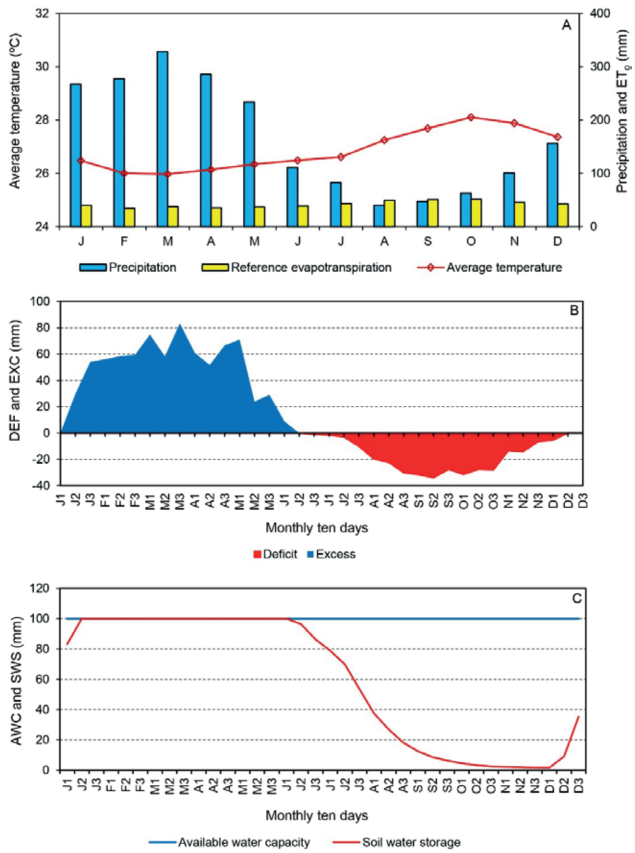

Figure 1. (A) Normal climatological readings for average temperature, precipitation and reference evapotranspiration (ET_o); (B) normal climatological water balance; and (C) normal soil water storage for the region of Juruti-PA, Brazil.

2.2. Implementing and conducting the experiments

An area of 576 m^2 was used for the experiments. The area was limed by the application and incorporation of dolomitic limestone 60 days before the beginning of the experiments. The experimental design adopted was randomized blocks, with six blocks and six treatments (varieties), totaling 36 experimental units. Each experimental unit consisted of 15 plants distributed in three rows with 1 m between rows and 0.8 m spacing between plants. For the agronomic performance evaluations of the varieties, the three central plants of the central row were used, excluding the plants at the ends. The six cassava varieties evaluated were BRS Poti, BRS Mari, BRS Formosa, Jurará, Manivão and Coraci. The genetic materials used in this

Table 1. Chemical analysis (macro- and micro-nutrients) of soil in the experimental area.

Layers	pH	M.O.	Ca	Mg	Al	H+Al	P	K+	B	Zn	Mn	Cu	Fe
meters	H_2O	dag·dm^{-3}		cmol$_c$·dm^{-3}						mg·dm^{-3}			
0 – 0.20	4.5	1.9	0.1	0.1	1.1	6.4	2.7	0.02	0.2	0.1	0.6	0.1	158
0.20 – 0.40	4.5	2.6	0.1	0.1	1.3	6.5	3.9	0.02	0.3	0.2	0.5	0.1	130

pH - hydrogen potential; M.O. - organic matter; P - phosphorus; K - potassium; Ca - calcium; Mg - magnesium; H+Al - hydrogen + aluminum; Cu - copper; Fe - iron; Zn - zinc; Mn - manganese; B - boron.

research come from the germplasm bank located in the municipality of Tracuateua, PA, Brazil, with the exception of the Coraci variety, which has been widely cultivated in the municipality of Juruti, PA, Brazil, for a long time.

The planting holes were made with a hoe, similar to the way used by local farmers. The cuttings for planting were made at a right angle with a machete, allowing the distribution of the roots in a more uniform way than a bevel cut. The cuttings were planted manually in the holes in a horizontal position, at a depth of approximately 0.10 m.

Before planting, 50 g of single superphosphate fertilizer (18% P_2O_5) was applied per hole. At 40 and 70 days after planting (DAP), the soil was top-dressed with 40 g of 20-0-20 fertilizer per hole. The management of pests, diseases and invasive plants was carried out in accordance with the agronomic recommendations for the cultivation of cassava in a planting system used in family farming.

2.3. Agronomic performance evaluations

Different methods of evaluating the agronomic performance of the cassava varieties studied were carried out. For the emergence index (EI), the number of plants that emerged in each plot at 30 DAP was counted, and then expressed as a ratio of the number of cutting planted, according to equation 1:

$$EI = \left(\frac{Pe}{Pst}\right) \quad (1)$$

where EI is the emergence index, Pe is the number of plants that emerged and Pst is the number of cuttings planted.

The survival index (SI) was evaluated by counting the number of plants that survived in each plot at the end of the evaluation period as a ratio of the number of cuttings planted, according to equation 2:

$$SI = \left(\frac{Ps}{Pst}\right) \quad (2)$$

where SI is the survival index, Ps is the number of plants that survived and Pst is the number of cuttings planted.

Plant height (PH) was measured monthly, with the first measurement performed at 30 DAP. PH data were obtained with the aid of a ruler and a measuring tape attached to a piece of wood, adopting the distance between the plant collar and the apical bud of the main branch as the criterion. For the stem diameter (SD), the measurements started at 90 DAP, because some plants did not reach a height of 0.10 m. Measurements were performed using a digital caliper.

The above-ground biomass was obtained by weighing all the material collected from the neck of the plant to the highest point. Storage root biomass was determined by weighing the roots of usable plants in a plot. The weighing procedure was carried out in the experimental area with the aid of a digital electronic scale and a portable power generator. Conversions of above-ground and storage root biomass to yield values were performed using Equations 3 and 4.

$$Yab = \left(\frac{By\ Pn}{1000}\right) \quad (3)$$

where Yab is the aerial biomass yield in $Mg{\cdot}ha^{-1}$, By is the above-ground biomass in kg of the useful plants in the plot and Pn is the number of plants per hectare for a spacing of 1.0 x 0.8 m.

$$Ysr = \left(\frac{Bsr\ Pn}{1000}\right) \quad (4)$$

where Ysr is the yield of storage roots in $Mg{\cdot}ha^{-1}$, Bsr is the storage root biomass of useful plants in the plot in kg and Pn is the number of plants per hectare considering the spacing of 1.0 x 0.8 m.

The harvest index (HI) was calculated as the ratio of the storage root biomass to total plant biomass (storage root biomass + above-ground biomass) using equation 5:

$$HI = \left(\frac{Bsr}{Bt}\right) \quad (5)$$

where HI is the harvest index, Bsr is the storage root biomass of the plot's useful plants in kg, and Bt is the total plant biomass in kg.

The percentage of reducing sugars (RS) was determined by the dinitrosalicylic acid (DNS) method (Miller, 1959) and the percentage of total soluble sugars (TSS) by the anthrone method (Morris, 1948; Yemm and Willis, 1954). Absorbance values were obtained using a UV-Vis spectrophotometer.

2.4. Data analysis

The F test was used to verify significant differences between treatments and the Tukey test at 5% probability to compare means. Analysis of variance and comparison of means were performed using the Sisvar software, version 5.8.

3. RESULTS AND DISCUSSION

3.1. Predominant environmental conditions

The predominant environmental conditions in the research period (December 2021 to November 2022) are shown in Figure 2. The monthly averages of maximum and minimum temperature did not show significant vari-

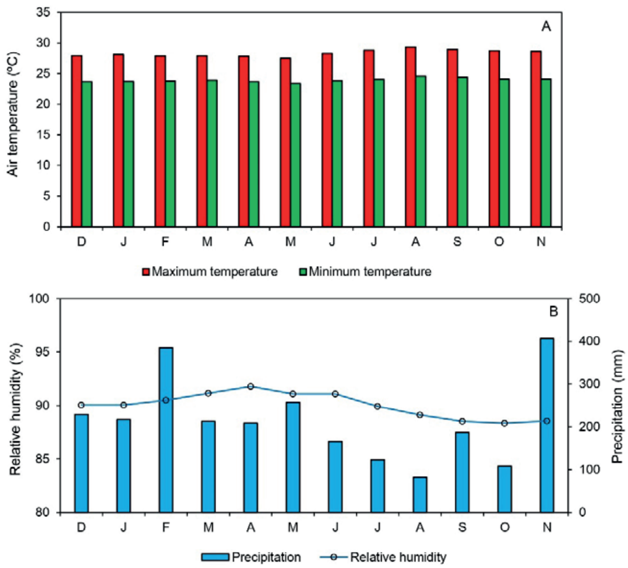

Figure 2. Monthly averages of meteorological variables (maximum and minimum temperature, relative humidity) and total monthly precipitation obtained in the region of Juruti-PA, Brazil, from December 2021 to November 2022.

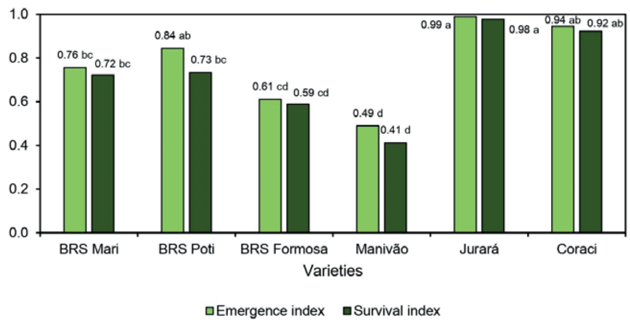

Figure 3. Emergence and survival indices of cassava varieties cultivated in the Juruti-PA region, Brazil. Different letters indicate significant differences between experimental means at the 5% probability level by Tukey's test.

ations within the analysis period. The monthly maximum temperature was around 28 °C and the monthly minimum temperature was around 24 °C. The small variation in monthly average values of maximum and minimum temperature throughout the year is common in equatorial or low-latitude regions. The geographic location of the region of Juruti-PA, Brazil implies a minimization of the effects of the inclination of the Earth's axis in relation to the sun, characterizing a climate pattern in which there are no significant environmental variations between the seasons.

Monthly precipitation was higher in February and November 2022, with totals of 385 and 406 mm, respectively. The months with the lowest values of monthly precipitation totals were August and October 2022, with 83 and 108 mm, respectively. Accumulated precipitation during the research period was 2582 mm, which was higher than the normal annual average for the region. The monthly averages of relative air humidity were around 90% throughout the research period. The registered environmental conditions were characteristic of the predominant climate in the Amazon region, which is classified as humid equatorial.

3.2 Emergence and survival indices, plant height and main stem diameter

The cassava varieties that showed the lowest EI were Manivão and BRS Formosa with values of 0.49 and 0.61, respectively (Fig. 3). The other studied varieties had EIs >0.75, with the Jurará variety showing an EI of 0.99. As for the SI values, the lowest performance was found for the Manivão and BRS Formosa varieties, with values of 0.41 and 0.59, respectively. The other varieties studied had SIs >0.70, again highlighting the Jurará variety, which had a SI of 0.98.

PH values varied according to the variety (Table 2). In the first month of the evaluation period, BRS Poti had the highest PH value at 0.12 m. At the end of the evaluation period, the Coraci, BRS Mari and Manivão varieties showed the highest PH values at 2.15, 2.40 and 2.70 m, respectively. The BRS Formosa, BRS Poti and Jurará varieties showed PH values < 2 m at the end of the evaluation period. PH is an important variable for deter-

Table 2. Plant heights (meters) of cassava varieties throughout the growing season.

Date	Variety					
	BRS Mari	BRS Poti	BRS Formosa	Manivão	Jurará	Coraci
Jan 19	0.07 b	0.12 a	0.08 b	0.07 b	0.08 b	0.08 b
Feb 19	0.19 a	0.21 a	0.18 a	0.19 a	0.19 a	0.20 a
Mar 27	0.52 a	0.52 a	0.50 a	0.65 a	0.61 a	0.56 a
Apr 24	0.79 a	0.74 a	0.72 a	0.96 a	0.82 a	0.83 a
May 21	1.03 a	0.94 a	0.93 a	1.29 a	1.03 a	1.08 a
Jun 19	1.22 ab	1.09 b	1.12 b	1.64 a	1.18 ab	1.33 ab
Jul 24	1.54 ab	1.25 b	1.23 b	1.94 a	1.40 b	1.58 ab
Aug 20	1.78 ab	1.41 b	1.37 b	2.14 a	1.57 b	1.78 ab
Sep 24	2.04 ab	1.59 bc	1.53 c	2.40 a	1.75 bc	1.92 abc
Oct 22	2.24 ab	1.75 bc	1.60 c	2.56 a	1.85 bc	2.06 abc
Nov 19	2.40 ab	1.91 bc	1.67 c	2.70 a	1.94 bc	2.15 bc

Different letters on the same line mean significant differences between varieties using Tukey's test ($p < 0.05$).

Table 3. Stem diameters (meters) of cassava varieties throughout the growing season.

Date	Variety					
	BRS Mari	BRS Poti	BRS Formosa	Manivão	Jurará	Coraci
Feb 19	0.002 a	0.003 a	0.003 a	0.003 a	0.004 a	0.003 a
Mar 27	0.007 a	0.008 a	0.008 a	0.010 a	0.010 a	0.009 a
Apr 24	0.010 a	0.010 a	0.011 a	0.013 a	0.012 a	0.011 a
May 21	0.012 a	0.011 a	0.013 a	0.015 a	0.013 a	0.013 a
Jun 19	0.014 a	0.012 a	0.014 a	0.016 a	0.014 a	0.014 a
Jul 24	0.015 ab	0.012 b	0.015 ab	0.018 a	0.014 ab	0.015 ab
Aug 20	0.016 ab	0.013 b	0.015 ab	0.019 a	0.015 ab	0.016 ab
Sep 24	0.018 ab	0.013 b	0.017 ab	0.021 a	0.016 ab	0.017 ab
Oct 22	0.020 a	0.014 b	0.017 ab	0.022 a	0.017 ab	0.018 ab
Nov 19	0.021 ab	0.015 c	0.018 abc	0.023 a	0.017 bc	0.018 abc

Different letters on the same line mean significant differences between varieties using Tukey's test ($p < 0.05$).

mining spacing, for choosing varieties that can be used in a consortium and for weed management (Rós et al., 2011). Thus, the Coraci, BRS Mari and Manivão varieties showed excellent soil coverage, which reduced takeovers by invasive plants. In addition, these varieties were promising as suppliers of cuttings for mechanized planting, since the larger the branch, the greater the operational yield of the planting machine (Vidigal Filho et al., 2000; Borges et al., 2002; Azevedo et al., 2006). The BRS Formosa, BRS Poti and Jurará varieties showed a low yield of stem cuttings, in addition to hampering cultivation practices such as weeding and fertilization.

Stem diameter values did not show significant differences between the cassava varieties studied until the sixth month of evaluation (Table 3). After the sixth month, significant differences were observed between the cassava varieties studied. At the end of the evaluation period, the BRS Mari and Manivão varieties had the highest SD values at 0.021 and 0.023 m, respectively. At the end of the evaluation period, the BRS Poti, BRS Formosa, Jurará and Coraci varieties had SD values that were <0.02 m.

3.3. Yield and energy potential of cassava varieties

The cassava varieties studied showed significant differences in above-ground biomass yield (Yab). The Manivão variety had the highest average Yab at 21 Mg·ha^{-1}, while BRS Poti showed the lowest average Yab, 8 Mg·ha^{-1}. The BRS Mari, BRS Formosa, Jurará and Coraci varieties showed average Yab values of 15, 14, 10 and 15 Mg·ha^{-1}, respectively (Fig. 4). The Yab performance of the Manivão variety revealed its potential for use in animal feed and to minimize costs for the acquisition and transport of propagation material.

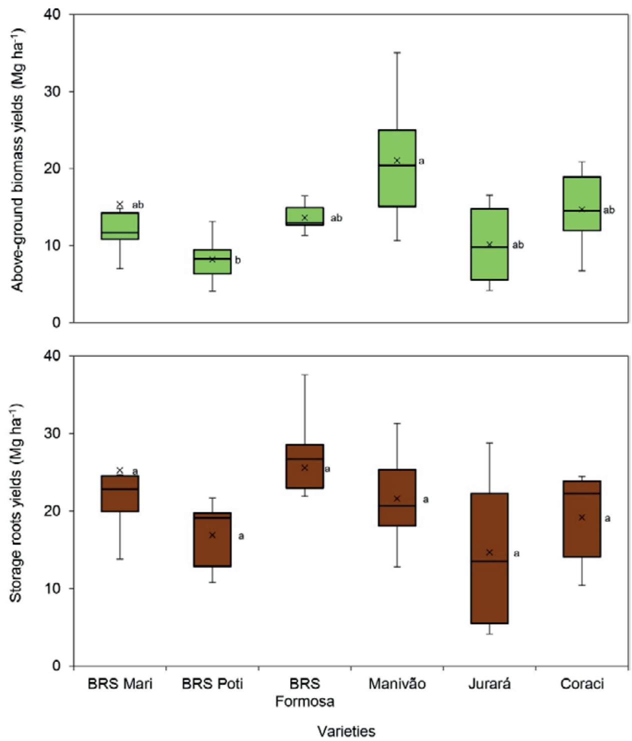

Figure 4. Above-ground biomass and storage root yields of cassava varieties cultivated in the Juruti-PA region, Brazil. Different letters indicate significant differences between experimental means at the 5% probability level by Tukey's test.

With regard to the storage root yield (Ysr), the cassava varieties studied did not show significant differences. The average values of Ysr for the BRS Mari, BRS Poti, BRS Formosa, Manivão, Jurará and Coraci varieties were 26, 17, 26, 22, 15 and 19 Mg·ha^{-1}, respectively. The Ysr of these varieties was greater than or equal to the average yield recorded in Brazil in 2021, which was 15 Mg·ha^{-1} (FAOSTAT, 2023). The results showed a range of Ysr of 15 to 26 Mg·ha^{-1}for the genetic materials evaluated, showing that the replacement of varieties in use by farmers could increase the cassava crop yield in the Amazon region.

Considering the harvest index, the cassava varieties studied showed significant differences between them (Fig. 5). The varieties that presented the highest average HI values were BRS Mari (0.64), BRS Poti (0.68) and BRS Formosa (0.64). The varieties that presented the lowest average HI values were Manivão (0.52), Jurará (0.56) and Coraci (0.57). The HI reflects the efficiency of the varieties in root production, identifying those with the greatest capacity to

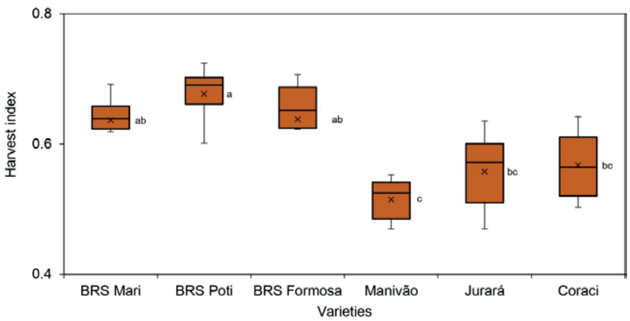

Figure 5. Harvest index of cassava varieties cultivated in the Juruti-PA region, Brazil. Different letters indicate significant differences between experimental means at the 5% probability level by Tukey's test.

direct the carbohydrates produced in the leaves to the production of roots (Silva et al., 2021). According to Peixoto et al. (2005), the harvest index is considered satisfactory when it exceeds 50%. Thus, all varieties evaluated in this research presented satisfactory values.

The BRS Mari variety had the highest RS value (2.91%) followed by the Coraci variety (2.41%). The BRS Formosa (2.34%), Jurará (2.33%) and Manivão (2.31%) varieties were statistically equal (Fig. 6). Bezerra et al. (2002) stated that the sugar content in the cassava roots could be influenced by the harvest time and the storage period, but mainly by the variety. The BRS Poti variety had the lowest RS value (1.55%). In terms of TSS, the BRS Formosa variety had the highest values (2.66%), followed by th BRS Mari variety (2.56%), BRS Poti (2.41%), Jurará (2.33%), Coraci (2.31%) and Manivão (1.91%).

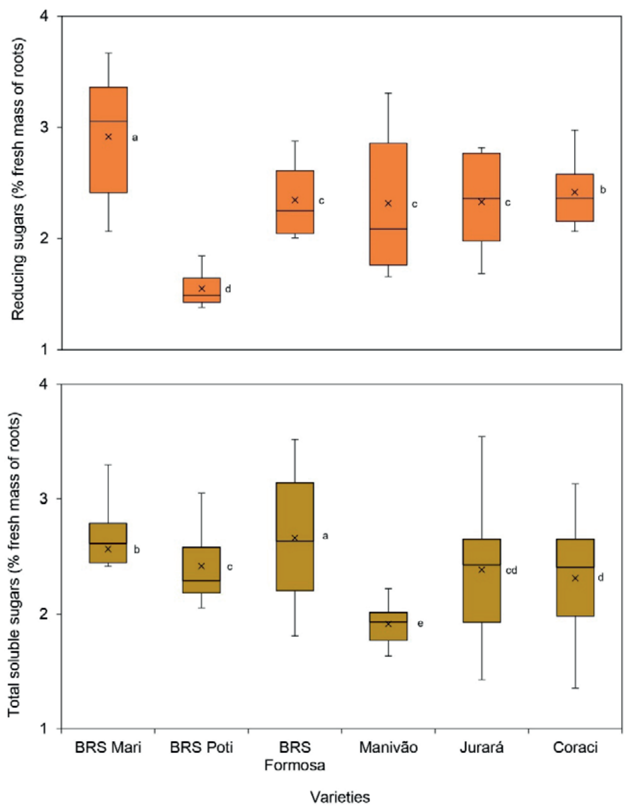

Figure 6. Reducing sugars and total soluble sugars of cassava varieties cultivated in the Juruti-PA region, Brazil. Different letters indicate significant differences between experimental means at the 5% probability level by Tukey's test.

4. CONCLUSIONS

The cassava varieties BRS Mari, BRS Poti, BRS Formosa, Manivão, Jurará and Coraci showed a satisfactory agronomic performance when cultivated in Amazonian edaphoclimatic conditions. The Jurará and Coraci varieties stood out in terms of emergence and survival indices, with average values above 0.9 for these two variables. The Manivão variety had the highest average values for plant height and stem diameter at the end of the evaluation period, 2.7 and 0.023 m, respectively.

The BRS Mari variety had the highest reducing sugar content among the studied varieties, while the BRS Formosa variety had the highest total soluble sugar content, with average values of 2.91 and 2.66%, respectively. All cassava varieties evaluated had a HI >50%, a range of storage root yields between 15 and 26 $Mg{\cdot}ha^{-1}$and aboveground biomass yields between 8 and 21 $Mg{\cdot}ha^{-1}$, indicating good potential for the dual purpose of shoots and roots production, with good adaptation to the Amazonian edaphoclimatic conditions, thus, these varieties represent good options for rural producers in this region.

ACKNOWLEDGEMENTS

We wish to thank to the Secretary of Agricultural Development and Fisheries of Para State (SEDAP) and the Federal University of West Para (UFOPA) for financial support.

REFERENCES

Adiele, J.G., Schut, A.G.T., Van Den Beuken, R.P.M., Ezui, K.S., Pypers, P., Ano, A.O., Giller, K.E., 2021. A recalibrated and tested LINTUL-Cassava simulation model provides insight into the high yield potential of cassava under rainfed conditions. Eur. J. Agron. 124, 126242. https://doi.org/10.1016/j.eja.2021.126242

Alves-Pereira, A., Peroni, N., Abreu, A.G., Gribel, R., Clement, C.R., 2011. Genetic structure of traditional varieties of bitter manioc in three soils in Central Amazonia. Genetica 139, 1259-1271. https://doi.org/10.1007/s10709-011-9627-4

Azevedo, E.B., Nörnberg, J.L., Kessler, J.D., Brüning, G., David, D.B., Falkenberg, J.R., Chielle, Z.G., 2006. Aerial part silage of cassava cultivars. Cienc. Rural 36, 1902-1908. https://doi.org/10.1590/S0103-84782006000600037

Bezerra, V.S., Pereira, R.G.F.A., Carvalho, V.D., Vilela, E.R. 2002. Minimally processed cassava roots: effect of blanching on quality and conservation. Cienc. Agrotec. 26, 564-575.

Borges, M.D.F., Fukuda, W.M.G., Rossetti, A.G., 2002. Evaluation of cassava varieties for human consumption. Pesq. Agropec. Bras. 37, 1559-1565. https://doi.org/10.1590/S0100-204X2002001100006

Brito, R.S., Brito, R.S., Moreira, J.G.V., Oliveira, A.V., 2019. Productivity of cassava in the region of Juruá valley, southerstern amazon. Sci. Nat., 1, 1-9.

FAOSTAT, Food and Agriculture Organization of the United Nations, 2023. Data-Dataset-Crops-National production. Available in: <www.fao.org>. Accessed on: May 1, 2023.

Farias Neto, J.T.D., Moura, E.F., Resende, M.D.V.D., Celestino Filho, P., Augusto, S.G., 2013. Genetic parameters and simultaneous selection for root yield, adaptability and stability of cassava genotypes. Pesq. Agropec. Bras. 48, 1562-1568. https://doi.org/10.1590/S0100-204X2013001200005

Figueiredo, P.G., Bicudo, S.J., Moraes-Dallaqua, M.A., Tanamati, F.Y., Aguiar, E.B., 2014. Yield components and morphology of cassava roots under different tillage. Bragantia 73, 357-364. https://doi.org/10.1590/1678-4499.0150

Filgueiras, G.C., Homma, A.K.O., 2016. Cassava crop: socioeconomic aspects, genetical enhancement, cultivation systems, management of pests and diseases and agroindustry. EMBRAPA: Brasília-DF. 36p.

Fiorda, F.A., Soares Júnior, M.S., Silva, F.A.D., Souto, L.R.F., Grossmann, M.V.E., 2013. Cassava bagasse flour: byproduct utilization and comparison with cassava starch. Pesqui. Agropecu. Trop. 43, 408-416. https://doi.org/10.1590/S1983-40632013000400005

Kizito, E.B., Chiwona-Karltun, L., Egwang, T., Fregene, M., Westerbergh, A., 2007. Genetic diversity and variety composition of cassava on small-scale farms in Uganda: an interdisciplinary study using genetic markers and farmer interviews. Genetica, 130, 301-318. https://doi.org/10.1007/s10709-006-9107-4

Lima, R.F., Silva, A.O., Dias, P.H.B., Silva, B.C., Guimarães, W.R., Vasconcelos, E.S., Silva, D.A.S., 2020. The production of cassava (*Manihot esculenta* Crantz) in family agriculture in the Northeast Parasian region: a study from the community of Jacarequara, Capanema, Pará. Braz. J. Animal Environ. Res. 3, 1284-1296. https://doi.org/10.34188/bjaerv3n3-047

Miller, G.L. 1959. Use of dinitrosalicylic acid reagent for determination of reducing sugar. Anal. Chem. 31, 426-428. https://doi.org/10.1021/ac60147a030

Morris, D.L. 1948. Quantitative determination of carbohydrates with Dreywood's anthrone reagent. Science 107, 254-255. https://doi.org/10.1126/science.107.2775.254

Peixoto, J.R., Bernardes, S.R., Santos, C.M., Bonnas, D.S., Fialho, J.F., Oliveira, J.A., 2005. Agronomic performance of sweet cassava varieties in Uberlândia, MG. Rev. Bras. Mandioca. 18, 19-24.

Rosa, J.M.O., Oliveira, S.A.D., Jordão, A.L., Siviero, A., Oliveira, C.M.G.D., 2014. Plant parasitic nematodes on cassava cultivated in the Brazilian Amazon. Acta Amaz. 44, 271-275. https://doi.org/10.1590/S0044-59672014000200013

Rós, A.B., Hirata, A.C.S., Araújo, H.S.D., Narita, N., 2011. Cassava cultivars growth, phenology and yield. Pesqui. Agropecu. Trop. 41, 552-558. https://doi.org/10.5216/pat.v41i4.11075

Silva, D.V., Santos, J.B., Ferreira, E.A., Silva, A.A., França, A.C., Sediyama, T., 2012. Weed management in cassava. Planta daninha 30, 901-910. https://doi.org/10.1590/S0100-83582012000400025

Silva, E.H., Colares, D.S., Ferreira, V.E., Silva Junior, A.J.S., Campos, G.A., 2021. Agronomic performance of cassava varieties in irrigated system. Rev. Agr. Environ. Sci. 7, 1-10. https://doi.org/10.36725/agries.v7i1.5250

Somavilla, A., Massem, D.S., Fronza, R.T.L., Medeiros, V.V., Michelon, C.J., Junges, E., Deon, B.C., 2022. Cassava yield under organic fertilization in different cultivation sites. Braz. J. Dev. 8, 11644-11654

Streck, N.A., Pinheiro, D.G., Junior Zanon, A., Gabriel, L.F., Rocha, T.S.M., Souza, A.T.D., Silva, M.R.D., 2014. Effect of plant spacing on growth, development and yield of cassava in a subtropical environment. Bragantia 73, 407-415. https://doi.org/10.1590/1678-4499.0159

Vidigal Filho, P.S., Pequeno, M.G., Scapim, C.A., Vidigal, M.C.G., Maia, R.R., Sagrilo, E., Simon, G.A., Lima, R.S., 2000. Evaluation of cassava cultivars in northwest region of Paraná State, Brazil. Bragantia 59, 69-75. https://doi.org/10.1590/S0006-87052000000100011

Yemm, E.W., Willis, A. 1954. The estimation of carbohydrates in plant extracts by anthrone. Biochem. J. 57, 508. https://doi.org/10.1042/bj0570508

Italian Journal of Agrometeorology
Rivista Italiana di Agrometeorologia

Firenze University Press
www.fupress.com/ijam

Citation: Dessale, S., Fenta, T., Wondatir, S., & Mollaw, G. (2023). Effect of different soil moisture regimes on yield and water use efficiency of groundnut at Kobo irrigation scheme, Kobo Ethiopia. *Italian Journal of Agrometeorology* (2): 41-48. doi: 10.36253/ijam-2201

Received: June 24, 2023

Accepted: November 14, 2023

Published: January 20, 2024

Data Availability Statement: All relevant data are within the paper and its Supporting Information files.

Competing Interests: The Author(s) declare(s) no conflict of interest.

ORCID:

SD: 0000-0001-6654-6477

Contributions

Sisay Dessale. Performed the experiments, collect, analyzed and interpret the data, and wrote the manuscript. Tigabu Fenta performs data collection and frequent follow-up at the field level. Solomon Wondatir and Gebeyaw Mollaw edited the paper throughout the manuscript work.

Effect of different soil moisture regimes on yield and water use efficiency of groundnut at Kobo irrigation scheme, Kobo Ethiopia

Sisay Dessale*, Tigabu Fenta†, Solomon Wondatir†, Gebeyaw Mollaw†

Sirinka Agricultural Research Center, P.O.Box 74, Sirinka, Ethiopia
*Corresponding author. E-mail: sisay1943@gmail.com

Abstract. In the arid and semi-arid part of Eastern Amhara, water is the most important yield-limiting factor for agricultural production. Application of the right amount of irrigation water at a right time helps to optimize water loss and increases crop yield. Therefore, a field experiment was conducted at Kobo irrigation scheme to determine the optimal crop water requirement and irrigation frequency for yield and water use efficiency of groundnut. The CROPWAT model could generate the 100% irrigation scheduling as 40 mm irrigation water with 8 days. Field base validation and ground truthing is vital. Therefore, the treatments were formulated by the factorial combinations of the three crop water levels as 75% ETc (30 mm), 100% ETc (40 mm), 125% ETc (50 mm) with three irrigation intervals (6 days, 8 days and 10 days). The treatments arranged in randomized complete block design with three replications. The statistical analysis was carried out using Genstat 15.0 software and the mean comparison was done using least significant difference (LSD) test. The analysis revealed that the crop water use efficiency was significantly ($p<0.05$) affected by the main effects of crop water levels, irrigation interval and by their interaction, whereas the grain yield does not show a significant ($p>0.05$) response. As the water levels declined and the irrigation intervals varied, the grain yield tends a fairly constant trend. However, based on the commerciality of the crop, application 75% ETc (30 mm) with 8 days irrigation interval gave numerically maximum grain yield of 3466.9 kg/ha and it has nearly more than 200 kg relative yield advantage over most treatments. The highest water use efficiency (0.9 kg/m^3) was recorded from the combination 75% ETc (30 mm) with 10 days; while it was statistically at par with 75% ETc with 8 days interval (0.8 kg/m^3) applied treatment. From the result, it could be concluded that the maximum yield and maximum water productivity were simultaneously achieved by combined application of 75% ETc with 8 days interval and saves 4600 m^3 water to irrigate an additional 1.2 ha compared with 125% (50 mm) ETc with 6 days interval applied treatment.

Keywords: crop water level, crop water use efficiency, grain yield, irrigation interval.

1. INTRODUCTION

Groundnut (*Arachis hypogaea* L.) is an important monoecious annual legume to make oils and animal feed all over the world (Upadhyaya et al., 2006). It is the main source of food in various forms and used as a component of crop rotation in many countries (Waktole, 2018). As a legume, it improves soil fertility by fixing nitrogen and thereby increasing the productivity of the semi-arid cereal cropping systems (Sanogo et al., 2017). Groundnut is also a high-value crop; that can be marketed with little processing and it is the second-largest source of vegetable oils next to soybeans (Okello et al., 2010).

Groundnuts are also a significant source of cash income in developing countries that contribute significantly to food security and alleviate poverty (Baiphethi and Jacobs, 2009). The lowlands and rift valley areas of Ethiopia have considerable potential for increased oil crop production including groundnut. The national average area coverage and seed yield of groundnut were 64,649.3 hectares and 1.6 t ha-1 respectively (Kebede et al., 2017). Similarly, in Kobo valley pulse crops like groundnut (*eta*) variety were highly adaptable and gave a better production.

However, food production in many parts of Ethiopia is challenged by the inadequate and unreliable supply of water. The fact that the country's water use in general and agricultural water, in particular, is inefficient due to increases the water demand in all water use sectors (Ayana et al., 2015). "In arid and semi-arid parts of Eastern Amhara, including Kobo Girana valley, water is the most important yield-limiting factor for agricultural production as the rainfall is erratic and non-uniform in time and space". This leads to a common phenomenon of recurrent drought and crop failure (Getahun, 2014; Sisay, 2021). The Raya Kobo valley has good potential in terms of ground and surface water, fertile land and livestock production. Due to the lack of appropriate on-farm water management, many productive lands are posed by soil salinity and alkalinity. The poor practices of irrigation management discourage efforts in the irrigation development sector (Getahun, 2014; Sisay, 2021). For the long-term sustainability of an irrigation system, improvements of the current on-farm water management seem to be more necessary than any other practice (Sarwar et al., 2001).

The two main reasons for studying irrigation scheduling are to save water and protect the environment. However, for farmers and irrigation managers, the usual driving pressure for adopting irrigation scheduling is economic – scheduling is used because it makes or saves money (Henggeler, 2004). The Food and Agriculture Organization (FAO) created the CROPWAT software application to aid irrigation engineers and agronomists in doing common calculations for water irrigation studies, as well as in the management and design of irrigation systems (Allen et al., 1998). To provide better irrigation water management today, anticipated crop water use and irrigation timing should be validated on the field (USDA, 1993). Application of the right amount of irrigation water at a right time helps to optimize water loss and increases crop yield. Hence, the present study was focused to determine optimal crop water depth and frequency on yield and water use efficiency of groundnut at the kobo valley irrigation scheme.

2. MATERIALS AND METHODS

2.1. Description of the study area

The field experiment was conducted at Kobo experimental site from January 25 to June 9 and January 18 to June 2 for 2016 and 2017 respectively. The site is found at about 50 km from Woldia town to the North-East direction and 570 km in the North of Addis Ababa. Geographically, it is located between12.03°-12.08°N latitudes and 39.28°-39.42°E longitudes with an altitude of 1470 m.a.s.l. (Figure 1).

2.2. Climate

The average annual rainfall, mean monthly minimum and maximum temperatures are 644.08 mm, 8.49 °C, and 36.58 °C respectively (Figure 2). "As indicated in Figure 2, ten years (2006-2015) of long-term climatic data (mean rainfall, maximum and minimum temperature) of the study site was collected from Kobo metrological station".

2.3. Irrigation scheduling

ET_0 values were calculated using the FAO Penman-Monteith method with the aid of CROPWAT 8.0 model. The climatic data's (relative humidity, wind speed, sunshine hour, solar radiation, maximum and minimum temperature) were considered by the model for ET_0 simulation. The actual evapotranspiration (ET_c) was calculated as:

$$ET_c = ET_0 * kc \quad (1)$$

where ET_c = actual evapotranspiration;
ET_0 = Reference evapotranspiration;
Kc = Crop factor.

In addition to the climatic parameters, the crop (Kc, length of total growing season, length of each growth

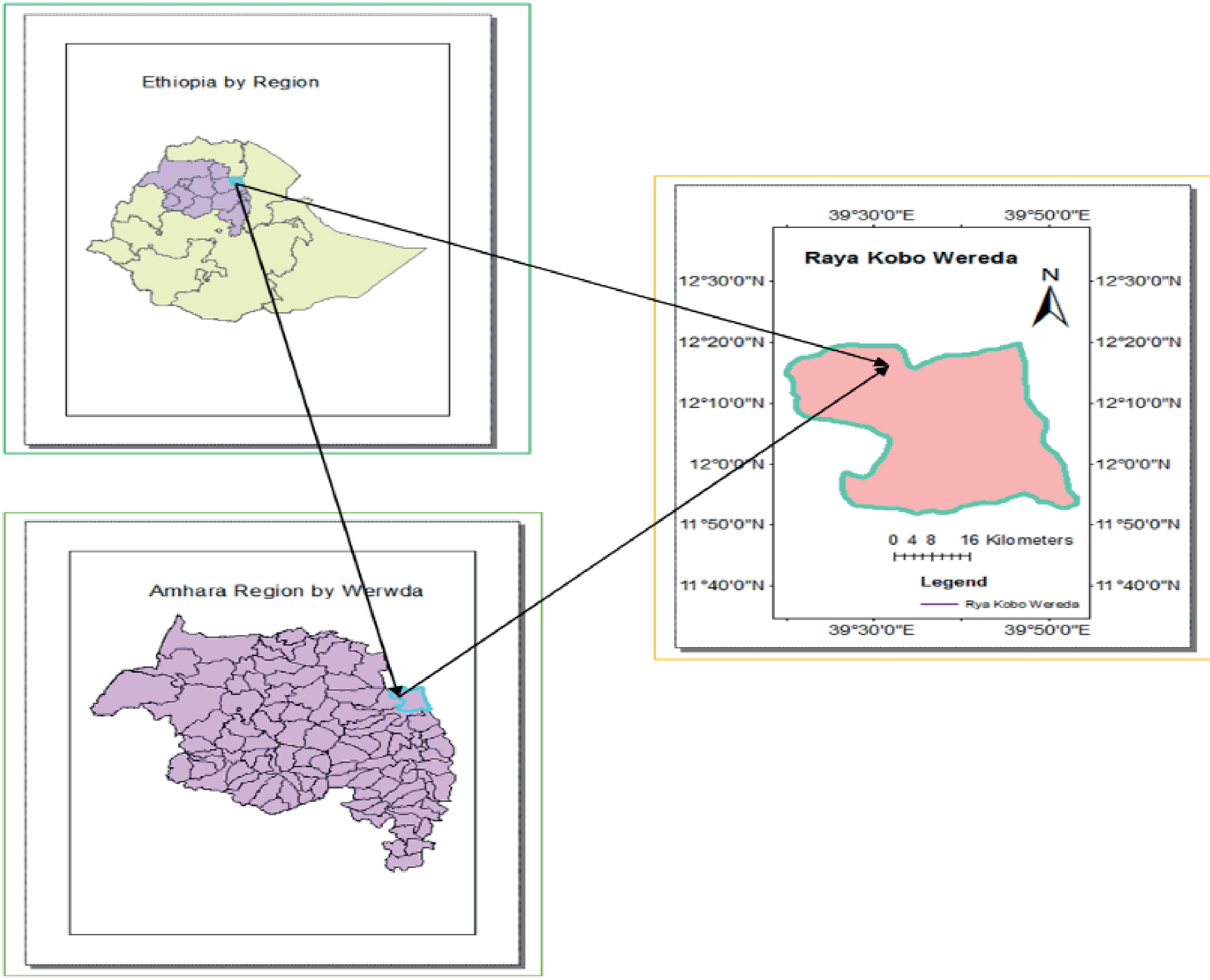

Figure 1. Map of the study area.

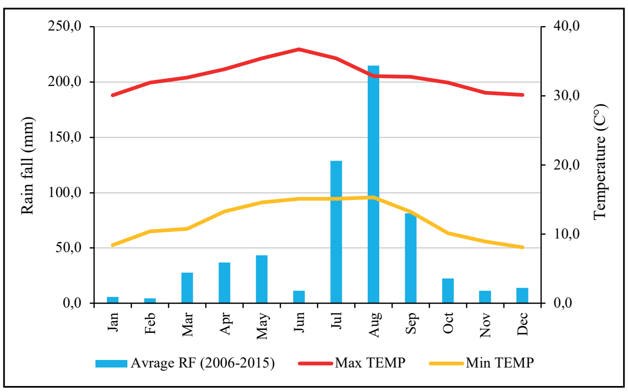

Figure 2. Mean monthly rainfall (mm), maximum and minimum temperature of the study area (2006-2015).

stage, critical depletion level (p) and maximum effective rooting depth) and soil data's (field capacity, permanent wilting point, and soil type) were needed by the model to compute the 100% irrigation scheduling of groundnut. The FAO Penman-Monteith modeling used as a preliminary study for irrigation planning and design purposes. The modeling approach has always certain deviations for under or overestimates of scheduling. During irrigation scheduling, the researcher should always pay attention and consider the simulated ET_c and irrigation interval (100%) as the initial starting point. Field evaluations and ground-truthing should be utilize to fine-tune the estimations used in irrigation system planning (USDA, 1993).

The irrigation requirement at each event was computed by monitoring daily actual rainfall data throughout the experimental season (Kobo meteorological station 2016 and 2017). It estimated as:

Table 1. Crop parameters as an input for CROPWAT model (Allen et al., 1998).

Growth stage	Initial	Development	Mid	Late	Total
Stage lengths (days)	35	35	35	35	140
Crop coefficient (Kc)	0.50	>>	1.05	0.75	
Rooting depth (m)	0.2	>>	0.5	0.3	
Depletion levels (P)	0.50	0.50	0.50	0.50	

$$IR = ET_c - P_{eff} \quad (2)$$

where IR = Net irrigation requirement (mm),
ET_c = Crop water requirement (mm) and
P_{eff} = Effective rainfall (mm).

Effective rainfall is a part of rainfall that entered into the soil and is made available for crop production. The effective rainfall throughout the growing season was calculated as (Allen et al., 1998):

$$P_{eff} = 0.6*P - 10/3 \quad \text{If } P < \frac{70}{3} \quad (3)$$

$$P_{eff} = 0.8*P - \frac{24}{3} \quad \text{If } P > \frac{70}{3} \quad (4)$$

where, P = precipitation (mm/month)
P_{eff} = monthly decades of effective rainfall (mm).

2.4. Experimental setup

The full irrigation scheduling (100%) which was simulated by the Penman-Monteith equation mostly varied with the approximation of 20% probability level (Rhoades et al., 1992; Allen et al., 1998). To validate the model output the three water levels of 75% (30 mm), 100% (40 mm) and 125% (50 mm) of the ETc with 75% (6 days), 100% (8 days), and 125% (10 days) of the optimal irrigation interval were tested on the field. Totally nine treatments were examined in a factorial randomized complete block design with three replications. The plot size was 3 m * 2.4 m = 7.2 m^2, and the distance between blocks and plots were 2 m and 1 m, respectively. The spacing between rows and plants were 30 and 10 cm respectively. Totally 240 plants were found on each experimental (7.2 m^2). Two days prior to sowing an equal amount of irrigation water was applied up to field capacity (mm) for one irrigation event to initiate seed germination. The irrigation scheduling experimental treatments were started 6 days after sowing. The amount of irrigation water was applied using a partial flume flow measuring device. The treatment combinations were constructed as in Table 2.

Table 2. Treatment combinations.

Factor 1 (Crop water levels in mm)	Factor 2 (Irrigation intervals in days)		
75% ETc (30 mm depth)	6	8	10
100% ETc (40 mm depth)	6	8	10
125% ETc (50 mm depth)	6	8	10

Table 3. Volume of used by the crop.

Treatments	Volume of water used (m^3/ha)	
	2016	2017
30 mm-6	5100	5100
40 mm-6	6800	6800
50 mm-6	8500	8500
30 mm-8	**3900**	**3900**
40 mm-8	5200	5200
50 mm-8	6500	6500
30 mm-10	**3000**	**3000**
40 mm-10	4000	4000
50 mm-10	5000	5000

2.5. Volume of water used

The total amount of water used by the individual treatments were recorded (Table 3).

2.6. Data collection and analysis

Agronomic parameters like plant height at maturity, number of pod per plant, number of seed per pod and grain yield were recorded from each net plot and changed to hectare base to make it ready for statistical analysis. However, water use efficiency is a derived parameter calculated as (Sinclair, 1984):

$$WUE = \frac{\text{Grain yield (kg)}}{\text{Amount of water used by the crop (cubic meter)}} \quad (5)$$

where, WUE= water use efficiency (kgm^{-3})

2.7. Statistical analysis

The Grain yield, plant height, and number of seed per plant and stand count were analaysed using Genstat 15.0 software following the statistical procedure described by Gomez and Gomez (1984). The mean separation was carried out using least significant difference (LSD) test.

3. RESULTS AND DISCUSSION

3.1. Soil properties of the experimental site

Based on the soil analytical result the textural classes of the three soil layers (0-30 cm, 30-60 cm and 60-90 cm) categorized as silty clay loam (Table 4). The clay content shows an increasing tendency down the depth from 52% to 62.5% for 0-30 cm and 60-90 cm respectively. Buol et al., (2003) reported that the increasing of clay content down the depth indicates the presence of eluviation and illuviation processes or translocation of clay particles within the layers. The soil water content at FC shows increasing tendency from 31% to 33% for 0-30 to 60-90 cm depths respectively (Table 4**).** It indicates that, the relative proportion of higher clay content provides for sufficient moisture retention. The study agreed with many findings reported that soils with a relatively higher clay content could enhance a greater water retention capacity and lower permeability than sandy soils (Rengasamy, 2006; Seita et al., 2011). The bulk density varies within the range of 1.28 and 1.14 gm cm^{-3} for 0-30 to 60-90 cm depth respectively (Table 4). It classified as "well aggregated soil" (White, 2006).

3.2. Effect of crop water levels and irrigation frequency on yield-related parameters

A significant difference ($p<0.05$) was exhibited for mean plant height due to the interaction effect of water application depth and irrigation frequency in each year and combined over years (Table 5). The highest mean combined plant height (50.7 cm) was noted by the uniform application of 125% (50 mm) ETc with 8 days interval followed by 100% (40 mm) ETc with 8 days interval applied treatment as 48 cm. As the crop water level varied with the increasing trend the plant height tends to increase. This indicates that the application of moisture depth (50 mm) in the optimal scheduling (8 days) can enhance leaf production, root penetration and stem elongation, which agreed with the findings of Firake and Shinde (2000). "However, application of 50 mm crop water depth with a closer frequency (6 days) could decrease the plant height". In fact, the application of relatively larger crop water depth (50 mm) in a short irrigation interval promote surplus moisture, which influence aeration, plant growth and nutrients through leaching. On the other hand, the crop height was restricted as a maximum crop water level (50 mm) applied in a wider frequency (10 days) due to the relative moisture stress compared with 50 mm with 8 days applied treatment. The study agrees with the findings of MALLIC et al. (2018) state that uniform application of 50 mm depth through the growth period has a greater response in the plant height of groundnut.

Application of crop water levels with variable irrigation interval (Table 5) showed non-significant interaction effects ($p>0.05$) on the number of pods per plant in 2016 and combined over years. Nevertheless, during 2017 there was an interaction effect ($p<0.05$). Based on the combined result the numerically higher number of pods per plant (25) was obtained by the applications of 50 mm and 40 mm crop water depth with 8 days, and 40 mm in 6 days intervals. This implies that the number of pods per plant has not been much affected by variable irrigation scheduling. Similar experiences have been reported as the application of a slightly variable depth of water does not significantly affect the number of pods of groundnut (Aruna, 2017).

3.3. Effect of crop water levels and irrigation interval on grain yield

The interaction effect of crop water levels and irrigation frequency in Table 6 revealed a non-significant difference ($p>0.05$) on grain yield of groundnut in each year and combined of two years (2016 and 2017). Whereas the stand count of the treatments were similar. A comparatively yield reduction of treatments that receive the maximum amount of water (50 mm) with a rela-

Table 4. Effects of irrigation scheduling on yield related parameters of groundnut ($p<0.05$).

Depth (cm)	Particle size distribution (%)			Textural class	ρ (gm cm^{-3})	Soil moisture content		
	Clay	Silt	Sand			FC (%v)	PWP (%v)	TAW (mm)
0-30	52	28.6	19.4	SCL	1.28	31	19	36
30-60	57.5	26.5	16	SCL	1.21	32..2	19.8	47.2
60-30	62.5	22.5	15	SL	1.14	33	20.4	37.8
Average	57.3	25.9	16.8	SCL	1.2	32.1	19.7	∑111

Where, SCL- silty clay loam; SL- silty loam; ρ_b – bulk density; gm- gram.

Table 5. Effects of irrigation scheduling on yield related parameters of groundnut using least significant difference test (p<0.05).

Treatments	Plant height (cm)			Number of pods per plant		
	2016	2017	Combined	2016	2017	Combined
30 mm-6	41.8^{ab}	42.1^{bc}	42.1^{cde}	27.0	18.0^{b}	23.0
40 mm-6	44.9^{ab}	45.6^{b}	45.2^{bcd}	28.0	22.0^{ab}	25.0
50 mm-6	46.9^{ab}	44.7^{bc}	45.8^{bc}	23.0	21.0^{ab}	22.0
30 mm-8	44.3^{ab}	44.3^{bc}	44.8^{bcde}	24.0	23.0^{ab}	23.0
40 mm-8	45.9^{ab}	50.9^{a}	48.0^{ab}	24.0	23.0^{ab}	25.0
50 mm-8	47.9^{a}	53.6^{a}	50.7^{a}	25.0	25.0^{a}	25.0
30 mm-10	41.3^{ab}	42.6^{bc}	42.0^{de}	24.0	20.0^{b}	22.0
40 mm-10	40.7^{b}	41.5^{c}	41.1^{e}	27.0	20.0^{b}	24.0
50 mm-10	43.9^{ab}	44.9^{bc}	44.3^{bcde}	26.0	18.0^{b}	24.0
CV (%)	9.3	4.4	7.31	16.4	10.9	17.1

Where, ns: non-significant difference, CV (%): coefficient of variation in percent, 30, 40 and 50 mm are crop water levels, 6, 8 and 10 days are irrigation intervals.

Table 6. Effects of water application depth and irrigation frequency on grain yield using least significant difference test (p>0.05).

Treatments	Grain yield (kg/ha)		Combined over years
	2016	2017	
30 mm-6	2889.8	3383.6	3110.7
40 mm-6	3265.9	3283.1	3274.5
50 mm-6	2978.6	3080.7	3029.7
30 mm-8	**3435.5**	**3308.1**	**3466.9**
40 mm-8	3361.1	3571.9	3464.4
50 mm-8	3228.0	3468	3348.0
30 mm-10	3094.5	3022.4	3058.4
40 mm-10	3117.4	3427.3	3272.4
50 mm-10	3070.8	3371.1	3209.9
CV (%)	19.0	12.9	15.3
LSD (5 %)	ns	ns	ns

Where, ns: non-significant difference, CV (%): coefficient of variation in percent, 30, 40 and 50 mm are crop water levels, 6, 8 and 10 days are irrigation intervals.

tively closer frequency (6 days) could be due to a result of poor aeration and nutrient leaching. This implies that the application of the right amount of water at the right time optimizes water stress, water loss and nutrient uptake to attain comparatively higher yield. The study in line with the finding of Aruna (2017) states that the availability of the right amount of water enhances the development and final yield of groundnut as reduction imposes stress thus making use of available nutrients for growth and yield.

3.4. Effect of crop water levels and irrigation frequency on water use efficiency

The interaction of crop water levels and irrigation interval (Table 7) showed a significant effect (p<0.05) for water use efficiency in each year and combined over years. Based on the combined result, application of 75% (30 mm) crop water depth with 10 days irrigation interval gave the highest mean water use efficiency (0.9 kg/m^3) followed by 75% (30 mm) crop water depth with 8 days irrigation interval (0.8 kg/m^3). Especially, maximum yield and maximum water productivity were simultaneously achieved by the application of 75% crop water depth with 8 days. This treatment saves 4600 m^3 water and can be irrigated an additional 1.2 ha compared with 50 mm crop water depth with 6 days interval applied treatment. In comparing with the full irrigation (100%) which generated by the CROPWAT model (40 mm with 10 days interval) application of 30 mm crop water depth with 8 days interval has a comparative advantage to save 1400 m^3 water for 0.33 ha groundnut production.

Based on the result as indicated in Table 8, applications of crop water levels in a variable rate were significant impact on water use efficiency. As the water levels increased from 75 to 125% the water use efficiency also linearly decreased from 0.79 to 0.48 kg/m^3. The maximum water use efficiency of 0.79 kg/m^3 was recorded from the 75% ETc applied treatment.

The effect of irrigation interval on crop water use efficiency was exhibited a significant difference (Table 9).

Table 7. Effects of crop water depth and irrigation frequency on water use efficiency using least significant difference test (p<0.05).

Treatments	Crop water use efficiency (kg/m^3)		
	2016	2017	Combined
30 mm-6	0.60^{cd}	0.70^{bc}	0.60^{de}
40 mm-6	0.50^{cd}	0.50^{de}	0.45^{fg}
50 mm-6	0.40^{d}	0.40^{e}	0.30^{g}
30 mm-8	**0.90^{ab}**	**0.70^{ab}**	**0.80^{ab}**
40 mm-8	0.65^{c}	0.70^{bc}	0.60^{bc}
50 mm-8	0.50^{cd}	0.50^{cd}	0.50^{ef}
30 mm-10	**1.03^{a}**	**1.01^{a}**	**0.90^{a}**
40 mm-10	0.80^{bc}	0.90^{a}	0.85^{ab}
50 mm-10	0.60^{c}	0.70^{bc}	0.60^{de}
CV (%)	20.71	12.89	16.4
LSD (0.05)			

CV (%): coefficient of variation in percent, LSD: list significant difference, 30, 40 and 50 mm are crop water levels, 6, 8 and 10 days are irrigation intervals.

Table 8. Effects of crop water levels on crop water use efficiency using least significant difference test ($p<0.05$).

Water application level	Crop water use efficiency (kg/m^3)		
	2016	2017	Combined
75% (30 mm)	0.8^a	0.85^a	0.79^a
100% (40 mm)	0.60^b	0.65^b	0.65^b
125% (50 mm)	0.47^b	0.49^c	0.48^c
CV	16.3	11.5	15.5
LSD	0.13	0.085	0.09

CV (%): coefficient of variation in percent, LSD: list significant difference.

Table 9. Effects of irrigation interval on crop water use efficiency using least significant difference test ($p<0.05$).

Irrigation frequency (day)	Crop water use efficiency (kg/m^3)		
	2016	2017	Combined
6	0.49^b	0.52^c	0.5^c
8	0.65^a	0.67^b	0.65^b
10	0.77^a	0.82^a	0.8^a
CV	16.30	11.50	15.50
LSD	0.13	0.09	0.09

CV (%): coefficient of variation in percent, LSD: list significant difference.

As the interval between irrigation events increased from 6 to 10 day the mean crop water use efficiency tends to increase from 0.5 to 0.8 kg/m^3 respectively. The highest mean combined crop water use efficiency of 0.8 kg/m^3 was recorded by the application of 10 day irrigation interval.

4. CONCLUSION AND RECOMMENDATIONS

The effects of treatments were examined using plant height, number of pods per plant, grain yield and crop water use efficiency. The overall result indicates that the crop water levels and irrigation intervals as the main effect do not have a significant response on grain yield. On the other hand, the crop water use efficiency tends to increase due to the decreased and increased of water levels and irrigation intervals respectively. The interaction of 75% ETc with 8 days irrigation interval provides to achieve a simultaneously higher grain yield, water use efficiency and can save a substantial amount of water to irrigate additional land. The present study concludes that for the Kobo irrigation scheme combined application 75 % (30 mm) ETc with 8 days irrigation interval gave the highest crop water use efficiency without affecting the grain yield.

ACKNOWLEDGMENT

I would like to express my priceless thanks to "Almighty God", for his protection and kindness in my entire life. My sincere gratitude extends to Sirinka Agricultural Research Kobo Sub-center for providing me all the necessary research aid and equipments for the successful completion of the study. My genuine gratitude extends to Sirinka Agricultural Research Center soil and water managements directorate researchers for their valuable support to finish this study. I wish to express my thanks to Amhara Agricultural Research Institute for the financial support. Last but not the least, i would like to express my grateful thanks to Dr. Tesfaye Feyisa and Kindu Gashu, for their professional support and providing me with valuable comments.

REFERENCES

Allen, R.G., Pereira, L.S., Raes, D. and Smith, M. 1998. Crop evapotranspiration guidelines for computing crop water requirements. *FAO Irrigation and drainage paper* 56. *FAO, Rome*, 300(9), p. Do5109.

Aruna, K.T., Kumar, U.S., Reddy, G.S., Gowda, A.A. and Shanwad, U.K. 2017. Water Use Efficiency, Yield and Crop Coefficient (Kc) of Groundnut Crop at Different Water Regimes under Agro Climatic Condition of Raichur, Karnataka, India. *Int. J. Curr. Microbiol. App. Sci*, *6*(12), pp.1956-1963.

Ayana, M., Teklay, G., Abate, M., Eshetu, F. and Mada, M. 2015. Irrigation water pricing in Awash River Basin of Ethiopia: Evaluation of its impact on scheme-level irrigation performances and willingness to pay. *African Journal of Agricultural Research*, *10*(6), pp.554-565.

Baiphethi, M.N. and Jacobs, P.T. 2009. The contribution of subsistence farming to food security in South Africa. *Agrekon*, *48*(4), pp.459-482.

Buol, SW., Southard, R.J., Graham, R.C., McDaniel, P.A., 2003. Soil genesis and classification, 5th edition. *Iowa State University Press-Blackwell, Ames, IA*.

Firake N.N. and Shinde, S.H. 2000. Performance of planting geometry and micro-sprinkler layouts in summer groundnut. Journal of Maharashtra Agricultural Universities, *25*(2), pp.206-208

Getahun Wendmkun Adane 2014. *Groundwater modeling and optimization of irrigation water use efficiency to sustain irrigation in Kobo Valley, Ethiopia* (M.Sc. Thesis, UNESCO-IHE).

Gomez, K.A. and Gomez, A.A., 1984. Statistical procedures for agricultural research. *John Wiley and Sons, second edition, New York*.

Henggeler, J. 13 Irrigation scheduling. *Hampshire*, *6*, pp.3-7. USDA, (2004).

Kebede, A., Abady, S., Endale, D., Abdulahi, J., Getahun, A., Robsa, A. and Petros, Y., 2017. Registration of 'Babile-1','Babile-2', and 'Babile-3'groundnut varieties. *East African Journal of Sciences*, *11*(1), pp.59-64.

Mallic, A.N., Gunri, S.K., Paul, S., Barman, M., Mukherjee, A. and Sengupta, A. 2018. Effect of different depths of irrigation water on yield and water use pattern of summer groundnut (Arachis hypogaea L.). *The Indian Society of Oilseeds Research*, p.33.

Okello, D.K., Biruma, M. and Deom, C.M. 2010. Overview of groundnuts research in Uganda: Past, present and future. *African Journal of Biotechnology*, *9*(39), pp.6448-6459.

Rengasamy, P., 2006. World salinization with emphasis on Australia. *Journal of experimental botany,* 57(5), pp. 1017-1023.

Rhoades, J. D., A. Kandiah, and A. M. Mashali 1992. "The use of saline waters for crop production-FAO irrigation and drainage paper 48." *FAO, Rome* 133.

Sanogo, D., Ndour, B.Y., Sall, M., Toure, K., Diop, M., Camara, B.A., N'Diaye, O. and Thiam, D. 2017. Participatory diagnosis and development of climate change adaptive capacity in the groundnut basin of Senegal: building a climate-smart village model. *Agriculture & Food Security*, *6*(1), p.13.

Sarwar, A. and Bastiaanssen, W.G. 2001. Long-term effects of irrigation water conservation on crop production and environment in semiarid areas. *Journal of irrigation and drainage engineering*, *127*(6), pp.331-338.

Setia, R., Marschner, P., Baldock, J., Chittleborough, D., Smith, P. and Smith, J., 2011. Salinity effects on carbon mineralization in soils of varying texture. Soil biology and biochemistry, *43(9), pp. 1908-1916.*

Sinclair, T. R., Tanner, C. B. and Bennett, J. M. 1984. Water-Use Efficiency in Crop Production. American Institute of Biological Sciences, 34: 36-40.

Sisay, D., Belayneh, M. and Ahmed, F. 2021. Reclamation and amelioration of saline-sodic soil using gypsum and halophytic grasses: Case of Golina-Addisalem irrigation scheme, Raya Kobo Valley, Ethiopia. *Cogent Food & Agriculture*, *7*(1), p.1859847.

Upadhyaya, H.D., Reddy, L.J., Gowda, C.L.L. and Singh, S. 2006. Identification of diverse groundnut germplasm: sources of early maturity in a core collection. *Field Crops Research*, *97*(2-3), pp.261-271.

USDA, 1993. Chapter: 2 Irrigation Water Requirements. *Part 623 National Engineering Handbook.*

U.S. Department of Agriculture 1993. Chapter: 2 Irrigation Water Requirements. *Part 623 National Engineering Handbook.*

Waktole, G. 2018. In-Vitro Induction of Mutation in Groundnut (Arachis hypogea L.) by Using Sodium Azide Mutagens and Its Impact on Selected Agronomic Traits. *Annals of Ecology and Environmental Science*, *2*(3), pp.27-32.

White, E., 2006. *Principles and practices of soil science: Soil as a natural resource, 4th ed*, pp.133-154.

Italian Journal of Agrometeorology
Rivista Italiana di Agrometeorologia

Firenze University Press
www.fupress.com/ijam

OPEN ACCESS

Citation: Lupi Edao, A., Dechassa, N., Merga, F., Alemayehu, Y., & Abebe, T. (2023). Analysis of projected climate change in sorghum growing semi-arid rift valley of Ethiopia. *Italian Journal of Agrometeorology* (2): 49-68. doi: 10.36253/ijam-2194

Received: June 21, 2023

Accepted: October 6, 2023

Published: January 20, 2024

Data Availability Statement: All relevant data are within the paper and its Supporting Information files.

Competing Interests: The Author(s) declare(s) no conflict of interest.

Credit authorship contribution statement

Agere Lupi Edao: Data curation, Writing of the original draft.
Nigussie Dechassa: Data curation, reviewing an original draft.
Feyera Merga: Data curation, reviewing the original draft
Yibekal Alemayehu: Data curation, reviewing the original draft and
Tewodros Mesfin: Data curation, reviewing the original draft

Analysis of projected climate change in sorghum growing semi-arid rift valley of Ethiopia

Agere Lupi Edao[1,*], Nigussie Dechassa[1,2], Feyera Merga[2,3], Yibekal Alemayehu[1], Tewodros Abebe[2]

[1] *Haramaya University, School of plant Science P.O.Box 138 Dire Dawa, Ethiopia*
[2] *Melkassa Agricultural Research Center, P.O. Box 436 Adama, Ethiopia*
[3] *Alliance of Biodiversity International and CIAT.ILRI, Guard Shola Area, P.O. Box 5689 Addis Ababa, Ethiopia*
*Corresponding author. E-mail: agere97@gmail.com

Abstract. Global warming projected to have a significant impact on agricultural water availability for crops in Africa in particularly in Ethiopia. Therefore, the study was conducted to analyze the projected change of temperature and rainfall in sorghum growing semi-arid rift valley of Ethiopia. The weather data for 11 stations were generated using AgiMP5 technique for RCP 4.5 and 8.5 and for the period of 2050s and 2080s. MAKESENS employed for the detection of trend of extreme indices. InStat v3.37 were used for the analysis of start, end, and length of growth season. Under RCP 4.5, the projected mean annual minimum air temperatures in CRV, ERVE and NRVE could increase respectively by 1.9 °C (2050s) and 2.6 °C (2080s), 1.8 °C (2050s) and 2.5 °C (2080s) and 1.88 °C (2050s) and 2.69 °C (2080s). Under RCP 8.5, however, with same location it will projected to increase in both time frames (2050s and 2080s) in all studied sites. The mean annual maximum air temperature, projected under RCP 4.5 in the CRV, ERV and NRVE will increase by 1.59 °C (2050s) and 2.18°C (2080s),1.42 °C (2050s) and 2.08 °C (2080s) and 1.46 °C (2050s) and 2.09 °C (2080s) respectively. However, under the RCP 8.5, at same regions it projected to rise in both periods (2050s and 2080s). This will be convoy with increase of the hot and cold extremes' indices in regions. The mean percentage change of annual rainfall is projected to decrease insignificantly in (0.6-5.5% and 2.6%) and increase (0.85-12.3% and 22.3%) in half of the stations located in CRV and ERVE, whereas, in NRVE it will projected to increase (6.1-14.6%) under RCP 4.5 in all stations in 2050s. Though the annual projected rainfall under RCP 4.5 in 2080s will decline in range of 2.1-10.1%, 3.12-4.5% and 0.9-4.6% at CRV, ERVE and NRVE respectively. In most of the location in CRV and ERVE stations growing season rainfall will projected to decline from 1.45% to 53.8% and 0.8 to 8.8%, whereas, in NRVE it will projected to increase in 9.2 to 19% under RCP 4.5 in period of 2050. The projected SOS will be changed in mixed pattern, whereas and LGP will prolonged in most locations. The findings indicated that there has been a change of projected climate change in semi-arid RV, which will be alter the agricultural practices in depletion of soil moisture. Therefore, in adjusting planting timing and using early/medium maturation sorghum varieties, may be necessary for farmers in the region. Soil and water management needs attention.

Keywords: climate change, air temperature and rainfall change, extreme indices, SOS, EOS and LGP.

1. INTRODUCTION

According to the United Nations Framework Convention on Climate Change (UNFCCC, 2017), developing nations are greatly susceptible to the consequences of climate change since they possess fewer resources to facilitate adaptation. Niang et al. (2014) and the Intergovernmental panel on Climate change (IPCC 2014, 2019) point out that Africa is among the continents that are significantly influenced by climate change and variability. In recent years, several global proceedings, such as the IPCC (2014) and the World Bank (2019), have raised concerns about the exacerbation of food security and economic insecurity. These concerns are particularly relevant in Sub-Saharan Africa (SSA), which has the highest prevalence of undernourishment according to Sonwa et al. (2017), OECD/FAO (2016). Furthermore, key economic sectors in SSA are highly vulnerable to climate change and variability, as depicted in various studies, including Mahoo et al. (2013), Ceci et al. (2021), and Sonwa et al. (2017). The resulting economic consequences have been significant as reported by Sonwa et al. (2017) and the OECD and FAO (2016). Sub-Saharan Africa (SSA) is a key concern in region food security (FAO, 2011). Within the SSA region, Eastern Africa and Ethiopia, in particular, are identified as being the most vulnerable to climate inconsistency and change by USAID (2015) and NAP (2019). This vulnerability is due to the region's reliance on rain-based agriculture (Schlenker and Lobell, 2010; IMF, 2020; World Bank, 2019). Additionally, the relatively limited capacity of the region to absorb shocks further exacerbates the situation (Schlenker and Lobell, 2010; World Bank, 2019). In the coming fifty years and subsequent periods, it is projected that climate change will significantly affect the agricultural sector of Ethiopia and its overall societal progress (Arndt et al., 2011; Thomas et al., 2019), highlighting the urgent need for proactive measures to address this concern.

According to various scholarly sources, it has been projected that during the 21st century, the rate of temperature increase in Africa will exceed the global average (Joshi et al., 2011; Sanderson et al., 2011; James and Washington, 2013). According to the Intergovernmental Panel on Climate Change (IPCC, 2007), Africa has experienced an excessively substantial influence from climate change compared to other continents. The continent is poised to face significant vulnerability arising from its geographical location, characterized by a notably diminished adaptive capacity that is further compounded by the prevalence of poverty and a preexisting shortage of development (IPCC, 2007). Due to climate change the East African region, specifically Ethiopia, is projected to experience a rise in temperatures with increase by 1.8 °C in the mid-century and 3.7 °C in the end-century, as reported by the IPCC (2019), Irish Aid (2018), and the CCKP (2020). Various climate models produce only slightly varying projections for temperature increase while presenting differing anticipations for changes in rainfal patterns. The accuracy of Ethiopia's projected rainfall remains uncertain. Nevertheless, projection suggest a marginal increase in the country's cumulative rainfal (USAID, 2015; IPCC, 2019; CCKP, 2020). The high-emission scenarios: projected to result in a relatively low mean annual rainfall rate, which increase significantly by the end of the century (CCKP, 2020).

The phenomenon of climate change has already had a significant adverse impact on various aspects of people's livelihoods, with projected future exacerbations as posited by the IPCC, (2019). According to Mahoo et al. (2013), there is a significant susceptibility of Ethiopia's economy to the impacts of climate change and variability. The projected posits that by the year 2050, the gross domestic product (GDP) of Ethiopia may experience a decline ranging from 8% to 10%. (CIAT; BFS/USAID, 2017; World Bank, 2021) This decline is mainly attributable to the impact of climate change on agricultural productivity, with drought serving as a major contributing factor (CIAT; BFS/USAID, 2017). The nation's gross domestic product (GDP) has been negatively impacted by up to 4% as a result of recent severe droughts (USAID, 2016) Furthermore, it has been projected that rain-induced soil erosion may lead to an additional decrease in GDP by approximately 1% (CGIAR, 2018). However, the financial consequences of these environmental factors are primarily contingent on the levels of rainfall received annually, as well as the variations and extremes of temperature (CGIAR, 2018).

Furthermore, global warming is projected to have a significant impact on agriculture water availability in Africa.in particularly in Ethiopia Agriculture. The literature suggests that there will be a reduction in growing periods and an increase in water stress in many parts of the continent (World Bank, 2021). Specifically, studies have shown that the expected warming patterns in Ethiopia may exacerbate current rainfall deficits, leading to elevated levels of water scarcity (MoFE, 2015; USAID, 2016). Moreover, research indicates that there exists a negative correlation between annual rainfall and the productivity of important crops such as millet, sorghum, and maize in the northern region of Ghana (Ndamani and Watanabe, 2015). Additionally, there is evidence that rising temperatures, coupled with an increase in the frequency and intensity of droughts, have had a significant impact on Ethiopia's grain yield (WFP, 2014; USAID, 2015; World Bank, 2019). According to Shanahan et al. (2013), it is anticipated that there will be an increase in flooding and extreme rainfall, causing substantial detrimental impacts on Ethiopian production output and environmental conditions. Low temperature extremes are a critical determinant of the pace of plant growth and development, and the distribution of plant genotypes in diverse geographic localities across the globe (Ramankutty et al., 2008; Yadav, 2009). The research conducted by Maulana and Tesso (2013) indicates that the impact of cold extremes on the growth rate and duration of flowering of sorghum plants differs across various genotypes in the semi-arid region of Ethiopia.

Rainfed cereal production and limited livestock rearing support households in semi-arid Rift valley. High rainfall variability and drought cause crop failure and famine in the central rift valley (Kassie et al., 2013; Getent and Alister, 2012). The region is a significant land portion of the country that is environmentally vulnerable to climate change (Kassie et al., 2013; Hadgu et al., 2013; Muluneh, 2017). In order to develop effective climate change adaptation strategies for agricultural systems, an investigation into both the variability and predictability of forthcoming rainfall and air temperature changes is imperative (Thornton et al., 2009; Kassie et al., 2013). The task of monitoring changes in regional climate is vital for exploiting agricultural advancements that could potentially heighten productivity, while concurrently steering clear of circumstances that may give rise to substantial stress (Thornton et al., 2009). The ability to accurately climate change projection patterns is largely contingent upon the availability of regional climatological data, as highlighted in previous research conducted by Oates et al. (2011). According to Ghosh and Mujumdar (2008), Global Circulation Models (GCMs) represent the most accurate means of modeling the response of the global climate system presently available. According to the Intergovernmental Panel on Climate Change's (IPCC, 2007), General Circulation Models (GCMs) are capable of providing estimates for alterations in multiple meteorological factors at grid cells typically measuring 250 km in width and 600 km in length. Consequently, the resolution they achieve is somewhat coarse. However, the results produced by General Circulation Models (GCMs) are seldom in a format that is applicable to a regional level, and substantial analysis is required prior to practical usage, to assess potential effects and suitable adaptation approaches (Jones and Thornton, 2013). The attainment of enhanced spatial resolution can be accomplished by down-sampling the outputs generated by coarse-scaled global climate models (GCMs). The climate impact community mostly accepted these methodologies that demonstrate empirical correlations between the output (predictors) of coarse-scale GCMs and local or station scale predictands (rainfall and/or) (Fowler et al., 2007; Green et al., 2011). Research on the implications of future climate change for agricultural production in the semi-arid rift valley of Ethiopia is currently is not enough or even lacking in most sorghum producing areas. Despite the importance of obtaining locally-relevant information on future climate patterns to develop effective adaptation strategies, no more as such studies have been conducted in this region. Therefore, the purpose of this study was to characterize and analyze the rainfall and air temperature outputs at a local scale, derived from selected GCMs climate change scenarios in the semi-arid rift valley of Ethiopia's sorghum producing region. Noteworthy, rainfed crop production in this area has experienced substantial growth in recent years (Jansen et al., 2007).

2. MATERIALS AND METHODS

2.1. Description of the study areas

The prominent geological feature of the Main Rift Valley in Ethiopia is characterized by its intricate terrain, which is marked by noteworthy tectonic escarpments that demarcate the rift floor from the adjacent plateaus. According to Corti (2013), this area is situated between the topographical elevations of the Ethiopian and Somali Plateaus. According to Keir et al. (2005) and Agostini et al. (2010), it is presently postulated that the faults situated in the northern Rift valley escarpment are in a state of quiescence. However, in the southern region, they are expected to remain tectonically and seismically active. The Ethiopian highlands are a notable geographical feature, resulting from the formation of the Main Rift Valley on either flank, as observed by Agostini et al. (2010).

This study focuses on the semi-arid rift valley of Ethiopia, which is located from 38°.07'–41°.11'E and 7°.85'-12°.42'N. It includes the heart and corridor of the Ethiopian Rift Valley, and encompasses semi-arid lowlands in the northwest and eastern areas. The CRV has a central valley floor at 1500-1700 m a.s.l. and is flanked by northern, western, and eastern escarpments exceeding 4000 m a.s.l. (Jansen et al., 2007). The CRV has a weak bi-modal rainfall pattern, typical for the central, eastern, and northern parts of Ethiopia. Valley floor gets 175-358 mm rain in the short season (Mar-May) and 420-680 mm in the main season (Jun-Sep). Eastern and northern rift valleys escarpments get 833 mm in the main season and 603 mm in the short season annually.

Andosol (orthic) is the most dominant soil, followed by phaeozems (ortic) and chromic luvisols (orthic) (FAO, 1984), due to the prevalence of silt and ash (white, volcanic) with high-water infiltration capacity. Due to agriculture and dense population, the flora is scarce, causing soil erosion in sloping areas with andosols.

Cereals, including teff, maize, sorghum, common beans, and wheat are the main crops. Past rainfall was analyzed for eleven stations in the CRV floor and its semi-arid escapements. Studied areas: CRV floor (Adami Tullu, Melkassa, Dhera, Matahara, Mieso, Melka Werer), Easter RV escapement (Abomsa, Gololcha), and northern RV escapement (Kobo, Sirinka, Alamata). All known for sorghum production and similar weather.

2.2. Historical meteorological data and future climate scenarios analysis

National Meteorology Agency Service (NMAS) provided historical daily rainfall, maximum and minimum air temperature data for different locations across the study region from 1989 to 2019. These climate data were used as baseline data to prepare local future climate scenarios. The site-specific future climate change scenarios were generated following the Agricultural Model Inter comparison and Improvement Project (AgMIP) technique, which uses the delta statistics approach (Hudson and Ruane, 2015). Downscaled future climate data as shown in Table 1 derived from five ensemble representative GCMs, namely, CSIRO-Mk3.6.0, HadGEM2-ES, IPSL.CM5A-MR, MIROC5 and MRI.GCM3 were selected out of the 20 GCMs that are available in the AgMIP climate scenario (Hudson and Ruane, 2015; Rosenzweig et al., 2015) ensembled for two RCP's (RCP 4.5 and RCP 8.5) and two time periods; 2050s (2040-2069) and 2080s (2070-2099) including the baseline scenario (1989-2019). These five GCMs were selected due to their long history of development and evaluation, a preference for higher resolution, and established performance in monsoon regions (Rosenzweig et al., 2013b).

The name of the global circulation models (GCM's) used for this study and their institutions is presented in Table 1. The projected future scenario data applied to analysis and characterize the future climate change in sorghum growing semi-arid Rift Valley under the medium (4.5 W/m^2) and maximum (8.5 W/m^2) irradiance energy striking the earth. RCPs usually refer to the portion of the concentration pathway extending up to 2100, for which Integrated Assessment Models have produced corresponding emission scenarios (IPCC, 2013). The RCP 8.5 is a high emission scenario, corresponding to projections of high human population (12 billion by 2100), high rates of urbanization, and limited rates of technological change, all resulting in emissions approaching 30 Gt of carbon by 2100 compared with 8Gt in 2000 (Riahi et al., 2007). The RCP 4.5 scenario is an intermediate mitigation scenario characterized by a continuously increasing human population, but at a rate lower than in the RCP 8.5 scenario, intermediate levels of economic development and less rapid and more diverse technological change (Moss et al., 2010).

The projected changes of air temperature were calculated absolute difference (eq. 1) and the rainfall relative change of percentage(eq. 2), respectively.

$$\Delta T = Tmp - Tmb \quad (1)$$

$$RF\% = \frac{RFp - RFb}{RFb} * 100 \quad (2)$$

where ΔT is the absolute change of temperature, Tmp = projected temperature and Tmb baseline temperature and RF% = relative change of percentage of rainfall, RFp = projected rainfall, and RFb is baseline rainfall.

2.3. Data quality check and analysis of indices

Data quality control is essential for reliable indices. The data displayed for visual inspection and the detection of outliers to prevent potential issues that could affect the seasonal cycle (Abbas et al., 2013). The Expert Team on Climate Change Detection, Monitoring and Indices (ETCCDMI) of the Climate Research Branch of the Meteorological Service of Canada created the data and the technique in the RClimDex 1.3 program was used to further quality check the data. Its key function is to detect processing errors, including manual data entry mistakes. An assessment was done on daily air temperatures, and any values outside the user's range are considered outliers. Zhang et al. (2005) defined the findings within the range of the climatological mean value and four standard deviation (SD). The daily temperature was manually assessed and edited if it deviated from the prescribed range. RClimDex (1.3) computes 27 indices for extreme weather conditions in temperature and rainfall. ETCCDMI defined 27 core indices that include the most R.ClimDex (V.1.3) indices. In the study, 8 temperature indices and 10 rainfall indices were analyzed (Table 2).

2.4. Analysis of rainfall and air temperature indices trends

Non-parametric technique in Excel, the Mann-Kendall and Sen's (MAKESEN) slope estimator test utilized to find trends in the climate variables caused by climate

Table 1. Coupled Model Inter-comparison Project phase 5 (CMIP5) and general circulation models (GCM's) were used for this study.

No.	Institution	Model Name	Resolution		Reference	Country
			Lat	Long		
1	Commonwealth Scientific and Industrial Research Organization and the Queensland Climate Change Centre of Excellence	CSIRO-Mk3. 6-0	1.875	1.875	Collier et al. (2011)	Australia
2	Met Office Hadley Centre	HadGEM2-ES	1.75	1.25	Collins et al. (2011).	UK
3	Institute Pierre-Simon Laplace	IPSL CM5A-MR	1,2587	2.5	Dufresne et al. (2013).	France
4	Japan Agency for Marine-Earth Science and Technology, Atmosphere and Ocean Research Institute (The University of Tokyo), and National Institute for Environmental Studies	MIROC5	1.4063	1.4063	Watanabe et al. (2010).	Japan
5	Meteorological Research Institute	MRI-GCM3	1.12	1.12	Yukimoto (2012).	Japan

Source: (IPCC, 2013).

Table 2. Temperature and rainfall indices used in the analysis.

s/n	Index	Index name	Definition of the index	Unit
Temperature indices				
1	TXx	Hottest day	Max Tmax: monthly maximum value of daily maximum temperature	°C
2	TNx	Hottest night	Max Tmin: monthly maximum value of daily minimum temperature	°C
3	TXn	Coolest day	Min Tmax: monthly minimum value of daily maximum temperature	°C
4	TNn	Coolest night	Min Tmin: monthly minimum value of daily minimum temperature	°C
5	TN10p	Cool night frequency	Percentage of days when TN <10th percentile of the baseline period	Days
6	TX10p	Cool day frequency	Percentage of days when TX <10th percentile of the baseline period	Days
7	TX90p	Hot day frequency	Percentage of days when TX >90th percentile of the baseline period	Days
8	TN90P	Hot night frequency	Percentage of days when TN >90th percentile of the baseline period	Days
Rainfall Indices				
1	RX1da y	Max 1-day rainfall amount	Monthly maximum 1-day rainfall	mm
2	Rx5day	Max 5-day rainfall amount	Monthly maximum consecutive 5-day rainfall	mm
3	R10	Number of heavy rainfall days	Annual count of days with rainfall ≥10 mm	Days
4	R20	Number of very heavy rainfal days	Annual count of days with rainfall ≥20 mm	Days
5	CDD	Consecutive dry days	Maximum number of consecutive days with rainfall <1 mm	Days
6	CWD	Consecutive wet days	Maximum number of consecutive days with rainfall ≥1 mm	Days
7	PRCPTOT	Annual total wet-day rainfal	Annual total rainfall from days ≥1 mm	mm
8	SDII	Simple daily intensity index	Simple rainfal intensity index	mm/day
9	R95P	Very wet days	Annual total rainfal when RR>95 percentile	mm
10	R99P	Extremely wet days	Annual total rainfal when RR>99 percentile	mm

change, (Timo et al., 2002). According to Da Silva et al (2015), the main benefits of non-parametric methods include the ability to use datasets with missing values and the fact that the data need not follow a specific distribution and to identify whether there is a positive or negative trend based on statistical significance (Amadi et al., 2014).

A non-parametric method called the Mann-Kendall (MK) test is frequently used in different trend identification research (Karaburun et al., 2011). Given the possibility of ties (i.e., equal values) in the x values, the variance of S is as below:

$$var(S) = 1/18\left|N(N\text{-}1)(2N\text{+}5)\text{-}\Sigma^{M}_{i=1} ti(ti\text{-}1)(2ti\text{+}5)\right| \quad (3)$$

where: M is the number of tied groups in the data set and *ti*is the number of data points in the *ith* tied group. For n larger than 10, *ZMK* approximates the standard normal distribution (Partal and Kahya, 2006; Yenigun et al., 2008) and computed as follows:

for n larger than 10, the standard normal Z test statistic used and computed from eq. 8 as

$$Z = \begin{cases} \frac{s-1}{\sqrt{var(s)}} & ifs > 0 \\ & ifs = 0 \\ \frac{s+1}{\sqrt{var(s)}} & ifs < 0 \end{cases} \quad (4)$$

The presence of a statistically significant trend was evaluated using the Z value. A positive or negative value of Z indicates an upward or downward trend. The statistic Z has a normal distribution. In a two-sided test for trend, the null hypothesis Ho should accept if $|ZMK| < Z1-\alpha2$ at a given level of significance. $Z1-\alpha2$ is the critical value of ZMK from the standard normal table. e.g., for 5% significance level, the value of $Z1-\alpha2$ is 1.96…

The Sen's estimator of slope; to estimate the true slope or magnitude of an existing trend (as change per year). The Sen's method can be used in cases where the trend can assume to be linear. This method could be used with missing data and remain unaffected by outliers or gross errors (Karpouzos et al., 2010). Then, the slope magnitude (change per unit time) was estimated for both rainfall and temperature:

$$Q = Q_{\frac{N+1}{2}} \quad \text{if } N \text{ is odd number} \quad (5)$$

$$Q = \frac{1}{2}(Q_{\left(\frac{N}{2}\right)} + Q_{\left[\frac{N+2}{2}\right]}) \quad \text{if } N \text{ is even} \quad (6)$$

2.5 Determination of the start, end, and length of growing period

Various authors use different threshold values to determine the start (SOS) and the end of the growing season (EOS). The criteria used in this study were a rainfall of 20 mm or more accumulated over three consecutive rainy days after a specified date (in this case June first) with no dry spell greater than 9 days in the next 21 days (Girma, 2005; Liben, 2013; Edao et al., 2018). SOS is calculated as (eq. 7):

$$\boldsymbol{SOS = D\,\frac{(20-F)}{R}} \quad (7)$$

where; D is the total number of days in the first month with effective rain (MER: accumulated rainfall totals equal or exceeds 20 mm). F (mm) is the accumulated rainfall total of earlier months and R is the accumulated rainfall within the MER.

Moreover, the end of the season (EOS), was defined as the date when the available soil water content dropped to 10 mm m^{-1} of available water (Dodd and Jollite, 2001; Tesfaye and Walker, 2004; Girma, 2005; Liben, 2013; Edao et al., 2018) in October. Rainfall end dates were also calculated using (eq. 8):

$$\boldsymbol{EOS = b + 275} \quad (8)$$

where EOS is any day from 1st October after which there are more than 7 consecutive days of rainfall amounts below 50% of the soil water requirement and "b" denotes the number of days in which there is maximum build-up of pre-season moisture.

The Length of the growing period (LGP): is a key factor in deciding on the maturity of cultivars to be grown in dissimilar rainfall regimes. Therefore, LGP is considered as the period from the SOS to the EOS. (eq 9)

$$LGP = EOS - SOS + 1 \quad (9)$$

3. RESULTS AND DISCUSSIONS

3.1. Projected change of air temperature in the semi-arid rift valley

3.1.1. Projected change of maximum and minimum air temperature

The findings of this study reveal that the projected future mean annual minimum and maximum air temperatures across several locations in the semi-arid Rift Valley will increase under both RCP scenarios (4.5 and 8.5) and time frames (2050s and 2080s) based on an ensemble of five General Circulation Models (GCMs) namely CSIRO-Mk3.6.0, HadGEM2-ES, IPSL CM5A-MR, MIROC5, and MRI-GCM3 (Table 3). Only in Melka Werer there is no value in 2080 for the mean annual maximum air temperature due to high uncertainty in period of RCP 8.5, while the other studied areas will experience an increase in air temperature. Furthermore, the study indicates that the average increase in minimum air temperature in the CRV region could potentially reach 1.91 °C and 2.56 °C under the RCP 4.5 scenario in 2050s and 2080s and under the RCP 8.5 in the year 2050s and 2080s and 2.61 °C and 4.82 °C respectively (Table 3). For RCP 4.5, the mean of the projected minimum air temperature increase in the Eastern(ERVE) and Northern Rift Valley Escapements(NRVE) is 1.8°C and 2.57 °C, and 1.88 °C and 2.66 °C by mid-century and end of century respectively. The projected increase for the RCP 8.5 in the mid and end of the century are much higher, up to 2.53 and 4.76 °C and 2.67 and 4.88 °C, respectively (Table 3).

Based on the findings stated earlier, the minimum air temperature is projected to be higher in the NRVE followed by CRV then ERVE in both analyzed periods and scenarios (Table 3). The end of the century, the minimum air temperature in both scenarios will be

Table 3. Projected change of annual air temperature in CRV, floor, ERVE, and NRVE of Ethiopia in 2050s and 2080s using five GCM models for RCP 4.5 and RCP 8.5 scenarios.

Locations /Sites LSites		Minimum Temperature change				Maximum Temperature change				Mean Temperature change			
		2050		2080		2050		2080		2050		2080	
		RCP 4.5	RCP 8.5	RCP 4.5	RCP 8.5	RCP 4.5	RCP 8.5	RCP 4.5	RCP 8.5	RCP 4.5	RCP 8.5	RCP 4.5	RCP 8.5
CRV	AdamiTullu	1.66	2	2	3.65	1.46	2.33	2.34	4.36	1.56	2.17	2.17	4
	Melkassa	1.84	2.61	2.55	4.91	1.43	2	2.05	3.61	1.63	2.3	2.3	4.26
	Dhera	1.83	2.60	2.54	4.91	1.43	2	2.05	3.61	1.63	2.3	2.29	4.26
	Abomsa	2.28	3.06	2.89	5.36	1.88	2.45	2.3	4.03	2.8	3.75	2.54	4.69
	Matahara	1.95	2.75	2.68	5.03	1.94	2.10	2.17	3.68	1.94	2.42	2.43	4.35
	Melka Werer	1,90	2.67	2.72	5.03	1.44	2.08	2.19	-	1.67	2.36	2.46	3.59
	mean	1.91	2.61	2.56	4.82	1.59	2.16	2.18	3.85	1.87	2.55	2.37	4.19
ERVE	Mieso	1.78	2.46	2.6	4.78	1.42	2.09	2.03	3.61	1.6	2.32	2.27	4.19
	Gololcha	1.82	2.59	2.54	4.74	1.41	2.04	2.06	3.28	1.62	2.32	2.3	4.01
	mean	1.8	2.53	2.57	4.76	1.42	2.07	2.05	3.45	1.62	2.32	2.29	4.1
NRVE	Kobo	1.9	2.8	2.7	4.9	1.9	2.1	2.0	3.8	1.7	3.85	2.45	4.4
	Sirinka	1.77	2.55	2.45	4.77	1.44	2.05	2.12	3.67	1.605	2.3	2.285	4.22
	Alamata	1.97	2.65	2.84	4.97	1.44	2.1	2.07	3.81	1.71	2.38	2.46	4.39
	mean	1.88	2.67	2.66	4.88	1.46	2.08	2.09	3.76	2.51	2.84	2.39	4.34

CRV=central rift valley, ERVE=eastern rift valley escapement, NRVE= northern rift valley escapement.

warmer compared to the mid-century. Within the studied three locations, the highest change in minimum air temperature is projected in Abomsa and the lowest will be encountered in Adami Tullu across all stations examined, in both time frames (2050s and 2080s) and scenarios (4.5 and 8.5) (Table 3). Table 3 reveals that both emission scenarios (4.5 and 8.5) exhibit a trend of 2080s minimum air temperatures will be warmer compared to baseline period (1989-2019) during the mid-century across all stations examined. Specifically, the RCP 4.5 displays this pattern at all analyzed stations.

For the RCP 4.5, the projected mean change in the maximum air temperature of the CRV floor is projected to rise in 1.59 and 2.18 °C for the periods of 2050s and 2080s, respectively (Table 3). Similarly, for the RCP 4.5, it found that the mean change of the projected maximum air temperature rise in the ERVE and NRVE will be 1.42 and 2.08 °C and 1.46 and 2.09 °C, respectively, for the periods of 2050s and 2080s. Furthermore, in the RCP 8.5 the projected changes in the maximum air temperature will be identified as increasing by 2.16 and 3.85 °C in the CRV floor, 2.04 and 3.45 °C at ERVE, and 2.08 and 3.76 °C in the NRVE during the periods of 2050s and 2080s, respectively (Table 3). The analysis indicated that the projected maximum air temperature towards 2080s will be warmer than 2050s expected for CRV during 2080s and less warm than in 2050s (Table 3). The CRV will experience higher air temperatures under the RCP 4.5 in both 2050s and 2080s compared to the ERVE and NRVE areas. Additionally, during the 2050s period, the CRV will be even warmer compared to the baseline period (1989-2019), in contrast to the ERVE and NRVE areas for the RCP 8.5.

In the coming decades, specifically during the 2050s and 2080s, it is projected that the mean air temperature in the CRV, ERVE and NRVE areas will rise significantly in both emission scenarios (4.5 and 8.5). The projected mean air temperature increase will be around 1.85 °C, 1.62 °C, and 2.52 °C for the RCP 4.5, and around 2.55 °C, 2.33 °C, and 2.84 °C for the RCP 8.5 during 2050s respectively in CRV, ERVE and NRVE. Towards the end of the century, there is an expected rise in the mean air temperature in the CRV, ERVE, and NRVE areas to be around 2.37 °C, 2.29, and 2.39 °C for the RCP 4.5, and around 4.19, 4.1 and 4.34 °C for the RCP 8.5, respectively (Table 3).This confirms IPCC's (2014) postulation that the average temperature will increase by 2-3 °C by the mid-century and by 4-6 °C by the end of the 21st century over East Africa including Ethiopia. The projected future temperature increase was also shown by Gebrechorkos et al. (2023), Weldegebriel and Prowse (2013) for East Africa, by World Bank (2022) particularly in Ethiopia, by Adem and Abebe (2022) in Northern Ethiopia, by Teshoma (2022) in Eastern Ethiopia, and by Kassie et al. (2013) in CRV.

The change in the projected future mean air temperature is more dramatic in minimum air temperature than in maximum air temperature, and the magnitude of the change depends on location, emission scenarios, and time frames. The results of the analysis suggest that, at RCP 4.5, CRV is projected to exhibit higher air temperatures than two other regions, namely, ERVE and NRVE, in 2050s. However, under RCP 8.5, NRVE is expected to experience greater levels of warmth during 2080s than 2050s. The current findings are consistent with publications by IPCC (2013) and Gebrechorkos et al. (2023) for east Africa, and Kassie et al. (2013) for the CRV, in which the expected future shift in minimum air temperature is higher than maximum air temperature. According to Halfield et al. (2011) report, the projected increase in air temperature may result in a reduction in yield by an estimated ranging between 2.5% to 10% across several crop species. Abera's (2022) conflicting findings suggest that a 1% increase in mean air temperature during the crop's growth phase results in a proportional yield increase of 2.4% in the sorghum crop.

3.1.2. Projected change in seasonal mean air temperature

The projected main rainy season mean air temperature experience an increase pattern across all examined regions. Specifically, there will be an increase by 1.65 °C, 1.56 °C, and 1.69 °C in the 2050s for the CRV, ERVE and NRVE, respectively. Furthermore, in the 2080s, it is expected that there will be a change in mean air temperature, with an increase by 2.29 °C, 2.26 °C and 2.42 °C under RCP 4.5 for the same areas (Table 4). For the RCP 8.5, it is projected that the future mean air temperature during the main rainy season will increase by 2.36, 2.28, and 2.42 °C for the 2050s, and by 4.18, 3.87, and 4.38 °C for the 2080s, respectively in the CRV, ERVE and NRVE (Table 4). The findings have demonstrated that, during the main growing season, the projected mean air temperature in the NRVE will be warmer than both areas, with the CRV following in subsequent order. As shows in Table 4 that the short rainy season projected future mean air temperature is to be increase in the range of 1.74 °C (CRV)-1.61 °C (ERVE) in 2050s and 2.38 °C (ERVE)-2.45 °C (NRVE) in 2080s for the RCP 4.5. By the 2050s and 2080s respectively, the projected future short rainy season mean air temperature will be expected to rise by 2.35 °C (ERVE)-2.43 °C (CRV) and 4.31 °C (NRVE)-4.35 °C (CRV) for the RCP 8.5 (Table 4). The projected dry season mean air temperature in the semi-arid rift valley locations is expected to rise in range of between 1.63 °C (NRVE) and 1.77 °C (CRV) in 2050s and during 2080s it will rise in range of 2.23 °C (ERVE)-2.37 °C (NRVE) for the RCP 4.5. The dry season projected mean air temperature rise will be expected in range of 2. 44 °C (ERVE) to 2.52 °C (CRV) by the 2050s and increase range of 4.26 °C (ERVE) to 5.55 °C (CRV) in 2080s for the RCP 8.5 (Table 4). As showed in Table 4, due to high uncertainty there is no value of the Melka Werer site located in CRV for the main rainy season, short rainy season and dry season.

During 2050s in CRV floor and ERVE, the mean seasonal air temperature will increase consistently from main rainy season to dry season in both RCP 4.5 and 8.5,

Table 4. Projected future mean air temperature (°C) change for the main rainy, short rainy, and dry season as compared to baseline period (1989-2019) under RCP 4.5 and RCP 8.5 scenarios in CRV floor, ERVE and NRVE of Ethiopia

Time Slices	Scenario	Season	CRV							ERVE			NRVE			
			Adami Tullu	Melkas-sa	Dhera	Abomsa	Mata-hara	Melka Werer	Mean	Miesso	Golol-cha	Mean	Kobo	Sirinka	Alamata	Mean
2050	RCP 4.5	MRS	1.57	1.53	1.52	1.99	1.65	1.65	1.65	1.56	1.56	1.56	1.73	1.61	1.74	1.69
		SRS	1.52	1.66	1.65	2.137	1.79	1.71	1.74	1.57	1.65	1.61	1.71	1.55	1.73	1.66
		DS	1.6	1.71	1.71	2.135	1.81	1.65	1.77	1.67	1.67	1.67	1.66	1.59	1.65	1.63
	RCP 8.5	MRS	2.2	2.18	2.17	2.64	2.29	2.26	2.29	2.22	2.21	2.22	2.56	2.27	2.39	2.41
		SRS	2.24	2.33	2.31	2.79	2.46	2.42	2.43	2.34	2.35	2.35	2.41	2.32	2.49	2.41
		DS	2.2	2.42	2.42	2.85	2.87	2.41	2.52	2.47	2.41	2.44	2.57	2.34	2.34	2.46
2080	RCP 4.5	MRS	2.2	2.28	2.27	2.56	2.39	2.47	2.36	2.26	2.29	2.28	2.44	2.34	2.48	2.42
		SRS	2.23	2.36	2.35	2.68	2.49	2.54	2.44	2.38	2.38	2.38	2.52	2.31	2.51	2.45
		DS	2.12	2.28	2.28	2.57	2.39	2.38	2.34	2.21	2.25	2.23	2.42	2.29	2.40	2.37
	RCP 8.5	MRS	4.06	4.1	4.07	4.50	4.16	-	4.18	3.98	3.75	3.87	4.43	4.25	4.48	4.38
		SRS	3.92	4.3	4.31	4.79	4.45	-	4.35	4.32	4.1	4.21	4.4	4.18	4.36	4.31
		DS	4.06	4.41	4.41	4.82	4.48	-	5.55	4.31	4.21	4.26	0.55	4.22	4.35	3.04

CRV=central rift valley, ERVE=eastern rift valley escapement, NRVE= northern rift valley escapement, MRS=main rainy season, SRS=short rainy season, DS=dry season but in NRVE there will be consistently increasing season mean air temperature from dry season to main rainy season in RCP 4.5. This indicated that in CRV and ERVE the dry season will warmer followed by the short rainy season, but in NRVE the main rainy season will warmer followed by the short rainy season. During the 2080s in CRV of Ethiopia, the dry season will warmer followed by the short rainy season, in RCP 8.5, whereas, in RCP 4.5 the short rainy season warmer than all followed by main rainy season .However, the short rainy season air temperature will warmer in ERVE and NRVE for RCP 4.5, but in 2080s for ERVE dry season and NRVE main rainy season will rapid warmer followed by a short rainy season for RCP 8.5 (Table 4). The report of Kassie et al. (2013) the seasonal projected future temperature in the CRV expected to increase, and Hadgu et al. (2013) and Adame and Abebe (2022) also reported that the seasonal air temperature in the northern expected to rise. This result reveals that growing season air temperature during crop growing season leads to aggravated evaporations and resulting in moisture stress suffered crops (Segele and Lamb, 2005). The ensembled climate models indicate that in the future the semi-arid rift valley of Ethiopia might be one of the most affected areas due to climate change and variability, with a simulated mean seasonal air temperature increase up to 4.82 °C in the mid and end century during the main rainy season compared to baseline (1989-2019) (Table 4). This finding corroborated by the finding of Mathur and Jajoo (2014), who noted that high air temperatures have an adverse impact on a variety of cellular processes involved in plant performance, which is directly linked to a decline in photosynthetic productivity and, ultimately, crop output. The use of long-duration cultivars is replaced by short-maturation ones, which have reduced yield potential, because of a rise in temperature (Wylie, 2008).

3.1.3. Projected extreme air temperature trend analysis in sorghum growing areas

Hot extremes. As indicated in Table 5, the trend analysis of the hottest day (TXx) and night (TNx) of the projected future maximum and minimum temperatures and their frequencies (TX90p and TN90p) will increase in the 2050s and 2080s under RCP 4.5 and 8.5 scenarios at Melkassa (CRV) and Mieso (ERVE) stations. However, the trend of the projected future TXx will decrease non significantly but the TNx and TX90P and TN90P will increase under RCP 4.5 and 8.5 during mid and end century at Kobo (NRVE) (Table 5). The TXx are projected to increase more than TNx at Melkassa and TNx are projected to increase than TXx at Mieso site. Other disagreeing reports found the projected future hot day and night frequency will be expected to decrease in the mid and end century in Ethiopia (McSweeney et al., 2008).

The projected future TNx will expect to increase more rapidly than the TXx over Melkassa and Mieso, whereas in the Kobo region the projected TXx to increase more than the TNx (Table 5). Consistent with the findings of this study, Omondi et al (2014), Dosio et al. (2018), and Kharin et al. (2018) indicated increasing trends in TXx and TNx over east Africa. This implies that extreme temperature rises as well as the increase in the frequency and intensity of droughts and floods are likely to reduce crop yields (World Bank, 2020). In Ethiopia, the projected future TXx and TNx are likely to increase, which will mostly affect the arid and semi-arid and pastoral areas in the country (McSweeney et al., 2008; Murken et al., 2020).

Cold extremes. The present study reveals that the analysis of the cool temperature metrics, namely, the coolest day (TXn) and coolest night (TNn), indicates an upward trend across the selected regions under two RCP, namely 4.5 and 8.5, during the 2050s and 2080s. However, it is noteworthy that the projected TNn will expected to show a non-significant decrease exclusively in the Kobbo region (Table 5). In contrast to Mieso region where the projected frequency of the coolest day (TX10P) does not exhibit a statistically significant decline, it is observed that both Melkassa and Kobo regions experience a notable decrease in the TX10P (Table 5). According to the findings, the projected frequency of the coolest night (TN10P) exhibited a non-significant decrease across both the 2050s and 2080s, as well as the RCP 4.5 and 8.5, in the Melkassa area. Furthermore, a decrease will be observed in Mieso for the RCP 4.5 across both time frames (2050s and 2080s). The findings suggest that the TN10P in Kobo is expected to increase in RCP 4.5 and 8.5, as well as in 2050s and 2080s. Additionally, an increase in the occurrence of TN10P is predicted for Mieso under the RCP 8.5, encompassing the time frames of 2050s and 2080s (Table 5). Cold extremes are a key factor in the rate of plant growth and development, as well as the distribution of plant genotypes in various regions of the planet (Ramankutty et al., 2008; Yadav, 2009). The consequence of cold extremes on plant growth rate and days to flowering varies among sorghum genotypes (Maulana and Tesso, 2013).

3.2. Projected change of rainfall in semi-arid CRV

3.2.1. Changes in annual and seasonal rainfall

Annual total rainfall change. As indicated by Table 6, the average projected future mean annual rainfall

Table 5. Trends in air temperature indices in the baseline period (1989-2019) and in 2050s and 2080s for the selected three stations in CRV floor, ERVE, and NRVE of Ethiopia under RCP 4.5 and 8.5 scenarios.

Parameters	CRV floor					ERVE					NRVE				
	Melkassa					Miesso					Kobbo				
	baseline	RCP 4.5		RCP 8.5			RCP 4.5		RCP 8.5		baseline	RCP 4.5		RCP 8.5	
	2019	2050	2080	2050	2080	2019	2050	2080	2050	2080	2019	2050	2080	2050	2080
TXx	0.071	0.072	0.076	0.07	0.068	0.022	0.004	0.004	0.001	0.0012	0.035	-0.017	-0.013	0.05	-0.13
TNx	0.0095	0.022	0.028	0.026	0.033	0.053	0.057	0.053	0.056	0.053	0.036	0.03	0.031	0.03	0.033
TXn	0.067	0.071	0.067	0.067	0.065	0.066	0.058	0.063	0.067	0.068	0.065	0.15	0.14	0.15	0.14
TNn	-0.01	0.004	0.002	0.002	0.005	0.01	0.025	0.024	0.02	0.034	0.015	-0.025	-0.02	-0.008	-0.015
TN10P	-0.035	-0.05	-0.04	-0.04	-0.046	-0.39	-0.305	-0.32	0.305	0.31	0.19	0.11	0.13	0.11	0.125
TX10P	-0.26	-0.18	-0.19	-0.18	-0.19	-0.15	-0.11	-0.15	-0.11	-0.15	-0.41	-0.17	-0.19	-0.17	-0.19
TN90P	0.21	0.14	0.14	**0.15**	0.14	0.42	0.24	0.25	0.24	0.25	0.29	0.103	0.11	0.103	0.11
TX90P	0.31	0.23	0.23	0.23	0.23	0.18	0.11	0.12	0.12	0.12	0.65	0.23*	0.22*	0.22*	0.23*

Bolds figures indicates statistical significance at less than 5% alpha level.
CRV=central rift valley, ERVE=eastern rift valley escapement, NRVE= northern rift valley escapement.

output of five global circulation models (GCMs), namely, CSIRO-Mk3.6.0, HadGEM2-ES, IPSL-CM5AMR, MIROC5, and MRI -GCM3, suggests a mixed change in most of the stations located in the CRV floor and ERVE. The range of this decline is estimated to be between 0.6% (Dhera)-5.5% (Melka Werer) and 0.32% (Mieso) during the 2050s in the RCP 4.5, relative to the baseline period(1989-2019). Towards the 2080s, compared to the reference period of 1989-2019, it is projected that the annual average rainfall will decrease significantly in various regions. Specifically, the CRV floor, ERVE and NRVE are predicted to experience declines ranging from 0.67% (Melkassa)-10.1% (Melka Werer), 3.1% (Gololcha)-4.9% (Mieso), and 0.9% (Alamata)-4.6% (Sirinka) under RCP 4.5. The projected future annual rainfall as presented in Table 6, in some analyzed areas will be expected to rise in the range of 0.9 (Matahara)-12.3%(Abomsa), 22.3% (Golocha) and 6.1 (Alamata)-14.6% (Sirinka) respectively in the CRV, ERVE and NRVE during 2050s. In the other hands, the projected total annual rainfall will expected to be rise in NRVE in range of 6.1% (Alamata)-14.6% (Sirinka) during 2050s for the RCP 4.5.

The mid-century ensembles for mean annual rainfall in Ethiopia suggest significant uncertainty regarding both the magnitude and direction of changes across the models, particularly with respect to the RCP 4.5 (McSweeney et al., 2008; USAID, 2015). Various reports have offered distinct projections regarding the mean total rainfall in different regions of Ethiopia. For instance, some have suggested a decrease in north-east Ethiopia (MoFE, 2015), while others have predicted an increase in north Ethiopia (Adam and Abebe, 2022) and eastern Ethiopia (Teshoma et al., 2022). Meanwhile, other studies have observed a decrease in the CRV (Kassie et al., 2013) as well as northern Ethiopia (MoFE, 2015). In general, reported by McSweeney et al. (2008), different models projected in the ensemble are broadly consistent in indicating increases in annual rainfall in Ethiopia.

In a congruent manner, the RCP 8.5 projected for the 2050s and 2080s exhibits a discernible pattern of annual total rainfall increase across all examined locations (Table 6). In the context of a RCP 8.5 during the 2050s, the researched locations within the CRV, ERVE and NRVE will predicted to experience an annual increase in total rainfall within the ranges of 1.3-13.7%, 7.5%, and 16-18.4%, respectively (Table 6). Conversely, towards the 2080s under the same RCP 8.5, substantial increases in total rainfall will expected, with ranges of 9.3-40.9% for the CRV, 22.3% for the ERVE, and 31.3-32.5% for the NRVE (Table 6). This result is consistent with the reports of CCKP (2020), the annual mean rainfall slightly increases by the 2080s, under RCP 8.5 in Ethiopia and as reported by Nikulin et al. (2018) and Osima et al. (2018) the projected mean annual rainfall will be higher, particularly in the eastern parts of east Africa will expected.

Seasonal rainfall's change. As presented in Table 6, the ensemble output of the Global Circulation Models (GCMs) indicates a projected decrease in the future main rainy season rainfall. This reduction is expected to occur within the range of 1.45% to 53.8%, across more than 50% of locations in the CRV area. Only Mieso in ERVE exhibited such a decrease in 0.83% of rainy season rainfall. The

Table 6. Projected changes in percentage (%) of the annual and seasonal rainfall totals in CRV floor, ERVE, and NRVE of Ethiopia in 2050s and 2080s under RCP4.5 and 8.5 scenarios.

Rainfall	Time horizon	Scenarios	CRV floor						ERVE		NRVE		
			Adami Tullu	Melkassa	Dhera	Abomsa	Matahara	Melka Werer	Mieso	Gololcha	Kobbo	Sirinka	Almata
Annual	2050	RCP 4.5	-4.9	0.86	-0.6	12.3	0.9	-5.5	-0.32	22.3	10.2	14.6	6.1
		RCP 8.5	1.3	-3.5	7.9	24.4	13.7	5.04	-4.5	7.5	-2.4	18.4	16.6
	2080	RCP 4.5	-2.1	-0.67	-5.9	7.3	-2.3	-10.1	-4.9	-3.12	18.4	-4.6	-0.9
		RCP 8.5	9.3	-5	19.2	40.9	26.8	15.2	-55.6	22.3	32.5	31.3	32.4
Main Rainy Season	2050	RCP 4.5	-53.8	-1.45	0.62	9.1	-1.7	-8.8	-0.83	43.8	14.3	19.15	9.2
		RCP 8.5	-8.5	-8.01	7.9	16.2	6.6	-0.9	-13.2	0.8	-6.02	22.55	20.9
	2080	RCP 4.5	-10.4	-8.16	-6.14	0.6	-7.9	-15.05	-13.46	-10.8	23.9	-4.8	-4.35
		RCP 8.5	-7.2	-18.5	18.9	33.2	20.4	7.9	9.2	43.8	34.3	55.6	34.8
Short rainy season	2050	RCP 4.5	0.9	4.8	-5.1	3.1	2.5	-1.9	-0.12	28.8	10.3	4.35	3.6
		RCP 8.5	14.6	23.2	9.9	36.2	25.9	15.6	0.48	14.14	15.1	8.86	14.3
	2080	RCP 4.5	5.2	6.3	-3.6	16.6	6.2	-1.8	4.2	3.7	1.3	-1.3	0.43
		RCP 8.5	21.8	35.6	21.8	49.8	35.3	31.7	38.9	28.8	36.9	68	33.8

CRV=central rift valley, ERVE=eastern rift valley escapement, NRVE= northern rift valley escapement.

projected main rainy season in the CRV and ERVE will be more mixed change during mid-century in the RCP 4.5 (Table 6). However, in the NRVE, an increase ranging from 9.2% to 19.15% is expected during the 2050s in the RCP 4.5 compared to the base period. In contrast to the base period at the 2080s, it is projected that there will be a decrease in the amount of rainfall during the main rainy season across all examined regions under the RCP 4.5 expected Abomsa increase (Table 6). According to the projections based on the RCP 8.5, it is projected that the main rainy season will experience an increase of 6.6-16.2%, 0.8%, and 20.9-22.5% in the CRV floor, ERVE and NRVE, respectively, during 2050s, relative to the baseline period. In the present study, it found that an increase in the percentage of the main rainy season is expected during the 2080s. Specifically, the CRV floor, ERVE and NRVE will be expected to experience an increase in the range of 7.9-33.2%, 9.2-43.8%, and 34.3-55.6%, respectively, in comparison to the baseline period spanning from 1989 to 2019. Moreover, the mean result indicated a decrease in the projected future main rainy season for Melkassa and Adami Tullu, while an increase will be observed for Abomsa under both time frames (2050s and 2080s) and scenarios (4.5 and 8.5) (Table 6). The similar reports indicated that (Gutierrez et al., 2021; Otieno and Anyah, 2013; Kent et al., 2015) the projected future main rainy season mean rainfall will expected to increase under 2080s in east Africa.

Compared to the baseline period, it is projected that the mean short rainy season rainfall in the semi-arid Rift Valley of Ethiopia will experience a notable increase in the future.in both emission scenarios (4.5 and 8.5) and time frames (2050s and 2080s). However, it is projected that there will be a decline in rainfall in the locations of Dhera, Melka Werer, and Mieso by 2050s in RCP 4.5 and decrease at Dhera, Melka Werer and Sirinka by 2080s in RCP 4.5 (Table 6). This result was confirmed with the reports of Masilin et al. (2020), during the short rainy season, a longer rainfall projected over East Africa.

Regarding the local effects of climate variables, the significance of seasonal values is much more relevant than that of annual values. The projected mean seasonal rainfall will be expected to increase in the short rainy season than the main rainy season and more increase in NRVE than CRV and ERVE (Table 6). Current research suggests that an increase in rainfall is likely to give rise to a rise in crop productivity. Furthermore, it has been observed that crop productivity is notably more responsive to variations in rainfall compared to those in temperature (Kang et al., 2009). Moreover, it is crucial to employ moisture harvesting techniques to optimize crop production.in regions.

3.2.2. Projected future rainfall extremes trends

Maximum 1- and 5-days rainfall (R1xdays and R5xdays). The analysis of trends in the projected future maximum average rainfall for R1xdays and R5xdays, as presented in Table 7, reveals that there will be a discernible decrease at Melkassa and Kobo. Meanwhile, at Mieso, there will be a slight upward trend during the 2050s and 2080s periods under RCP 4.5. The analysis of projected future trends for R1xdays and R5xdays, as presented in Table 7, indicates a slight decline in trend of Kobo under RCP 8.5 between the years 2050s and 2080s. Meanwhile, an increase in R5xdays will expect at Melkassa during the same period. Additionally, R1xdays will predict to increase in the year 2050s but decrease in 2080s under the aforesaid climate scenario. At the location of Mieso, it is projected that the trend regarding future R1xdays will exhibit a slight increase in the years 2050s and 2080s, while R5xdays are expected to experience a marginal increase during the 2050ss period, followed by a decrease in the 2080s period under the influence of RCP 8.5.

Heavy and very heavy rainfall days (R10 and R20). The projected annual number of days with heavy rainfall (R10) over Melkassa, Mieso, and Kobo showed a decreasing trend under RCP 4.5 and RCP 8.5 in 2050s and 2080s. Although the predicted occurrence of excessively rainy days (R20) in the studied regions is high, the trend of such days will be expected to decreasing in magnitude, but not in a systematic manner (Table 7).

Very and extremely wet days (R95P and R99P). According to the findings presented in Table 7, the analysis reveals that Mieso will be poised to experience non-significant positive trends in the frequency of both very wet (R95p) and extremely wet (R99) days under RCP 4.5 and 8.5 during the both periods (2050s and 2080s). Conversely, Kobo projected to experience a non-significantly decreased frequency of rainy days during the same period, as indicated by the aforesaid data. At the Melkassa location, the analysis of projected future very wet day (R95P) trends indicates an upward trajectory under RCP 4.5 and 8.5 during the time frames (2050s and 2080s). Conversely, there will be an insignificant decrease in the trend of extremely wet days (R99P) under RCP 4.5 regime in the year 2050s, while there is an increase under RCP 8.5 during 2050s, and a decline during 2080s (Table 7).

Total rainfall (PRCPTOT). A trend analysis of projected future total rainfall, as presented in Table 7, will demonstrate a statistically non-significant negative trend across all stations, under both emission scenarios (RCP 4.5 and 8.5), and time frames (2050s and 2080s). The current study discloses that the overall rainfall patterns at three distinct locations, namely, Melkassa in the CRV floor, Miesso in the ERVE, and Kobo in the NRVE, will be projected to experience a non-significant reduction ($P<0.05$) in the order of 1.47, 1, and 3.96 mm/day under the RCP 4.5 by mid-century. Furthermore, by the end of the century, the projected reduction in rainfall will be estimated to be 1.15, 1.07, and 3.65 mm/day for the aforesaid study sites. The total rainfall at aforeside studied sites will decrease statistically non-significantly($P<0.05$) by 1.91, 0.38, and 4.25 mm/day in the mid-century and during the end century will decline in 1.37, 1.8 and 5.2 mm/day. This indicated that the amount of rainfall decreases in the time extent, and the water requirement of rain-fed crops will be affected, thereby increasing increase the water demand for sup-

Table 7. Rainfall indices (per decade) trend in the 2050s and 2080s compared to base period (1989-2019) for the selected three stations Melkassa (CRV floor), Mieso (ERVE) and Kobo (NRVE) of Ethiopia under RCP 4.5 and 8.5 scenarios.

	CRV floor					ERVE					NRVE				
	Melkassa					Mieso					Kobo				
	RCP 4.5			RCP 8.5		RCP 4.5			RCP 8.5		RCP 4.5			RCP 8.5	
	2015	2050	2080	2050	2080	2015	2050	2080	2050	2080	2015	2050	2080	2050	2080
RX1da y	-0.20	-0.058	-0.17	0.023	-0.13	0.25	0.24	0.048	0.24	0.17	0.05	-0.32	-0.096	-0.25	-0.35
RX5da y	0.098	-0.09	-0.062	0.027	0.0008	0.13	0.068	0.076	0.08	-0.02	0.13	-0.5	-0.53	-0.35	-0.58
R10	-0.095	-0.13	-0.14	-0.22	-0.3	-0.07	-0.09	-0.13	-0.3	-0.55	-0.059	-0.1	-0.2	-0.17	-0.12
R20	0.02	-0.19	-0.17	-0.21	-0.25	-0.125	-0.15	-0.14	-.0.16	-0.06	0.055	-0.02	-0.016	-0.07	-0.13
CDD	0.67	0.95	0.72	1.05	0.77	0.67	1	1	1	1	0.33	0.35	0.36	0.17	0.36
CWD	0.04	0.04	0.04	0.04	0.04	-0.1	-0.1	-0.07	-0.25	-0.1	0.18	0.3	0.067	0.3	0.3
PRCPTOT	-0.41	-1.47	-1.15	-1.99	-1.37	-0.43	-1.	-1.07	-0.38	-1.8	-4.16	-3.96	-3.65	-4.25	-5.2
SDII	-0.02	-0.02	-0.018	-0.029	-0.017	0.04	0.06	0.06	0.05	0.06	0.0086	-0.017	-0.0053	-0.08	-0.11
R95P	1.2	1.01	0.84	0.68	1.47	0.72	0.93	0.1	0.64	0.4	-0.35	-1.65	-0.93	-0.81	-0.84
R99P	-0.0003	-0.77	-1.5	0.071	-1.8	1.3	2.2	2.3	2.3	0.02	0.075	-0.18	-0.15	-0.3	-0.28

CRV=central rift valley, ERVE=eastern rift valley escapement, NRVE= northern rift valley escapement.

plementary irrigation, and affecting groundwater potential in the semi-arid Rift Valley region of Ethiopia.

Consecutive dry and wet days (CDD and CWD). The results of the study suggest that the projected future trend of maximum consecutive days with less than 1mm rainfall (CDD) at the Melkassa, Mieso and Kobo study sites will exhibit an insignificant increase during 2050s and 2080s and in RCP 4.5 and 8.5 (Table 7).Alternatively, the projected maximum number of consecutive days with rainfall greater than 1mm (CWD) at Melkassa and Kobo sites will reveal an increasing trend during both time frames (2050s and 2080s) and emission scenarios (4.5 and 8.5) but decrease at Mieso in all conditions. The findings of the study reveal that the projected future consecutive dry days (CDD) featuring a rainfall amount below 1mm (CDD) will expected to exhibit an insignificant increase in trend, while the consecutive wet days (CWD) characterized by a rainfall quantity greater than 1mm (CWD) will predicted to exhibit an insignificant decrease in trend specifically at the locality of Mieso in ERVE under RCP 4.5 and 8.5, within the timeframes of 2050s and 2080s (Table 7). According to a report by the World Bank (2019), it has been confirmed that in East Africa, and particularly in Ethiopia, there is a probability of increased extremity in both dry and wet periods in the forthcoming.

Simple daily intensity index (SDII). The analysis of trends for the projected future SDII reveals a reduction in trend over the Melkassa and Kobo regions, while indicating an upward shift in trend over the Mieso region. This trend is observable across both the RCP 4.5 and 8.5 scenarios, except for a projected decrease in trend at Kobo, specifically in RCP 8.5 during the period spanning 2050s. The major climate extremes that significantly affect various socioeconomic activities are drought and floods, in which understanding the intensity and frequency of extreme is actual significant (Lyon and DeWitt, 2012). The annual projected upcoming rainy day with strong variability characterized with a significant trend during the mid and end century across the studied locations (Table 7). Increasing in the number of CDDS and decreasing in the number of CWDS in the study area, especially during the main rainy season, could affect crop growth and yield, water availability for irrigation, animals, and municipal uses.

3.2.3. Projected future growing season

The changes in the projected future onset and cessation of the main rainy season in the CRV, ERVE and NRVE in comparison with the baseline periods (1989-2019) presented in Table 8. The result reveals that the onset and cessation of the main rainy season as well as the length of the growing period will vary spatially among the stations considered in this study.

Start of the main rainy season (SOS). The projected onset of the rainy season will be expected to delayed in half of the studied sites by 2-4 (Dhera, Melkass and Abomsa) days in the CRV, by 5 (Mieso) days in the ERVE, and by 2 days in all sites in the NRVE during mid-century in RCP 4.5 (Table 8). However, extended in some sites in the CRV by 1-7 (Adami Tullu, Melka werer and Matahara) days and in the ERVE by 3 (Gololcha) days in RCP 4.5 during 2050s. By the 2080s, the onset of the rainy season will be expected to be delayed by 1-14 (Melkassa-Melka Werer). 3 (Mieso) and 1 (Kobo) days in the CRV, ERVE and NRVE, under RCP 4.5. In CRV and ERVE, the projected onset season will be extended by 2-4 days and by 8 days in RCP 4.5 during 2080s. In RCP 8.5 in more than half of the study sites, the onset of the rainy season in 2050s will be expected to be delayed by 1-13.8, 2-3 days in CRV, ERVE, and NRVE respectively (Table 8). The rainy season's onset will be delayed in most of the studies by 2-16, 1-9, and 2-4 days in the same location in 2080s under RCP 8.5 respectively. In CRV and ERVE, the onset will be extended by 4-6 and 3 days, respectively, in 2050s and 2080s. In CRV, it will be extended by 4-6 days in RCP 8.5. NRVE shows no delay in 2050s and 2080s. Moreover, the finding depicts, these changes have been observed in mixed change and more variability in rainy season onset expected in the analyzed areas in the upcoming. There will be more onset of the rainy season variability in RCP 8.5 than RCP 4.5. From the regions CRV is more variable followed by ERVE. Significant changes and variations in the onset of high rainy seasons will expected to occur more frequently in RCP 8.5 when compared to RCP 4.5.

End of the season (EOS). The projected end of the season in all examined sites is expected to be extended in both time frames (2050s and 2080s) and scenarios (4.5 and 8.5) as indicated in Table 8. Specifically, the end of the season is expected to be prolonged by a range of 1-8, 3-4, and 1-3 days in CRV, ERVE, and NRVE areas, correspondingly, under RCP 4.5 during 2050s. Likewise, in these same areas, the end of the season is expected to be extended by a range of 1-4, 2-3, and 1-3 days in RCP 4.5. However, under RCP 8.5, the end of the season is expected to be prolonged by 1-7 and 1-15 days in both time frames (2050s and 2080s). The persistence at the end of the season is expected to exhibit a more noticeable manifestation in the CRV compared to the ERVE and NRVE a outlet.

Length of the growing season (LGS). The expected length of the growing season for the CRV, ERVE, and

Table 8. Projected change of SOS, EOS, and LGP the absolute difference between projected and baseline periods (1989-2019) at different stations in the CRV floor, ERVE and NRVE of Ethiopia.

Feature	Scenarios	Periods	CRV floor						ERVE		NRVE		
			A/Tullu	Melkassa	Dhera	Abomisa	Matahara	M/Werer	Mieso	Gololcha	Kobo	Alamata	Sirinka
SOS		Baseline	189	182	169	183	191	197	200	180	198	201	186
	RCP4.5	2050	3	-2	-2	-4	7	1	-5	3	-2	-2	-2
		2080	4	-1	2	-2	4	-14	-3	8	-1	0	0
	RCP8.5	2050	4	-1	6	-4	-3	-13	-8	3	-3	0	-2
		2080	4	-2	6	-3	-2	-16	-9	-1	-3	-4	-2
EOS		Baseline	276	276	282	284	275	275	275	283	275	275	275
	RCP4.5	2050	1	2	2	8	1	0	3	4	3	3	1
		2080	0	2	2	4	1	0	3	2	3	2	1
	RCP 8.5	2050	1	1	2	7	1	0	3	3	2	2	1
		2080	1	8	5	15	2	0	4	10	4	3	3
LGP		Baseline	87	96	113	101	85	78	75	103	77	74	89
	RCP 4.5	2050	-3	2	2	2	1	-1	8	1	5	4	3
		2080	-4	-1	1	1	-4	12	0	-6	3	2	0
	RCP 8.5	2050	-3	0	-4	3	3	9	10	0	5	-1	3
		2080	-4	8	-1	10	3	14	12	11	7	7	5

CRV=central rift valley, ERVE=eastern rift valley escapement, NRVE= northern rift valley escapement.

NRVE regions during the period of 2050s under the RCP 4.5 scenario is projected to increase by 1-2, 1-8, and 3-8 days, respectively (Table 8). However, in the CRV and NRVE regions, the expected extension is projected to be upto12 and 3 days, respectively, during 2080s, while ERVE is expected to remain unchanged during the same period. Under the RCP 8.5 in some studied sites, the length of the growing season is expected to be prolonged by 3-9, 10, and 3-5 days, respectively, in the CRV, ERVE and NRVE during 2050s respectively. Additionally, in the same regions and scenario, the projected extension is expected to be 3-14, 11-12, and 5-7 days in 2080s, respectively. The existing empirical evidence suggests that significant heterogeneity exists regarding the length of the growing period in the areas under analysis. The current study presents a significant observation regarding deviation levels, which exhibit a pronounced increase in the CRV when compared to the ERVE and NRVE.

The present investigation focuses on examined regions, wherein the projected growing season characteristics including onset, end, and length exhibit notable variations and modifications within two distinct time frames, namely 2050s and 2080s, as well as under distinct scenarios: 4.5 and 8.5, when compared with the base period. Therefore,the findings suggest that alterations to agricultural practices, such as adjusting planting timing and utilizing sorghum varieties with early or medium maturation periods, may be necessary for farmers in the region to address the changes observed in onset and cessation dates. Management measures related to soil, particularly those addressing flooding and water logging problems, must receive considerable attention.

4. CONCLUSIONS AND RECOMMENDATIONS

The study shows an increasing projected annual and seasonal minimum and maximum air temperatures in the Sami-arid rift valley of Ethiopia based on both emission scenarios (RCP 4.5 and 8.5) and time frames (205 and 2080s). The change in the projected future mean air temperature is more dramatic in minimum air temperature than maximum air temperature, and the magnitude of the change depends on location, emission scenarios, and time frames. The results of the analysis suggest that, at RCP 4.5, CRV is projected to exhibit higher air temperatures than two other regions, namely, ERVE and NRVE, in 2050. However, under RCP 8.5, NRVE is expected to experience greater levels of warmth during 2080 than 2050. The result shows that, during the main growing season, the NRVE will be warmer followed by CRV in subsequent order. Hottest day and night temperatures and their frequencies will increase in both time frames (2050s and 2080s) and scenarios at Melkassa and Mieso stations. However, the trend for the projected hottest days will decrease non-significantly, while the hottest nights, day and night frequency will increase under RCP 4.5 and 8.5 at Kobbo during 2050 and 2080.

The percentage change of mean annual rainfall is projected to a mixed change in the stations located in CRV and ERVE, whereas, in NRVE it will projected to increase under RCP 4.5 in 2050s. However the projected annual rainfall under RCP 4.5 in 2080s will be decline in the analyzed semi-arid rift valley of Ethiopia. In most of the location in CRV and ERVE stations the projected rainy season rain will be decline, whereas, in NRVE it will projected to increase in period of 2050s under RCP 4.5. Rainfall will decrease in semi-arid rift valley except Abomsa during the main rainy season in 2080s under RCP 4.5. Future maximum average rainfall for R1xdays and R5xdays will decrease at Melkassa and Kobo, while in Mieso, a slight upward trend in 2050s and 2080s under RCP 4.5. In Kobo's R1xdays and R5xdays slightly decline by 2050s and 2080s under RCP 8.5. The annual heavy rainfall days (R10)will decrease in Melkassa, Mieso, and Kobo under RCP 4.5 and RCP 8.5 in 2050s and 2080s. Very heavy rainfall days (R20) days will still occur to decrease in magnitude. The trend analysis of R95P will experience to increase at Melkassa and Mieso but decrease at Kobbo in both time frames (2050s and 2080s) and scenario (4.5 and 8.5). While, the projected R99P will experienced to mixed change at Melkassa and decline at Kobo in both time frames(2050s and 2080s) and scenario(4.5 and 8.5). A trend analysis of projected future total rainfall (PRCPTOT) will demonstrate a negative trend across all stations, under both emission scenarios (RCP 4.5 and 8.5), and time frames (2050s and 2080s). This study shows that rainfall (PRCPTOT) patterns in Melkassa, Miesso, and Kobo will have reducting pattern by 2050s with RCP 4.5. Study results suggest CDD trends will insignificantly increase at Melkassa, Mieso, and Kobo by 2050s and 2080s under RCP 4.5 and 8.5. CWD trend will increase at Melkassa and Kobo, but decrease at Mieso in all conditions.

Additionally, the result reveals that the annual and main rainy season rainfall, onset, ends, and the length of growing period will vary spatially among the stations considered for the study. This would influence moderate variations in LGP in some stations. Consequently, the finding highlights the position of site-specific efforts to increase local adaptive capacity. Thus, farmers in the region might require a modification in agricultural operations such as planting time, early or medium maturing sorghum verity corresponding to the modification in onset and cessation dates. Furthermore, attentions needs to be given the management measures related to soil and moisture conservation practice in the studied areas.

FUNDING'S

This Research as part of its staff Capacity Programme which was funded by the EIAR'

REFERENCE

Abbas, F., A. Ahmad, M. Safeeq, S. Ali, F. Saleem, H.M. Hammad, W. Farhad, 2013. Change inrainfal extremes over arid to semiarid and subhumid Punjab, Pakistan. *Theoretical and AppliedClimatology*, 116: 671-680. https://doi.org/10.1007/s00704-013-0988-8.

Abera Gayesa Tirfi ,2022. Sorghum yield response to climate and other input factors in Ethiopia. International Journal of Agriculture and Food Science https://www.agriculturaljournals.com

Adem Mohammed and Abebe Misganaw2022 Modeling future climate change impacts on sorghum (Sorghum bicolor) production. CABI Agriculture and Bioscience (2022) 3:22, https://doi.org/10.1186/s43170-022-00092-9

Agostini A., Bonini M., Corti G., Sani F., Manetti P.; Distribution of Quaternary deformation in the central Main Ethiopian Rift, East Africa, Tectonics, 30, TC4010, https://doi.org/10.1029/2010TC002833.

Amadi S.O., S.O. Udo , and I.O. Ewona,2014 Trends And Variations Of Monthly Mean Minimum And Maximum Temperature Data Over Nigeria For The Period 1950-2012. International Journal of Pure and Applied Physics Vol.2,No.4, pp.1-27, December 2014Published by European Centre for Research Training and Development UK (www.eajournals.org).

Arndt, C.; Robinson, S.;Willenbockel, D. Ethiopia's growth prospects in a changing climate: A stochastic general equilibriumapproach. Glob. Environ. Chang. 2011, 21, 701–710. (CrossRef)

Ceci, P., Monforte, L., Perelli, C., Cicatiello, C., Branca, G., Franco, S., Binta, F., Diallo, S., Blasi, E., and Scarascia, G. (2021). Smallholder farmers' perception of climate change and drivers of adaptation in agriculture: A case study in Guinea. *Rev Dev Econ*, 00:1-22.

CGIAR (2018). Climate Resilient Green Economy Strategy. Sector-wise GTP II Implementation Monitoring Checklist. CGIAR Research Program on Climate Change, Agriculture and Food Security (CCAFS), East Africa. URL: https://ccafs.cgiar.org/publications/climate-resilient-green-economy-strategy#.

CIAT; BFS/USAID. 2017. Climate-Smart Agriculture in Ethiopia. CSA Country Profiles for Africa Series. International Center for Tropical Agriculture (CIAT); Bureau for Food Security, United States Agency for

International Development (BFS/USAID), Washington, D.C. 26 p.

Climate Change Knowledge Portal (CCKP, 2020)WB. Interactive Climate Indicator Dashboard Agriculture. Ethiopia.WoldBank,databaseURL:https://climatedata.worldbank.org/CRMePortal/web/agriculture/crops-and-land management?country=ETH&period=2080-2099.

Collins, W. J. et al. Development and evaluation of an earth-system model -hadgem2. Geosci. Model Devel. 4, 1051-1075 (2011).

Conway, D. and E.L.F. Schipper, 2011.Adaptation to climate change in Africa: challenges and opportunities identified in Ethiopia. Global Environmental Change, 21(1), 227-237.

Corti .G.. "The Ethiopian rift valley: geography and morphology". CNR-IGG. Retrieved 2013-08-02.

Da Silva, R.M., Santos, C.A.G., Moreira, M. et al., 2015. Rainfall and river flow trends using Mann–Kendall and Sen's slope estimator statistical tests in the Cobres River basin. Nat Hazards 77, 1205–1221 (2015). https://doi.org/10.1007/s11069-015-1644-7.

Dodd, D. and Jolliffe, I. 2001. Early Detection of the Start of the Wet Season in Semiarid Tropical Climates of WesternAfrica. *International Journal of Climatology*, 21, 1251-1262. https://doi.org/10.1002/joc.640 (CrossRef).

Dosio, A., Mentaschi, L., Fischer, E. M., Wyser, K., 2018. Extreme heat waves under 1.5°c and2°c global warming. Environ. Res. Lett. 13,054006. https://doi.org/10.1088/1748-9326/aab827

Dufresne, J. L. 2013. Climate change projections using the IPSL-CM5 Earth System Model: from CMIP3 to CMIP5. Climate Dynamics, 5:1-43.

Edao AL, Kibert K, Mamo G ,2018. Analysis of Start, End and Length of the Growing Season and Number of Rainy Days in Semi-Arid Central Refit Valley of Oromia State, Ethiopia. Adv Crop Sci Tech 6: 386. https://doi.org/10.4172/2329-8863.100038

FAO (Food and Agriculture Organization) (1984). Assistance with land use planning in Ethiopia:geomorphology and soil. Report prepared and submitted to the Government of Ethiopia. AGDA. ETH/78/003, Field Document 3.

FAO, 2011. The State of Food and Agriculture 2010–2011. FAO, Rome

Fowler, H.J., S. Blenkinsop, C. Tebaldi, 2007. Linking climate change modeling to impact studies:recent advances in downscaling techniques for hydrological modeling. Review *International Journal of Climatology*, 27: 1547-1578.

Gebrechorkos, S. H., Taye, M. T.,Birhanu, B., Solomon, D., & Demissie,T. (2023). Future changes in climate and hydroclimate extremes in East Africa.Earth's Future, 11, e2022EF003011. https://doi.org/10.1029/2022EF003011

Getinet, G., MacAlister, C., 2012. Integrated innovation and recommendation domains: Paradigm for developing,scaling-out, and targeting rainwater management innovations. Ecological Economics 76, 34-41.

Ghosh, S., P.P. Mujumdar, 2008. Statistical downscaling of GCM simulations to stream flow using relevance vector machine. *Advance Water Resource*, 31: 132–146.

Girma Mamo. 2005. Using seasonal climate outlook with advice on sorghum production in the Central Rift Valley of Ethiopia. PhD thesis, Blomefontein, Republic of South Africa

Green, T.R., M. Taniguchi, H. Kooi, J.J. Gurdak, D.M. Allen, K.M. Hiscock, H. Treidel, A. Aureli,2011. Beneath the surface of global change: Impacts of climate change on groundwater. *Journal of Hydrology*, 405: 532-560.

Gutiérrez, J. M., Jones, R. G., Narisma, G. T., Alves, L. M., Amjad, M., Gorodetskaya, I. V., Grose, M., Klutse, N. A. B., Krakovska, S., Li, J., Martínez-Castro, D., Mearns, L. O., Mernild, S. H., Ngo-Duc, T., Hurk, B. V. D. & Yoon, J.-H. 2021. Atlas. *In:* Masson-Delmotte, V., Zhai, P., Pirani, A., Connors, S. L., Péan, C., Berger, S., Caud, N., Chen, Y., Goldfarb, L., Gomis, M. I., Huang, M., Leitzell, K., Lonnoy, E., Matthews, J. B. R., Maycock, T. K., Waterfield, T., Yelekçi, O., Yu, R. & Zhou, B. (Eds.) *Climate Change 2021: The Physical Science Basis. Contribution Of Working Group I To The Sixth Assessment Report Of The Intergovernmental Panel On Climate Change* Cambridge, Uk.

Hadgu G, Tesfaye K, Mamo G, Kassa B (2013) Trend and variability of rainfall in Tigray, Northern Ethiopia: analysis of meteorological data and farmers'perception. Acad J Agric Res 1(6): 88-100

Hatfield, J.L.; Boote, K.J.; Kimball, B.A.; Ziska, L.H.; Izaurralde, R.C.; Ort, D.; Thomson, A.M.; Wolfe, D. Climate impacts on agriculture: Implications for crop production. Agron. J. 2011, 103, 351-370. https://doi.org/10.2134/agronj2010.0303

Hudson, N.I., and A.C. Ruane, 2015: Appendix 2. Guide for Running AgMIP Climate Scenario Generation Tools with R in Windows, Version 2.3. In *Handbook of Climate Change and Agroecosystems: The Agricultural Model Intercomparison and Improvement Project (AgMIP) Integrated Crop and Economic Assessments, Part 1*. C. Rosenzweig and D. Hillel, Eds., ICP Series on Climate Change Impacts, Adaptation, and Mitigation, vol. 3, Imperial College Press, pp. 387-440.

IMF (International monetary fund). 2020. Ethiopian statistical Appendix, Washington, DC, IMFcountry report no. 02/214.

IPCC, 2019: Summary for Policymakers. In: Climate Change and Land: an IPCC special report on climate change, desertification, land degradation, sustainable land management, food security, and greenhouse gas fluxes in terrestrial ecosystems [P.R. Shukla, J. Skea, E. Calvo Buendia, V. Masson-Delmotte, H.- O. Pörtner, D. C. Roberts, P. Zhai, R. Slade, S. Connors, R. van Diemen, M. Ferrat, E. Haughey, S. Luz, S. Neogi, M. Pathak, J. Petzold, J. Portugal Pereira, P. Vyas, E. Huntley, K. Kissick, M. Belkacemi, J. Malley, (eds.)]. In press.

IPCC, 2014. Summary for policymakers. In: Climate change 2014:Impacts, adaptation, and vulnerability. Part A: Global and sectoral aspects. Contribution of Working Group II to the Fifth Assessment Report of the Intergovermental Panel on Climate Change [Field CB, Barros VR, Dokken DJ, Mach KJ, Mastrandrea MD, Bilir TE, Chatterjee M, Ebi YL, Estrada YO, Genova RC, Girma B, Kissel ES, Levy AN, MacCracken S, Mastrandrea PR, White LL (eds)]. Cambridge University Press, Cambridge, UK and New York, USA. pp 1–32

IPCC, 2013. In: Stocker, T.F., Qin, D., Plattner, G.-K., Tignor, M., Allen, S.K.,Boschung, J., Nauels, A., Xia, Y., Bex, V. and Midgley, P.M. (Eds.) ClimateChange 2013: The Physical Science Basis. Contribution of Working Group Io the Fifth Assessment Report of the Intergovernmental Panel on Climate Change. Cambridge and New York, NY: Cambridge University Press, 1535 pp

IPCC, 2007. Summary for policymakers. In: Metz B, Davidson OR, Bosch PR, Dave R, Meyer LA (eds) Climatechange: mitigation. Contribution of Working Group III to the Fourth Assessment Report of the Intergovernmental Panel on Climate Change. Cambridge University Press; 2007.IPCC., 2018c. Global Warming of 1.5° C: An IPCC Special Report on the Impacts of GlobalWarming of 1.5° C Above Pre-Industrial Levels and Related Global Greenhouse Gas Emission Pathways, in the Context of Strengthening the Global Response to the Threat of Climate Change, Sustainable Development, and Efforts to Eradicate Poverty.Intergovernmental Panel on Climate Change

Irish AID, 2018. Ethiopia Country Climate Risk Assessment Report. Irish AID, Resilience and Economic Inclusion Team, Policy Unit. Available at: climathttps://www.climatelearningplatform.org/change team;%0A.

James Rachel and Washington Richard,2014. African Climate Change Uncertainty in Perturbed Physics Ensembles: Implications of Global Warming to 40C and Beyond . https://doi.org/10.1175/JCLI-D-13-00612.1

Jansen, H., Hengsdijk, H., Legesse, D., Ayenew, T., Hellegers, P., Spliethoff, P., 2007. Land and water resources assessment in the Ethiopian Central Rift Valley Alterra Report 1587. Wageningen, the Netherlands

Jones, P.G., P.K. Thornton. 2013. Generating downscaled weather data from a suite of climate models for agricultural modelling applications. *Agricultural Systems*, 114: 1-5.

Joshi Manoj, Ed Hawkins, Rowan Sutton1, Jason Lowe2 and David Frame, 2011.Projections of when temperature change will exceed 2 °C above preindustrial levels. Nature Climate Change, vol. 1, November 2011. www.nature.com/natureclimatechange

Kang Yinhong , Shahbaz Khan , Xiaoyi Maa,2009. Climate change impacts on crop yield, crop water productivity, and food security – A review. National Natural Science Foundation of China and Chinese Academy of Sciences. Published by Elsevier Limited and Science in China Press. All rights reserved. https://doi.org/10.1016/j.pnsc.2009.08.001

Karaburun, A., Demirci, A., Kara, F., 2011. Analysis of spatially distributed annual, seasonal, and monthly temperatures in Istanbul from 1975 to 2006. World Applied Sciences Journal 12, 1662-1675.

Karpouzos D K, Kavalieratou S and Babajimopoulos C 2010 Trend analysis of precipitationXGH6Ac9KhBw.

Kassie, B.T., R.P. Rotter, H. Hengsdijk, S. Asseng, M.K. Van Ittersum, H. Kahiluoto, H. Van Keulen,2013. Climate variability and change in the Central Rift Valley of Ethiopia: challenges for rainfed crop production. *Journal of Agricultural Science*, 152 (01): 58-74. https://doi.org/10.1017/S0021859612000986

Keir, D., Ebinger, C.J., Stuart, G.W., Daly, E. and Ayele A. Strain accommodation by magmatism and faulting as rifting proceeds to breakup: seismicity of the northern Ethiopian rift, Journal of Geophysical Research, 111(B5), B05314, doi: 10.1029/2005JB003748

Kent, C., R. Chadwick and D. P. Rowell, 2015: Understanding Uncertainties inFuture Projections of Seasonal Tropical Rainfal. Journal of Climate, 28(11), 4390-4413. https://doi.org/10.1175/JCLI-D-14-00613.1

Kharin, V.V.; Flato, G.M.; Zhang, X.; Gillett, N.P.; Zwiers, F.; Anderson, K.J. Risks from Climate Extremes Change Differently from1.5 _C to 2.0 _C Depending on Rarity. Earth's Future 2018, 6, 704–715. [CrossRef]

Liben F M., 2013.Evaluating RiskAssociEPCCated With Dry Soil Planting Of Sorghum [Sorghum Bicolor (L.) Moench] And Maize (Zea Mays L.) At Different Depths In Predictable Onset Of Rain In The Central Rift Valley, Ethiopia M.Sc. Thesis submitted to school of Graduate Study, Hramaya University, Ethiopia.

Lyon B, Dewitt DG (2012) A Recent and Abrupt Decline in the East African Long Rains 39:1–5. https://doi.org/10.1029/2011GL050337

Mahoo H, Radeny M, Kinyangi J, Cramer L, eds. 2013. Climate change vulnerability and risk assessment of agriculture and food security in Ethiopia: Which way forward? CCAFS Working Paper no. 59. CGIAR Research Program on Climate Change, Agriculture and Food Security (CCAFS).Copenhagen, Denmark. Available online at: www.ccafs.cgiar.org

Masilin G, Herbert O M, Zewdu T Segele, S. J., Jully O O. ,George O, Richard A, Victor S Indasi , Hussen Seid Endris , Sarah Osima6 ,Christopher Lennard , Modathir Zaroug, Emmah Mwangi , Alex Nimusiima, Alfred Kondowe Bob Ogwang5,, Guleid Artan and Zachary Atheru2020. Projected effects of 1.5 °C and 2 °C global warming levels on theintra-seasonal rainfall characteristics over the Greater Horn of Africa. Environ. Res. Lett. 15 (2020) 034037

Mathur, S.;Jajoo, A. Photosynthesis: Response to high-temperature stress. J. Photochem. Photobiol. B Biol. 2014, 137, 16-126, https://doi.org/10.1016/j.jphotobiol.2014.01.010.

Maulana F. and Tesso T. 2013 Cold Temperature Episode at Seedling and Flowering Stages Reduces Growth and Yield Components in Sorghum. crop science, vol. 53, march-april 2013. www.crops.org

McSweeney, C., New, M., and Lizcano, G. UNDP Country Climate Profiles: Ethiopia. 2008. [cited 3 August 2011]. Available from: http://countryprofiles.geog.ox.ac.uk/index.html?country=Ethiopia&d1=Repo.

MoFR(Ministry of Environment and Forest) ,2015. Ethiopia's Second National Communication to the United Nations Framework Convention on Climate Change (UNFCCC). The Federal Democratic Republic of Ethiopia. URL: https://unfccc.int/resource/docs/natc/ethnc2.pdf.

Moss, R. H., Edmonds, J. A., Hibbard, K. A., Manning, M. R., Rose, S. K., van Vuuren, D. P., … Wilbanks, T. J.(2010). The next generation of scenarios for climate change research and assessment. Nature, 463, 747-756. https://doi.org/10.1038/nature08823.

Muluneh Alemayehu, Saskia Keesstra, and Leo Stroosnijder ,2017.Bridging dry spells for maize cropping through supplemental irrigation in the Central Rift Valley of Ethiopia. Land Degradation and Development

Murken, L., Cartsburg, M., Chemura, A., Didovets, I., Gleixner, S., Koch, H., Lehmann, J., Liersch, S., Lüttringhaus, S., Rivas López, M. R., Noleppa, S., Roehrig, F., Schauberger, B., Shukla, R., Tomalka, J., Yalew, A. & Gornott, C., 2020. Climate risk analysis for identifying and weighing adaptation strategies in Ethiopia's agricultural sector. A report prepared by the Potsdam Institute for Climate Impact Research for the Deutsche Gesellschaft für Internationale Zusammenarbeit GmbH on behalf of the German Federal Ministry for Economic Cooperation and Development, 150 pp. https://doi.org/10.2312/pik.2020.003

NAP(National Adaptation Plan,2019 Ethiopia's Climate Resilient Green Economyhttps. https://doi.org/10.1111/rode.12815

Ndamani Francis, and Watanabe Tsunemi,Farmers'2015. Perceptions about Adaptation Practices to Climate Change and Barriers to Adaptation: A Micro-Level Study in Ghana Water 2015, 7, 4593-4604. https://doi.org/10.3390/w7094593 (CrossRef).

Niang I, Ruppel OC, Abdrabo MA, Essel A, Lennard C, Padgham J,Urquhart P (2014) Africa. In: Climate change 2014: impacts,adaptation and vulnerability. Contribution of Working Group II to the Fifth Assessment Report of the Intergovernmental Panel on Climate Change. Cambridge University Press, Cambridge FAO, 2011. The State of Food and Agriculture 2010-2011. FAO, Rome

Nikulin G, Lennard C, Dosio A et al (2018) The effects of 1.5 and 2 degrees of global warming on Africa in the CORDEX ensemble. Environ Res Lett 13(6): 065003(CrossRef).

Oates, N., D. Conway, R. Calow, 2011. 'mainstreaming' approach to climate change adaptation: insights from Ethiopia's water sector. Overseas Development Institute Background notes.www.odi.org.uk/50years, Accessed on 31/05/2011.

OECD/FAO (2016). OECD-FAO agricultural outlook 2016-2025. OECD Publishing

Omondi, P.A., J.L. Awange, E. Forootan et al., 2014 "Changes in temperature and rainfal extremes over the Greater Horn of Africa region from 1961 to 2010," *International Journal of Climatology*, vol. 34, no. 4, pp. 1262-1277.

Osima, S., Indasi, V.S., Zaroug, M., Endris, H.S., Gudoshava, M., Misiani, H.O., Dosio, A., 2018.Projected Climate over Greater Horn of Africa under 1.5°C and 2°C global warming. Environ.

Otieno, V.O. and Anyah, R.O. (2013) CMIP5 simulated climate conditions of the greater horn of Africa (GHA). Part 1: contemporary climate. Climate Dynamics, 41(7-8), 2081-2097. https://doi.org/10.1007/s00382-012-1549-z (CrossRef)

Otieno, V.O., Anyah, R.O. 2013a. CMIP5 simulated climate conditions of the Greater Horn of Africa (GHA). Part 1: Contemporary climate. Clim. Dyn., 41: 2081-2097. https://doi.org/10.1007/s00382-012-1549-z

Partal T. and Kahya E. 2006. Trend analysis of Turkish precipitation data. Hydrology Processes, 20: 2011-2026. https://doi.org/10.1002/hyp.5993

Ramankutty N, Evan AT, Monfreda C, Foley JA (2008). Farming theplanet: 1. Geographic distribution of global agricultural lands in theyear 2000. Global Biogeochemical Cycles 22.Res. Lett.13, 6. https://doi.org/10.1128/JVI.74.13.6223-6226.2000(cross ref).

Riahi, K., Grübler, A., & Nakicenovic, N. (2007). Scenarios of long-term socio-economic and environmental development under climate stabilization. *Technological Forecasting and Social Change, 74*, 887-935. https://doi.org/10.1016/j.techfore.2006.05.026

Rosenzweig, C., Jones, J., Hatfield, J., Antle, J., Ruane, A., Boote, K., … Mutter, C. (2013b). *AgMIP Guide forRegional Integrated Assessments: Handbook of Methods and Procedures Version 5.0*.

Rosenzweig, C.; Jones, J.W.; Hatfield, J.L.; Ruane, A.C.; Boote, K.J.; Thorburn, P.; Antle, J.M.; Nelson, G.C.; Porter, C.; Janssen, S.The agricultural model intercomparison and improvement project (AgMIP): Protocols and pilot studies. Agric. For. Meteorol. **2015**, 170, 166-182. [CrossRef]

Sanderson, M.G., D.L. Hemming, and R.A. Betts, 2011. Regional Temperature and Rainfal changes under warming. Philosophical Transactions of the Royal Society A, 36 9(1934), 85-98.

Schlenker, W., Lobell, D.B., 2010. Robust negative impacts of climate change on African agriculture. Environ. Res. Lett. 5, 1-8. https://doi.org/10.1088/1748-9326/5/1/ 014010

Segele Z. T. and Lamb P. J., "Characterization and variability of Kiremt rainy season over Ethiopia," *Meteorology and Atmospheric Physics*, vol. 89, no. 1-4, pp. 153-180, 2005.

Shanahan M, Shubert W, Scherer C and Corcoran T, 2013. Climate Change in Africa: A Guidebook for Journalists. Fackson Banda (ed). UNESCO Series on Journalism Education.

Sonwa dj, Dieye A, El Mzouri eh, Majule A, Mugabe ft, Omolo N, Wouapi H, Obando J and Brooks n (2017) drivers of climate risk in African agriculture. *Clim. Dev*. 9 (5) 383– 398. https://doi.org/10.1080/17565529.2016.1167659

Teshome, H.; Tesfaye, K.;Dechassa, N.; Tana, T.; Huber, M.Analysis of Past and ProjectedTrends of Rainfall and Temperature Parameters in Eastern and WesternHararghe Zones, Ethiopia. *Atmosphere* 2022, *13*, 67. https://doi.org/10.3390/atmos13010067

Thomas Timothy, Paul Dorosh, and Richard Robertson, 2019. Climate Change Impacts on Crop Yields in Ethiopia. Ethiopian Development Research Institute (EDRI) Strategy Support Program | Working Paper 130 | February 2019.

Thornton, P.K., P.G. Jones, A. Alagarswamy, J. Andresen, 2009. Spatial variation of crop yield responses to climate change in East Africa. *Global Environmental Change*, 19: 54-65.

Timo Salmi, Anu Määttä, Pia Anttila, Tuija Ruoho-Airola and Toni Amnell 2002. Detecting Trends of Annual Values of Atmospheric Pollutants by The Mann-Kendall Test and Sen's Slope Estimates the Excel Template Application MAKESENS

UNFCCC (United Nations Framework Convention on Climate Change, 2017). Climate Change: Impacts, Vulnerabilities and Adaptation in Developing Countries.

USAID, 2015. Climate Variability and Change in Ethiopia – Summary of Findings. Technical Report. URL: https://www.usaid.gov/sites/default/files/documents/1866/12.22.15%20%20ClimateVariabilityChange_Ethiopia_Dec2015%20%281%29.pdf

USAID, 2016. Climate Change Risk Profile – Ethiopia. Fact Sheet. URL: https://www.climatelinks.org/sites/default/files/asset/document/2016%20CRM%20Factsheet%20-%20Ethiopia_use%20this.pdf

Watanabe, M. 2010. Improved Climate Simulation by MIROC5: Mean States, Variability, and Climate Sensitivity. *Journal of Climate*, 23: 6312-6335.

Weldegebriel, ZB. and Prowse M. (2013) Climate change adaptation in Ethiopia: To what extent does social protection influence livelihood diversification? Development Policy Review 31: 35-56.

WFP (World Food Programme), 2014. Climate risk and food security in Ethiopia : Analysis of climate impacts on food security and livelihoods. World Food Programme (WFP).

World Bank, 2019. Action Plan on Climate Change Adaptation and Resilience: Managing risks for a more resilient future. Washington DC, USA. Available at: http://documents.worldbank.org/curated/en/519821547481031999/The-World-Bank-Groups-Action-Plan-on-Climate-Change-Adaptation-and-Resilience-Managing-Risks-for-a-More-Resilient-Future.pdf.

World Bank Data Bank ,2018. Health Nutrition and Population Statistics: Population estimates andprojections.Ethiopia.URL:https://databank.worldbank.org/data/reports.aspx?source=health-nutrition-and-population-statistics:-populationestimates-and-projections

World bank group (WBG,2021) Climate Change Knowledge Portal (CCKP, 2021). Ethiopia Water Dashboard. Data Description. URL: https://climateknowledgeportal.worldbank.org/country/ethiopia/climate-sector-water

World Bank, 2012. Ethiopia Overview. URL: http://www.worldbank.org/en/country/ethiopia/overview.

Wylie, P. Managing Sorghum for High Yields: A Blueprint for Doubling Sorghum Production; Grain Research and DevelopmentCorporation: Barton, ACT, Australia, 2008.

Yadav SK (2009). Cold stress tolerance mechanisms in plants: Areview. Agronomy for Sustainable Development 30: 515-527.

Yenigun K, Gumus V, Bulut H (2008). Trends in stream flow of the Euphrates basin, Turkey.Proceedings of the Institution of Civil Engineers Water Management. 161, 189-198. https://doi.org/10.1680/wama.2008.161.4.189

Yukimoto S (2012). A new global climate model of Meteorological Research Institute: MRI-CGCM3 – Model description and basic performance. J. Meteorol. Soc. Jpn., 90a, 23-64.

Zhang, X., Gabriele H, Francis W. Zwiers, Jesse K, 2005. Avoiding Inhomogeneity in Percentile-Based Indices of Temperature Extremes 005. Volume 18 Journal Of Climate 1 June 2005

Italian Journal of Agrometeorology
Rivista Italiana di Agrometeorologia

Firenze University Press
www.fupress.com/ijam

OPEN ACCESS

Citation: Tapparo, S.A., Duarte Coelho, R., de Oliveira Costa, J., Paulino Chaves, S.W., & Biscaro, G.A. (2023). Yield and quality responses of *Megathyrsus maximus* and *Cynodon* spp. forage grasses to irrigation. *Italian Journal of Agrometeorology* (2): 69-77. doi: 10.36253/ijam-2130

Received: May 2, 2023

Accepted: August 21, 2023

Published: January 20, 2024

Data Availability Statement: All relevant data are within the paper and its Supporting Information files.

Competing Interests: The Author(s) declare(s) no conflict of interest.

ORCID:

SAT: 0000-0002-8538-4060
RDC: 0000-0002-0472-8301
JdOC: 0000-0002-5387-7880
SWPC: 0000-0003-0110-420X
GAB: 0000-0001-6907-2756

Yield and quality responses of *Megathyrsus maximus* and *Cynodon* spp. forage grasses to irrigation

Sergio André Tapparo[1], Rubens Duarte Coelho[2], Jéfferson de Oliveira Costa[3,*], Sérgio Weine Paulino Chaves[4], Guilherme Augusto Biscaro[5]

[1] Federal Institute of Mato Grosso do Sul/IFMS, Ponta Porã Campus, highway BR-463, km 14, 79909-000, Ponta Porã, MS, Brazil
[2] University of São Paulo/USP-ESALQ, Biosystems Engineering Department, C.P. 09, 13418-900 Piracicaba, SP, Brazil
[3] Minas Gerais Agricultural Research Agency/EPAMIG, Experimental Field of Gorutuba, 39525-000 Nova Porteirinha, MG, Brazil
[4] Federal Rural University of the Semi-Arid/UFERSA, Agronomic and Forestry Sciences Department, Francisco Mota, 572, 59625-900, Mossoró, RN, Brazil
[5] Federal University of Grande Dourados/UFGD, College of Agrarian Sciences, highway Dourados/Itaum, km 12, CP 364, 79804-970, Dourados, MS, Brazil
*Corresponding author. E-mail: costajo@alumni.usp.br

Abstract. Periodic variations in rainfall have resulted in longer periods of drought in traditional rainfed livestock systems on savanna areas in Brazil. However, irrigation management techniques and rotational grazing have improved the productivity of these systems by mitigating soil water stress on forage grasses. The objectives of this research were to evaluate the response of *Megathyrsus maximus* cv. Tanzania and *Cynodon* spp. cv. Tifton 85 (*Cynodon nlemfuensis* × *Cynodon dactylon*) forage grasses to irrigation, and to determine their irrigation water productivity (IWP). The experiment was conducted at the University of São Paulo in Brazil. Plant height (PH), dry matter (DM), crude protein (CP), neutral detergent fiber (NDF) and acid detergent fiber (ADF) were measured, and IWP was calculated. Tifton 85 had a higher CP content than Tanzania but a lower average DM yield. The irrigation management (IM) treatments did not influence CP levels of both forage grasses, but in most situations, did affect their average DM yield. The IWP of Tanzania and Tifton 85 forage grasses did not differ among irrigation management treatments.

Keywords: *Cynodon* spp. cv. Tifton 85, irrigation water productivity, *Megathyrsus maximus* cv. Tanzania, soil depth.

HIGHLIGHTS

1) Pasture irrigation is a promising tool to mitigate the severe drought that has been occurring in savanna areas in Brazil;

2) *Cynodon* spp. had an average water productivity of 2.70 against 2.33 kg DM m^{-3} of *Megathyrsus maximus*;
3) Irrigation management treatments did not influence crude protein (CP) levels of forage grasses but did affect average dry matter (DM) yield;
4) *Cynodon* spp. had a higher CP content than *Megathyrsus maximus* and lower average DM yield under full irrigation.

1. INTRODUCTION

Among forage grasses, *Megathyrsus maximus* cv. Tanzania and *Cynodon* spp. cv. Tifton 85 (*Cynodon nlemfuensis* x *Cynodon dactylon*) are being used in different regions from Brazil for animal feed. These species, in particular, have been used in intensive rotational production systems, generally with high levels of fertilization and irrigation, aiming high rates of yield and forage quality (Lemos et al., 2019; Silva et al., 2019).

The use of technologies such as irrigation to increase livestock productivity is critical for meeting the growing demand for animal products; however, these technologies must be applied sustainably to minimize the impact of livestock on the environment and natural resources. The aim is to increase the pasture grass yield through rational use of irrigation, to increase milk and meat production. Irrigation of pasture is an efficient approach to minimize productivity losses due to rainfall seasonality. This strategy mitigates the effects of water stress on forages during the dry season and keeps the autumn/winter stocking rate close to that achieved in spring and summer (Neal et al., 2011; Mazzetto et al., 2015; Gheysari et al., 2017; Legesse et al., 2018; Yan et al., 2018; Balazadeh et al., 2021).

The rotational grazing method under irrigation is a complex practice in which the applied water depth must be varied according to the stage of pasture development. However, several studies have shown that irrigation practices most often use a constant depth for the total irrigated area, not taking into account the growth stage of the forage plants (Snyder et al., 2015; Rolando et al., 2017; Birendra et al., 2018).

When the irrigation depth is calculated using data collected from only one rotational grazing plot (reference plot), one can underestimate or overestimate the water consumption of pastures that present a leaf area index (LAI) different from the reference plot (Tapparo et al., 2022). The application of incorrect irrigation depth can increase the operational cost of the system, reduce the net revenue, and influence the quality of the grasses (Tapparo et al., 2019; Liao et al., 2021).

Measuring the yield and quality of irrigated forage grasses is important for improving irrigation management (IM), yet there have been no controlled studies on the effects of irrigation management treatments based on different soil depths (SD) on the yield and quality of Tanzania and Tifton 85 forage crops in irrigated savanna areas of Brazil.

Thus, this study aimed to evaluate the yield (dry matter) and quality (crude protein, neutral and acid detergent fiber) of irrigated *Megathyrsus maximus* cv. Tanzania and *Cynodon* spp. cv. Tifton 85 forage grasses, subjected to four irrigation management treatments based on four different soil depths. The effects of irrigation management treatments on yield were verified as irrigation water productivity (IWP).

2. MATERIALS AND METHODS

2.1. Description of the experimental area

The experiments were carried out in a rain out shelter at the University of São Paulo, Brazil (22°46'39"S, 47°17'45"W, altitude of 570 m). The rain out shelter had 160 m^2 of internal area, and 48 pots with a volume of 0.1 m^3 and dimensions of 0.60 × 0.40 × 0.45 m were used (Tapparo et al., 2019; Chaves et al., 2021; Almeida et al., 2022; Tapparo et al., 2022).

The soil in pots was characterized as Oxisol Typic Ustox with a sandy loam texture (17% clay, 8% silt and 75% sand). A drip irrigation system was used to apply water. The experimental design was randomized with eight treatments (two forage grasses and four irrigation management) and six replications. Irrigation management treatments were based on soil depth of 0.10 m (IM10), 0.20 m (IM20), 0.30 m (IM30), and 0.40 m (IM40). Soil depth was defined by vertical dimension in the pots, to simulate different conditions of soil fertility along the soil profile.

The meteorological data obtained over the entire period of the experiment is given in Figure 1. The maximum temperature ranged from 32.7 °C in July to 42 °C in March; the minimum temperature ranged from 12.3 °C in July to 20.5 °C in January. The monthly average of solar radiation ranged from 12.6 to 21.9 MJ m^{-2} day^{-1}. The relationship between the meteorological conditions inside a rain out shelter and the meteorological conditions outside the rain out shelter are discussed in Costa et al. (2015) and Chaves et al. (2021).

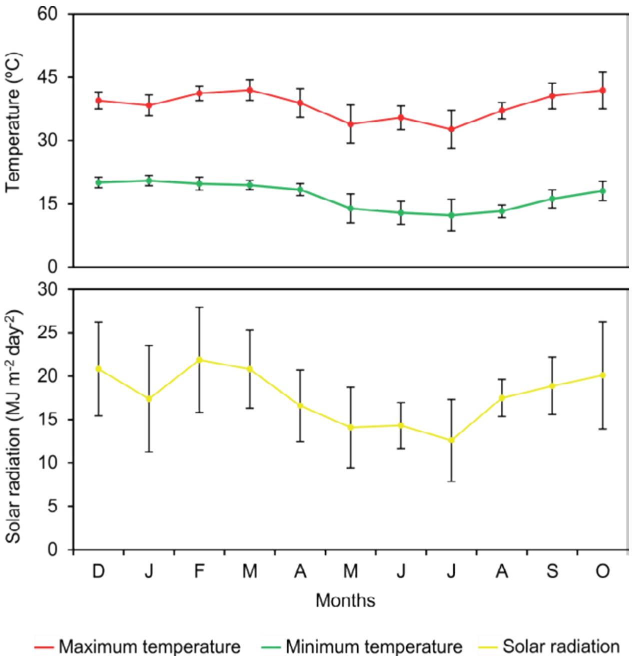

Figure 1. Monthly averages and standard deviations of weather data during the period of the experiment inside the rain out shelter.

2.2. Grass planting and experimental conditions

Before planting the forage grasses, soil samples were taken for liming and fertilization. Flow uniformity tests were also carried out on the drippers in the experimental area, and the system provided an excellent uniformity of water distribution to the plants (93%). Four months before beginning the evaluation, pots were planted with two types of grass: *Megathyrsus maximus* cv. Tanzania and *Cynodon* spp. cv. Tifton 85 (*Cynodon nlemfuensis* x *Cynodon dactylon*). Early planting was done so grasses could become well-established and cover the whole area of each pot. Pots were planted with Tanzania grass seeds, while seedlings were used for Tifton 85 grass.

Chemical analysis of the soil from the 0-0.40 m layer showed that there was no need for fertilization at planting; but after establishment, a soil analysis showed need for fertilization. Foliar chemical analysis was also performed to verify the nutritional status of the plants. The equivalent of 405 kg ha^{-1} of N, 190 kg ha^{-1} of K_2O, 115 kg ha^{-1} of P_2O_5 and 29 kg ha^{-1} of MgO was applied to each crop in five applications (three during summer and two in winter). Soil acidity correction and nutritional management were conducted according to Van Raij (1997) recommendations for grasses forage based on soil analysis results.

Tensiometers were installed at depths of 0.10, 0.20, 0.30 and 0.40 m, in the reference pots of each block. The irrigation management was based on soil matric potential, using the van Genuchten model (Van Genuchten, 1980) according to Eq. (1) to calculate the irrigation depth:

$$\theta\ (\psi m) = 0.246 + \frac{(0.564 - 0.246)}{(1 + (0.2187\ \Psi m)^{0.6068})^{0.8555}} \qquad (1)$$

where θ (ψm) is the soil volumetric water content (cm^3 cm^{-3}) as a function of the matric potential (ψm) (kPa).

Irrigation management calculations were performed in a spreadsheet developed in Microsoft Excel and used in other studies (Costa et al., 2020a; Costa et al., 2020b; Quiloango-Chimarro et al., 2021; Chaves et al., 2022). Treatments were kept at a moisture level corresponding to a reading of -5 kPa, the value chosen as the field capacity soil without drainage (Costa et al., 2018; Costa et al., 2019).

The irrigation depths applied in the different irrigation management treatments (IM10, IM20, IM30, and IM40) were based on soil depths different of 0.10, 0.20, 0.30, and 0.40 m, which affect the amount and frequency of water applied to each plot. The experiments were conducted over eleven months (December/2016 to October/2017), and involved eleven cuts of each forage grass (approximately 30 days of growth cycle) to simulate rotational grazing utilization.

2.3. Leaf water potential (LWP)

A Scholander chamber (model 3005) was used. Leaf samples were taken to the laboratory packed in ice to prevent necrosis or destruction of tissues and cells (Costa et al., 2018; Costa et al., 2020a; Costa et al., 2020b).

Six to eight leaves were collected from each pot between 6h00 and 6h30. The Tifton 85 grass samples included the entire tiller, while only leaves of Tanzania grass were collected. Before reading LWP, the leaves were standardized as follows: for Tanzania grass, the central part of the leaf was used without the central rib, as it was verified that pressing on the central rib caused pressure leakage; for Tifton 85 grass, only the 2+ or 3+ leaves were used.

2.4. Biomass production

Grass cutting in each pot was performed manually. Samples were taken from 0.18 to 0.24 m and 0.06 to 0.10 m for Tanzania and Tifton 85, respectively. This cutting height is the lowest for these species in rotational grazing systems with irrigation. Plant height (PH) was non-destructively measured using a ruler and a sheet of transparent acetate film placed next to each plant.

The use of transparent film prevented compression and allowed integration of an area of approximately 0.06 m^2. It was much faster and easier to mark the average height on the film than to measure a sufficient number of points to reach the same average height (Tapparo et al., 2019; Tapparo et al., 2022). For dry matter (DM) determinations, aboveground biomass was obtained within an area of 0.24 m^2, dried for 48 h at 65 °C, and weighed.

2.5. Quality measurements

Samples for crude protein (CP), neutral detergent fiber (NDF) and acid detergent fiber (ADF) analysis were obtained by mixing material from the same treatments, at spring, summer, autumn, and winter seasons. Samples were obtained in December, January, and February (summer); in March, April, and May (autumn); in June, July, and August (winter); and in September, October, and November (spring). The collected material was ground in a Wiley mill, passed through a 1 mm diameter sieve and placed in labeled plastic bags. The CP content was determined by combustion according to the Dumas method (Saint-Denis and Goupy, 2004) using a nitrogen self-analyzer, while the NDF and ADF fractions were determined with an Ankom 200 fiber analyzer (Spanghero et al., 2010).

2.6. Irrigation water productivity (IWP)

The IWP (kg m^{-3}) was obtained as the ratio of DM yield to the total irrigation water applied using Eq. (2) (Sadras, 2009). The IWP was calculated for each cut.

$$IWP = \frac{\text{DM yield}}{\text{IWA}} \quad (2)$$

where IWA is irrigation water applied in m^3 ha^{-1}. The IWA was obtained by adding the irrigation depths throughout the cutting cycle for each irrigation management treatment. This value was converted from L per pot to volumes applied in m^3 ha^{-1}.

2.7. Statistical analysis

The statistics software SAS (Statistical Analysis System Institute, 2001) was used. Data were checked for normal distribution using the Shapiro-Wilk method and tested by analysis of variance (ANOVA) to compare the means of the studied variables. Tukey's test of means was used at the 95% confidence level following the PROC GLM procedure, and graphical representation of the data was done on Microsoft Excel version 16.0.

3. RESULTS AND DISCUSSION

3.1. Irrigation water applied and leaf water potential

The average values of irrigation water applied (IWA), in the eleven cuts, for Tanzania grass were 151, 186, 222, and 258 mm at the treatments IM10, IM20, IM30, and IM40, respectively. For Tifton grass, the average values of IWA were 80, 103, 117, and 166 mm at the treatments IM10, IM20, IM30, and IM40, respectively (Figure 2).

Irrigation management treatments resulted in significant differences for the LWP of Tanzania and Tifton 85 grasses (Table 1). In comparing the LWP of Tanzania grass at different irrigation management treatments (Figure 3A), it was observed that the IM40 treatment resulted in the highest LWP value, -0.34 MPa. For the other IMs, mean LWP values varied from -0.55 to -0.46 MPa, confirming lower water potential in terms of soil-water

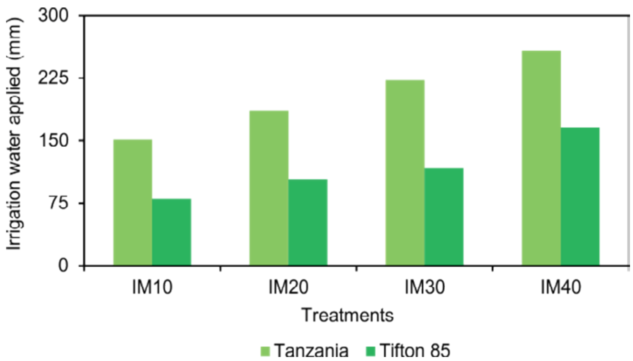

Figure 2. Average amount of irrigation water applied during the growing season of Tanzania and Tifton 85 forage grasses. Irrigation management based on soil depth of 0.10 m (IM10), 0.20 m (IM20), 0.30 m (IM30), and 0.40 m (IM40).

Table 1. Analysis of variance (ANOVA) to compare the means of the studied variables.

Variables	Sources of Variation	*p* value (Tanzania)	*p* value (Tifton 85)
Leaf water potential (LWP)	Irrigation management (IM) treatments	0.0057*	0.0401*
Plant height (PH)		0.1161^{ns}	0.2275^{ns}
Dry matter (DM) yield		0.0000*	0.0000*
Total dry matter		0.0007*	0.0031*
Crude protein (CD)		0.6864^{ns}	0.1039^{ns}
Total crude protein		0.0015*	0.0464*
Neutral detergent fiber (NDF)		0.0123*	0.0225*
Acid detergent fiber (ADF)		0.0131*	0.0327*
Irrigation water productivity (IWP)		0.2150^{ns}	0.6178^{ns}

^{ns} not significant; * significant at a probability level of 5%.

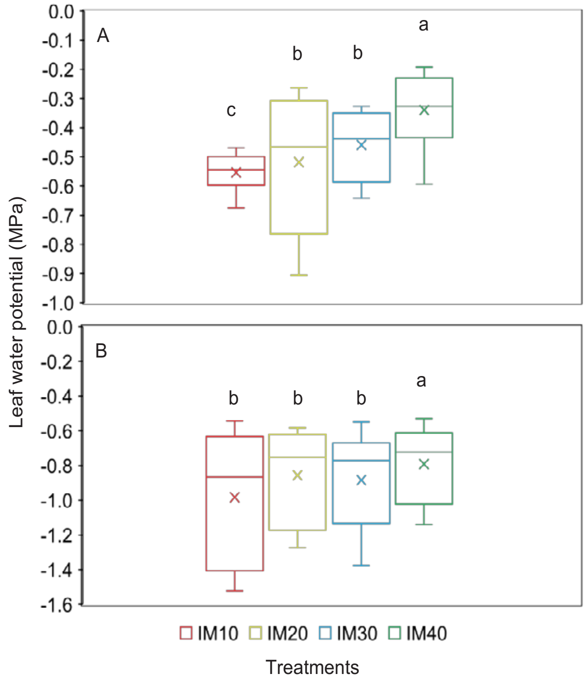

Figure 3. Leaf water potential (MPa) of Tanzania (A) and Tifton 85 (B) forage grasses subjected to irrigation management treatments. Irrigation management based on soil depth of 0.10 m (IM10), 0.20 m (IM20), 0.30 m (IM30), and 0.40 m (IM40). Treatments with same letters do not differ from each other at the 5% probability level by Tukey's test ($p < 0.05$).

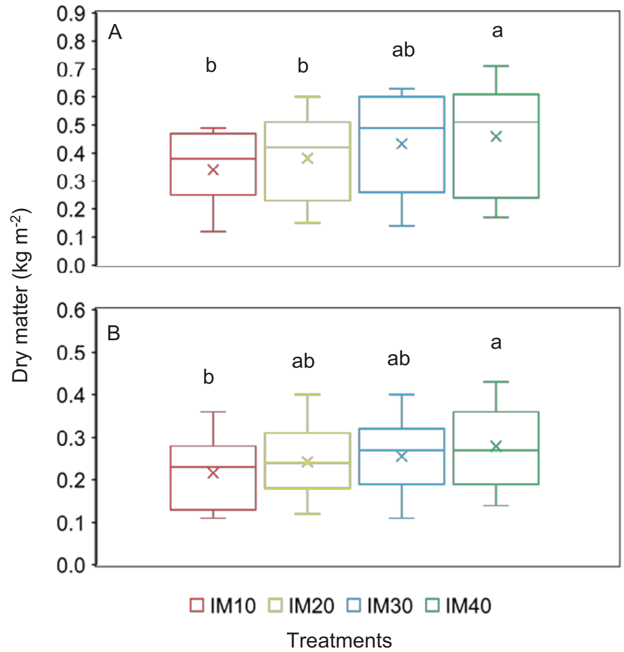

Figure 4. Mean dry matter (kg m^{-2}) yield per mowing of Tanzania (A) and Tifton 85 (B) forage grasses subjected to irrigation management treatments. Irrigation management based on soil depth of 0.10 m (IM10), 0.20 m (IM20), 0.30 m (IM30), and 0.40 m (IM40). Treatments with same letters do not differ from each other at the 5% probability level by Tukey's test ($p < 0.05$).

potential compared to the other treatments (Tapparo et al., 2022). In Tifton 85 grass at different irrigation management treatments (Figure 3B), mean LWP values were highest at the IM40 treatment, -0.79 MPa. Mean LWP values in plants grown at the other irrigation management treatments varied from -0.98 to -0.86 MPa. Korup et al. (2018) evaluated the LWP of perennial grasses during and after restrictive water conditions and found significant differences between irrigated and non-irrigated plants. Grasses subjected to water stress showed the lowest values, with a mean of -1.6 MPa, while the control plots had a mean LWP of -0.8 MPa. Mwendia et al. (2016) measured LWP in grass in East Africa, in the tropical environments of Muguga and Katumani, and reported mean values of -1.4 to -0.4 MPa, in agreement with the results of this research.

3.2. Grass yield responses to irrigation water

Analyzing the average height of the two grasses, it was observed that for both Tanzania and Tifton 85, there were no statistically significant differences ($p > 0.05$) for IM10, IM20, IM30, and IM40, which would suggest that irrigation management had little effect on PH (Table 1). The average PH values of Tanzania grass at the different irrigation management treatments were between 0.45 and 0.50 m, and 0.20 and 0.25 m for Tifton 85.

In comparing the average yields of DM, Tanzania and Tifton 85 grasses showed statistical differences ($p<0.05$) at the IM40 treatment when compared to the IM10 treatment (Table 1). In general, the largest DM yield was found at IM40 treatment compared to the averages obtained for the IM30, IM20, and IM10 treatments. The average DM values of Tanzania grass were 0.34, 0.38, 0.43, and 0.46 kg m^{-2} at IM10, IM20, IM30, and IM40, respectively (Figure 4A). Macedo et al. (2017) evaluated the structure and productivity of Tanzania grass under different defoliation rates in the State of Pará and observed that the forage DM was 0.23 kg m^{-2} at the 30-day frequency, similar to those found in this study. For Tifton 85, the average DM values were 0.22, 0.24, 0.26, and 0.28 kg m^{-2} at IM10, IM20, IM30, and IM40, respectively (Figure 4B). Fonseca et al. (2007) evaluated the yield of Tifton 85 grass under irrigation treatments in the State of São Paulo and observed that forage DM was 0.27 kg m^{-2} at the 30-day frequency, similar to those found in this study.

The accumulated DM yield for Tanzania grass was highest at IM40 and IM30 (Figure 5A). The average cumulative DM yield for Tanzania grass in the different treatments was 3.72, 4.18, 4.76, and 5.04 kg m^{-2} for IM10, IM20, IM30, and IM40, respectively. Pezzopane et al. (2012) determined the DM yield of Tanzania grass as a function of agrometeorological variables. They verified that the best statistical results in the development and validation of models were obtained for agrometeorological parameters that considered both the thermal and water effects as real evapotranspiration, accumulation of degree days corrected for water availability and climatic index of growth, based on average temperature, solar radiation, and water availability, showing that irrigation management treatments based on climate and soil data influence DM yield Tanzania grass.

For the Tifton 85 grass the accumulated DM yield was higher at the treatment IM40 compared to the IM10 treatment (Figure 5B). The average accumulated DM yield for Tifton 85 was 2.38, 2.74, 2.81, and 3.06 kg m^{-2} for IM10, IM20, IM30, and IM40. Oliveira et al. (2017) studied the performance of Tifton 85 grass in soils in the city of Lavras-MG and observed values of accumulated DM yield ranging from 2.3 to 4.0 kg m^{-2} over an evaluation period of 120 days. Pequeno et al. (2015) studying the forage accumulation of Tifton 85 with different cutting frequencies and irrigation, observed that the accumulated DM yield in dry conditions was, on average, 1.87 and 1.79 kg m^{-2} $year^{-1}$ for cut frequencies of 28 and 42 days, while under irrigated conditions, it was 1.97 and 2.11 kg m^{-2} $year^{-1}$.

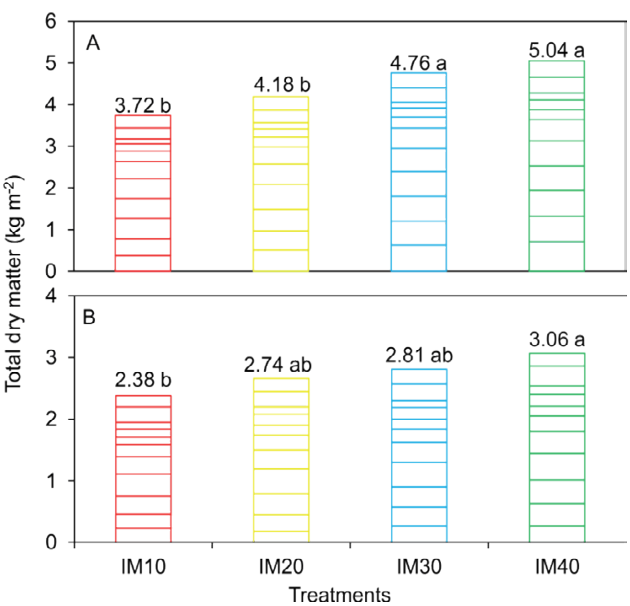

Figure 5. Total dry matter (kg m^{-2}) of Tanzania (A) and Tifton 85 (B) forage grasses subjected to irrigation management treatments. Irrigation management based on soil depth of 0.10 m (IM10), 0.20 m (IM20), 0.30 m (IM30), and 0.40 m (IM40). Treatments with same letters do not differ from each other at the 5% probability level by Tukey's test ($p < 0.05$).

3.3. Quality responses (crude protein and fiber yield) to irrigation water

The difference in % CP between Tifton 85 and Tanzania grasses was 7.2, 22.6, 16.9 and 26.7% in summer, autumn, winter, and spring, respectively (Table 2). Analyzing the average CP of the two grasses, it was observed that for both Tanzania and Tifton 85, there were no statistically significant differences (p> 0.05) for IM10, IM20, IM30, and IM40 (Table 1). For Tanzania grass, the average values were 11.4, 11.6, 12.2, and 11.3% for IM10, IM20, IM30, and IM40. Cecato et al. (2017), studying Tanzania grass in the State of Paraná observed that CP values from plants cut in the summer and autumn ranged from 9.2 to 11.0%.

For Tifton 85 grass, the averages values found were 13.9, 13.7, 14.2, and 14.7% for IM10, IM20, IM30, and IM40. Pequeno et al. (2015) examined the nutritional value of Tifton 85 grass and observed that the CP content under rain fed conditions was 14.6% and with irrigation it was 14%, meanwhile, Neres et al. (2011) found higher values (19.8%) and some that were close to values recorded in this research. At a forage cutting frequency of 28 days, the CP value was 15.3%, and at 42 days it was 13.4%. Comparing the amount of CP produced as a function of total DM for each forage, Tanzania grass produced total CP at the four irrigation management treatments (Figure 6) varying from 0.42 to 0.57 kg m^{-2}, while for Tifton 85 grass the range was 0.33 to 0.45 kg m^{-2}.

As for the medium values of NDF and ADF in the different periods analyzed, it was observed that Tanzania grass had an average value of 65.4% of DM and the Tifton 85 grass 66% of DM, showing that the two grass-

Table 2. Average values of crude protein at the four cutting periods.

Periods		Crude protein (%)		Difference (%)
		Tanzania	Tifton 85	
I	Summer	8.66 b	9.33 b	7.2
II	Autumn	9.81 b	12.68 b	22.6
III	Winter	15.31 a	18.42 a	16.9
IV	Spring	11.70 b	15.97 a	26.7

Treatments with same letters within a column do not differ from each other at the 5% probability level by Tukey's test ($p < 0.05$).

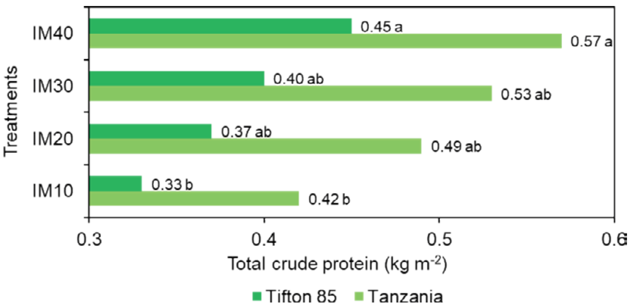

Figure 6. Total crude protein (kg m^{-2}) of Tanzania and Tifton 85 forage grasses subjected to irrigation management treatments. Irrigation management based on soil depth of 0.10 m (IM10), 0.20 m (IM20), 0.30 m (IM30), and 0.40 m (IM40). Treatments with same letters do not differ from each other at the 5% probability level by Tukey's test ($p < 0.05$), within a forage grass.

Table 3. Average values of neutral detergent and acid detergent fiber at the four cutting periods.

Periods		NDF (% DM)		ADF (% DM)	
		Tanzania	Tifton 85	Tanzania	Tifton 85
I	Summer	66.1 a	66.5 a	33.1 b	42.3 a
II	Autumn	65.6 a	65.1 a	34.3 ab	40.5 a
III	Winter	65.4 a	65.3 a	34.0 ab	38.7 a
IV	Spring	64.5 a	67.1 a	34.6 ab	40.5 a

Neutral detergent fiber (NDF), acid detergent fiber (ADF) and dry matter (DM). Treatments with same letters within a column do not differ from each other at the 5% probability level by Tukey's test ($p < 0.05$).

es studied presented similar quality responses for NDF (Table 3). For the ADF variable, it was observed that Tifton 85 grass presented medium values higher than Tanzania grass in the analyzed periods. Medium values ADF for Tifton 85 and Tanzania forage grasses were 40.5 and 34% of DM. The proportion of NDF of forage is important not only for the evaluation of its chemical composition, but also because the NDF is related to maximum DM consumption. Thus, plants with higher levels of NDF would have less consumption potential (Cecato et al., 2017; Pequeno et al., 2015).

3.4. Irrigation water productivity

Analyzing the average IWP of the two grasses, it was observed that for both Tanzania and Tifton 85, there were no statistically significant differences ($p > 0.05$) for IM10, IM20, IM30, and IM40 (Table 1). At the IM10, IM20, IM30, and IM40 treatments, the Tanzania grass had IWP averages of 2.10, 2.14, 2.51, and 2.55 kg DM m^{-3}, and Tifton 85 had IWP averages of 2.50, 2.69, 2.78, and 2.80 kg DM m^{-3}, respectively. Korup et al. (2018) found that IWP values of perennial grasses were between 3.61 and 2.62 kg DM m^{-3}, with the highest IWP in plots treated with water deficit and in sandy-clayey soil. Mazahih et al. (2016) verified that irrigation by 65% of reference evapotranspiration (ET_o) for Buffel grass gave the highest IWP value of 0.95 kg m^{-3}; and 42% of applied water can be saved to produce the same amount of DM of Rhodes grass.

Thus, our results demonstrated that IWP did not result in significant differences as a function of irrigation management for Tanzania and Tifton 85 forage grasses. However, when making a decision about the use of restrictive soil water levels, other factors must be taken into account, such as an economic analysis of the activity, where several variables such as water cost, crop production cost, can become limiting and thus must be optimized to guarantee good results. Maximum efficiency must be determined for each irrigation management.

4. CONCLUSIONS

The irrigation management (IM) treatments of irrigated Tanzania and Tifton 85 forage grasses resulted in significant differences in yield and quality responses but did not result in significant differences in irrigation water productivity (IWP).

Crude protein content varied with the cutting season, being winter the period with the highest concentration. Tifton 85 grass had higher CP content than Tanzania, although it showed a lower average dry matter (DM) yield. With respect to the amount of protein produced as a function of total DM and the protein content of each cutting, the Tanzania grass produced more total protein throughout the year. The irrigation management treatments based on different soil depth did not affect CP levels of Tanzania and Tifton 85 forage grasses in most situations; however, irrigation management treatment did changed the average DM yield of Tanzania and Tifton 85 grasses.

The IWP of Tanzanian and Tifton 85 forage grasses did not differ as a function of irrigation management treatments based on different SD. The average value found for IWP for Tanzania grass was 2.33 kg DM m^{-3} and for Tifton 85 grass it was 2.70 kg DM m^{-3}.

The irrigation management of forage grasses *Megathyrsus maximus* cv. Tanzania and *Cynodon* spp. cv. Tifton 85 (*Cynodon nlemfuensis* x *Cynodon dactylon*) based on monitoring the matric potential in the reference plot of the area under simulated grazing conditions was sufficient to maintain optimal levels of DM yield in the other irrigated plots with variable soil depth.

ACKNOWLEDGEMENTS

This study was financed in part by the 'Coordenação de Aperfeiçoamento de Pessoal de Nível Superior - Brasil (CAPES)' - Finance Code 001.

REFERENCES

Almeida, A.M.; Coelho, R.D.; Barros, T.H.S.; Costa, J.O.; Quiloango-Chimarro, C.A.; Moreno-Pizani, M.A.; Farias-Ramírez, A.J. 2022. Water productivity and canopy thermal response of pearl millet subjected to different irrigation levels. Agricultural Water Management 272, 107829.

Balazadeh, M.; Zamanian, M.; Golzardi, F.; Torkashvand, A.M. 2021. Effects of limited irrigation on forage yield, nutritive value and water use efficiency of Persian clover (*Trifolium resupinatum*) compared to berseem clover (*Trifolium alexandrinum*). Communications in Soil Science and Plant Analysis 52: 1927-1942.

Birendra, K.C.; Mohssen, M.; Chau, H.W.; Curtis, A.; Cuenca, R.; Bright, J.; Cameron, K. 2018. Impact of rotational grazing systems on the pasture crop coefficient for irrigation scheduling. Irrigation and Drainage 67: 441-453.

Cecato, U.; Junior, J.A.; Rego, F.C.A.; Galbeiro, S.; Paris, W.; Scapim, C.A.; Fakir, G.M. 2017. Animal performance, production, and quality of Tanzania grass fertilized with nitrogen. Semina 38: 3861-3870.

Chaves, S.W.P.; Coelho, R.D.; Costa, J.O.; Tapparo, S.A. 2021. Micrometeorological modeling and water consumption of tabasco pepper cultivated under greenhouse conditions. Italian Journal of Agrometeorology 1: 21-36.

Chaves, S.W.P.; Coelho, R.D.; Costa, J.O.; Tapparo, S.A. 2022. Vegetative and productive responses of tabasco pepper to fertigation and plastic mulching. Scientia Agricola 79: 1-9.

Costa, J.O.; Almeida, A.N.; Coelho, R.D.; Folegatti, M.V.; José, J.V. 2015. Estimation models of micrometeorological elements in a protected environment. Water Resources and Irrigation Management 4, 25-31.

Costa, J.O.; Coelho, R.D.; Barros, T.H.S.; Fraga Junior, E.F.; Fernandes, A.L.T. 2018. Physiological responses of coffee trees under different irrigation levels. Engenharia Agrícola 38: 648-656.

Costa, J.O.; Coelho, R.D.; Barros, T.H.S.; Fraga Junior, E.F.; Fernandes, A.L.T. 2019. Leaf area index and radiation extinction coefficient of a coffee canopy under variable drip irrigation levels. Acta Scientiarum. Agronomy 41: 1-8.

Costa, J.O.; Coelho, R.D.; Barros, T.H.S.; Fraga Junior, E.F.; Fernandes, A.L.T. 2020a. Canopy thermal response to water deficit of coffee plants under drip irrigation. Irrigation and Drainage 69: 472-482.

Costa, J.O.; Coelho, R.D.; Barros, T.H.S.; Fraga Junior, E.F.; Fernandes, A.L.T. 2020b. Tensiometry applied in the estimation of the water consumption of the coffee tree irrigated by drip irrigation. Revista Geama 6, 17-24.

Fonseca, A.F.; Melfi, A.J.; Monteiro, F.A.; Montes, C.R.; Almeida, V.V.; Herpin, U. 2007. Treated sewage effluent as a source of water and nitrogen for Tifton 85 bermudagrass. Agricultural Water Management 87, 328-336.

Gheysari, M.; Sadeghi, S.H.; Loescher, H.W.; Amiri, S.; Zareian, M.J.; Majidi, M.M.; Payero, J.O. 2017. Comparison of deficit irrigation management strategies on root, plant growth and biomass productivity of silage maize. Agricultural Water Management 182: 126-138.

Korup, K.; Laerke, P.E.; Baadsgaard, H.; Andersen, M.N.; Kristensen, K.; Munnich, C.; Jorgensen, U. 2018. Biomass production and water use efficiency in perennial grasses during and after drought stress. Gcb Bioenergy 10: 12-27.

Legesse, G.; Cordeiro, M.R.; Ominski, K.H.; Beauchemin, K.A.; Kroebel, R.; McGeough, E.J.; McAllister, T.A. 2018. Water use intensity of Canadian beef production in 1981 as compared to 2011. Science of the Total Environment 619: 1030-1039.

Lemos, N.L.S.; Ruggieri, A.C.; Costa, V.; Meister, N.C.; Oliveira Alari, F.; Malheiros, E. B. 2019. Residual leaf area index as strategy to management of pasture: structure of Tanzania grass. Revista Brasileira de Ciências Agrárias 14, 1-7.

Liao, R.; Zhang, S.; Zhang, X.; Wang, M.; Wu, H.; Zhangzhong, L. 2021. Development of smart irrigation systems based on real-time soil moisture data in a greenhouse: Proof of concept. Agricultural Water Management 245: 106632.

Macedo, V.H.M.; Cunha, A.M.Q.; Cândido, E.P.; Domingues, F.N.; Melo, D.D.M.; Rêgo, A.C.D. 2017. Structure and productivity of tanzania grass subjected to different defoliation frequencies. Ciência Animal Brasileira 18: 1-10.

Mazahrih, N.; Al-Wahaibi, H.; Al-Farsi, S.; Belgacem, A.O. 2016. Yield and water productivity of Buffel and Rhodes grasses under different irrigation water regimes using the sprinkler line-source system. Grassland science 62: 112-118.

Mazzetto, A.M.; Feigl, B.J.; Schils, R.L.M.; Cerri, C.E.P.; Cerri, C.C. 2015. Improved pasture and herd management to reduce greenhouse gas emissions from a Brazilian beef production system. Livestock Science 175: 101-112.

Mwendia, S.W.; Yunusa, I.A.; Sindel, B.M.; Whalley, R.D.; Kariuki, I.W. 2017. Assessment of Napier grass accessions in lowland and highland tropical environments of East Africa: water stress indices, water use and water use efficiency. Journal of the Science of Food and Agriculture 97, 1953-1961.

Neal, J.S.; Fulkerson, W.J.; Hacker, R.B. 2011. Differences in water use efficiency among annual forages used by the dairy industry under optimum and deficit irrigation. Agricultural Water Management 98: 759-774.

Neres, M.A.; Castagnara, D.D.; Mesquita, E.E.; Jobim, C.C.; Três, T.T.; Oliveira, P.S.R.; Oliveira, A.A.M.D.A. 2011. Production of Tifton 85 hay overseeded with white oats or ryegrass. Revista Brasileira de Zootecnia 40: 1638-1644.

Oliveira, J.F.D.; Rodrigues, F.N.; Fia, R.; Vilela, H.S.; Mafra, D.C. 2017. Performance of tifton 85 grass under fertirrigation with slaughterhouse wastewater. Engenharia Agrícola 37: 790-800.

Pequeno, D.N.; Pedreira, C.G.; Sollenberger, L.E.; Faria, A.F.; Silva, L.S. 2015. Forage accumulation and nutritive value of brachiariagrasses and Tifton 85 bermudagrass as affected by harvest frequency and irrigation. Agronomy Journal 107: 1741-1749.

Pezzopane, J.R.M.; Santos, P.M.; Mendonça, F.C.; Araujo, L.C.D.; Cruz, P.G.D. 2012. Dry matter production of Tanzania grass as a function of agrometeorological variables. Pesquisa Agropecuária Brasileira 47: 471-477.

Quiloango-Chimarro, C.; Coelho, R.D.; Costa, J.O.; Gomez-Arrieta, R. 2021. Crop water stress index for predicting yield loss in common bean. Irriga 4: 687-695.

Rolando, J.L.; Turin, C.; Ramírez, D.A.; Mares, V.; Monerris, J.; Quiroz, R. 2017. Key ecosystem services and ecological intensification of agriculture in the tropical high-Andean Puna as affected by land-use and climate changes. Agriculture, Ecosystems & Environment 236, 221-233.

Sadras, V.O. 2009. Does partial root-zone drying improve irrigation water productivity in the field? A meta-analysis. Irrigation Science 27, 183-190.

Saint-Denis, T.; Goupy, J. 2004. Optimization of a nitrogen analyser based on the Dumas method. Analytica Chimica Acta 515, 191-198.

Silva, W.L.; Costa, J.P.R.; Caputti, G.P.; Lage Filho, N.M.; Ruggieri, A.C.; Reis, R.A. 2019. Effects of grazing intensity and supplementation strategies on Tifton 85 production and on sheep performance. Small Ruminant Research 174, 118-124.

Snyder, R.L.; Pedras, C.; Montazar, A.; Henry, J.M.; Ackley, D. 2015. Advances in ET-based landscape irrigation management. Agricultural Water Management 147: 187-197.

Spanghero, M.; Berzaghi, P.; Fortina, R.; Masoero, F.; Rapetti, L.; Zanfi, C.; Ferlito, J. C. 2010. Precision and accuracy of in vitro digestion of neutral detergent fiber and predicted net energy of lactation content of fibrous feeds. Journal of Dairy Science 93, 4855-4859.

Tapparo, S.A.; Coelho, R.D.; Costa, J.O.; Chaves, S.W.P. 2019. Growth and establishment of irrigated lawns under fixed management conditions. Scientia Horticulturae 256: 1-7.

Tapparo, S.A.; Coelho, R.D.; Costa, J.O.; Chaves, S.W.P.; Quiloango-Chimarro, C.A.; Oliveira, E.D.S. 2022. Relationships between leaf water potential and soil water potential in grasses subjected to water stress. Revista Brasileira de Engenharia de Biossistemas 16: 1-7.

Van Genuchten, M.T. 1980. A closed-form equation for predicting the hydraulic conductivity of unsaturated soils. Soil Science Society of America Journal 44: 892–898.

Van Raij, B.; Cantarella, H.; Quaggio, J.A.; Furlani, A.M.C. 1997. Fertilization and liming recommendations for the São Paulo State. Campinas: Instituto Agronômico/Fundação IAC.

Yan, Y.; Wan, Z.; Chao, R.; Ge, Y.; Chen, Y.; Gu, R.; Yang, J. 2018. A comprehensive appraisal of four kinds of forage under irrigation in Xilingol, Inner Mongolia, China. The Rangeland Journal 40: 171-178.

Italian Journal of
Agrometeorology
Rivista Italiana di Agrometeorologia

Firenze University Press
www.fupress.com/ijam

OPEN ACCESS

Citation: Abdulqader Ibrahim, W., Gumus, V., & Seker, M. (2023). Investigating future projection of precipitation over Iraq using artificial neural network-based downscaling. *Italian Journal of Agrometeorology* (2): 79-94. doi: 10.36253/ijam-1929

Received: December 11, 2022

Accepted: October 6, 2023

Published: January 20, 2024

Data Availability Statement: All relevant data are within the paper and its Supporting Information files.

Competing Interests: The Author(s) declare(s) no conflict of interest.

ORCID:
WAI: 0000-0002-7210-6897
VG: 0000-0003-2321-9526
MS: 0000-0002-4007-0703

Author Statement:
WAI: Performing analysis, interpreting results, and writing the manuscript; VG: Conceptualization, coding, writing the manuscript; MS: Performing analysis, writing the manuscript and interpreting results.

Investigating future projection of precipitation over Iraq using artificial neural network-based downscaling

Wlat Abdulqader Ibrahim[1], Veysel Gumus[1,2,*], Mehmet Seker[1]

[1] *Department of Civil Engineering, Harran University, Sanliurfa 63050, Turkey*
[2] *Engineering Department, University of Durham, Durham, DH1 3LE, United Kingdom*
*Corresponding author. E-mail: gumus@harran.edu.tr

Abstract. Global climate change will affect the precipitation and the temperature, and its effects need to be investigated. General circulation models (GCM) are one of the most used approaches to assessing the future effects of climate change. However, different GCMs have been proposed by researchers, and their success in the regions needs to be tested. Therefore, in this study, the performance of 29 GCMs in predicting precipitation in the Iraq region for 102 stations is evaluated using the artificial neural network-based statistical downscaling method. In order to evaluate the performance of these models, Nash Sutcliffe Model Efficiency Coefficient (NSE), normalized root mean square error (nRMSE), Kling-Gupta Efficiency (KGE), The Modified Index of Agreement (md), and Comprehensive Rating Index (CRI) are used. A comparison of the results shows that NorESM1-ME, FGOALS-g2, and NorESM1-M models performed well in estimating the historical precipitation of the region, and NorESM1-ME had the best representation. As a final step, future precipitation changes in Iraq were analyzed spatially and temporally under the RCP4.5 and RCP8.5 scenarios.

Keywords: climate change, CMIP5, Iraq, precipitation, artificial neural network.

HIGHLIGHTS

- The performance of general circulation models (GCM) in predicting precipitation is evaluated in Iraq for 102 stations.
- The performance of 29 models is assessed via five different criteria
- The NorESM1-ME, FGOALS-g2, and NorESM1-M models performed well in estimating the historical precipitation of the region.
- Future precipitation changes in Iraq under different scenarios were evaluated temporally and spatially.

1. INTRODUCTION

Because of rapid human activities in industrial and economic development, land use change, and environmental degradation during the twentieth century, greenhouse gases have increased in the atmosphere on the planet. Since the second half of the twentieth century, most parts of the world have experienced a temperature increase and climate change due to this increase (Chen and Sun 2013). Climate change significantly impacts natural ecosystems, one of the most significant consequences. It is these changes that have an impact on the number of products and services available from these resources and, ultimately, their benefits. As a result of climate change, the quality and quantity of water resources will be affected. In addition, the condition of forests and pastures, green space, wildlife, aquatic animals, etc. The impact of climate change on water resources is one of the main concerns of scientists from various fields. It is essential to study and monitor climate change, as it greatly impacts all human activities (Feng et al. 2010). In this context, the World Meteorological Organization (WMO) and the United Nations Environment Organization (UNEP), which were established in 1988 under the leadership of the Intergovernmental Panel on Climate Change (IPCC), have been tasked with conducting essential studies on climate researchers worldwide. Several reports have been published by this organization in order to determine the extent and impact of climate change. According to the IPCC's Fifth Assessment Report (AR5), the Earth's average temperature has increased by 0.6 degrees Celsius over the past century. Additionally, if greenhouse gas emissions do not decrease in the 21st century, average global temperatures will rise by 1.1 to 6.4 degrees Celsius (IPCC 2013).

The use of climate modelling is one of the critical steps in predicting the future trend of climate change and the measures to be taken based on these forecasts. A global climate model (GCM) predicts possible future climate changes. It is a numerical instrument that simulates the physical processes of the land surface, ocean, and atmosphere in regional and hydro climatological studies (Sreelatha and Anand Raj 2019). Researchers in different countries have developed GCM models in recent decades to understand and predict climate change (Her et al. 2019). As part of the coupled model intercomparison project (CMIP), these models are combined into a global project with a common comparative framework to improve knowledge of climate change (climate in the past and present, as well as improving the performance of climate models for different species) (Demirel and Moradkhani 2015). In recent years, a new generation of climate models, known as Earth models, have been developed in the context of phase 5 of the CMIP (CMIP5) global projects, which aim to reduce the uncertainty associated with the previous phase 3 of CMIP (CMIP3) (Eyring et al. 2016). Compared to their predecessors' CMIP3 models, the CMIP5 models have significantly improved climate simulation and forecasting (Wang et al. 2016). According to (Taylor et al. 2012), the performance of CMIP5 is due to the inclusion of more favorable climate simulations from the previous year. In the AR5 report, scenarios known as Representative Concentration Pathways (RCP) were used in the development of GCMs published under CMIP5. Based on the RCP scenarios developed by a scientific committee under the auspices of the IPCC in 2010, the main causes of climate change can be traced. These results can be applied to climate models. The results of these scenarios are used in climate models to calculate greenhouse gas concentrations and emissions. In the same meeting, the literature was reviewed regarding the characteristics determined, and four RCP types were defined for radiative forcing levels and routes. From smallest to largest, these radiative forcing scenarios are RCP2.6, RCP4.5, RCP6.0, and RCP8.5.

In several studies, the GCM published under CMIP5 has been used to investigate climate change's impact on meteorological parameters (Afzali-Gorouh et al. 2018; Shiravand and Dostkamiyan 2019). For example, Srinivasa Raju et al. (2016) evaluated India's maximum and minimum temperature simulation performance using 36 general atmospheric circulation models from CMIP5. Ruan et al. (2018) examined CMIP5 to evaluate the score-based method's effectiveness in predicting precipitation in China (Lower Mekong Basin). Elsaeed et al. (2021), the daily precipitation characteristics of the Zab River were examined using the (CMIP5) model from 1979 to 2005, and the future precipitation changes were predicted using RCP4.5 and RCP8.5.

Even though GCMs are decent tools in climate studies, they cannot be applied directly because their outputs are too coarse to explain local climate changes (Shiru et al. 2019; Noor et al. 2020). Climate change simulations based on GCMs cannot provide practical information about spatial scales below 200 kilometers. Therefore, it is necessary to downscale coarse-resolution GCM simulated climate variables such as precipitation to regional scales for more realistic simulations (Su et al. 2016). By applying downscaling methods, it is possible to convert the output of GCM models into reliable predictions of climate precipitation variables at a regional scale. Downscaling methods can be categorized into two groups: statistical and dynamic downscaling. Dynamic downscaling allows the climate scale to be reduced for an area bounded by the GCM models. A statistical downscaling approach equates large-scale climatic features to local climate data (Wilby and Wigley 1997). However, dynamic downscaling, a method that relies on the complex physics of atmospheric processes, is both computationally expensive and time-consuming, requiring computers with high computing power and specialized personnel. On the other hand, the statistical downscaling method (SDSM) aims to find the relationship between the large-scale GCM outputs (predictors) and the climate variables at the basin scale (predictands) without providing any information about the physical area (Danandeh Mehr and Kahya 2016).

SDSM is based on establishing a relationship between predictors and predictands. However, many statistical downscaling methods are used in the literature. SDSMs are performed using either bias correction or regression methods, such as linear regression or machine learning. A significant advantage of bias correction methods is their simplicity and straightforward application. However, bias correction methods, such as the delta change approach, do possess limitations. Notably, they predominantly overlook variations in the temporal structure and variability of climate variables, including fluctuations in dry/wet spells or temperature (Maraun 2016). This is primarily because the delta change method assumes that biases are constant over time, and it does not consider changes in the distribution of climate parameters. Additionally, since bias correction methods use only the relevant GCM parameter as a predictor, other parameters are mostly ignored. In contrast, regression methods allow using different atmospheric variables in estimation (Seker and Gumus 2022). In this context, regression-based methods for statistical downscaling enable finding a relationship between the large-scale circulation variables of the GCM and the observed meteorological data. A particularly powerful tool in this regard is the Artificial Neural Network (ANN) regression method. It is capable of identifying complex relationships between predictors and basin-scale climate variables. The ANN method boasts distinct advantages over classical linear approaches, primarily its capacity to model intricate, non-linear relationships among multiple input and output variables. This ability is facilitated by the network's 'learning' nature, adapting its structure according to the data. Moreover, the ANN approach is robust against noise and offers considerable customization flexibility in terms of varying architectures, activation functions, and training algorithms (Nourani et al. 2013; Saraf and Regulwar 2016). This method in recent years have been mostly used in downscaling in different parts of the world. For example, Xu et al. (2020) used the ANN method to downscale GCMs in China's Upper Han River Basin, Rabezanahary Tanteliniaina et al. (2021) investigated the future impact of climate change on Africa (Mangoky River) using ANN techniques and soil and water assessment tool (SWAT) data. Seker and Gumus (2022) used ANN techniques for downscaling temperature and precipitation data in the Mediterranean region of Turkey.

Due to the differences in the ability of downscaled GCMs to simulate climate depending on the climatic zone, two methods have been used to select GCMs: past performance and envelope method (Srinivasa Raju et al. 2016; Salman et al. 2018; Iqbal et al. 2020). A GCM's past performance is mainly determined by its ability to reproduce the climate of the last few years and compare it with historical data (Wright et al. 2015). GCMs are generally chosen based on their ability to simulate past climates (Shiru et al. 2019; Iqbal et al. 2020; Khan et al. 2020), and it is generally accepted that if a GCM accurately simulates the past, it will also accurately simulate the future (Andrews et al. 2019).

The IPCC report (IPCC 2013) identifies North Africa and the Middle East region are particularly sensitive to climate change. The global average temperature changes much faster than in the Middle East and North Africa (Salman et al. 2018). Further, according to the World Meteorological Organization (WMO 2019), West Asia and the Middle East are experiencing one of the worst droughts and declining precipitation periods in human history. It is, therefore, imperative that climate change impacts precipitation, the primary source of water resources in these regions, to determine its impact.

The Middle East has been the subject of numerous studies over the past two decades on the impact of climate change on hydrological processes such as temperature, precipitation, and surface runoff. According to Zarenistanak (2018), precipitation might decrease under the RCP4.5 and RCP8.5 scenarios, according to most models under the Alborz Mountain area. Ostad-Ali-Askari et al. (2020) examined the prediction of future precipitation in Iran (Isfahan). Based on RCP4.5 results, a 17% decrease in precipitation is expected during winter. Also, RCP8.5 predicts 32.7% precipitation in the spring. According to RCP4.5 and RCP8.5, autumn had the lowest reduction in precipitation, 6.9% and 14.4%, respectively. Homsi et al. (2019) CMIP5 Precipitation predicted in Syria indicated precipitation decreased along the coast for all RCPs. A significant increase in precipitation (up to 76%) was observed in some areas in the northwest and southwest for RCPs 4.5 and 8.5. Precipitation decreased during the dry season, with the greatest reduction occurring in the coastal and northeast areas.

Regarding climate change, Iraq is an important region in the Middle East. Researchers have recently examined the effects of climate change on meteorological parameters in this region since it is sensitive to climate change. For example, Al-Mukhtar and Qasim (2019) used the HadCM3 model to predict precipitation in Iraq using (SDSM) and the daily precipitation. The results indicated a decrease in precipitation for all months. According to Mohammed and Hassan (2022), the LARS_WG model was used to predict future precipitation in southern Iraq. CSIRO-Mk3.6.0, HadGEM2-ES, CanESM2, MIROC5, and NorESM1-M models were used to predict precipitation and temperature under RCP4.5 and RCP8.5 scenarios. The results indicated that each model shows a different rate of precipitation reduction. According to Hashim et al. (2022), Iraq's future precipitation and temperature prediction indicate that the southern and southwestern parts are the most affected. Based on the 20 CMIP5 models, Khayyun et al. (2020) examined the future precipitation for 35 stations in Iraq. Following the final ranking of these 20 CMIP5 models, only four were suitable for data projection scenarios, namely HadGEM2-AO, HadGEM2-ES, CSIRO-Mk36, and MIROC5.

It is seen that the projection studies carried out in Iraq are mostly regional or is made with a limited number of stations. Additionally, to the authors' knowledge, there is no study in Iraq that used the ANN method in downscaling for precipitation. In this study, future precipitation projections were made using SWAT data from 102 grid points in Iraq. For this purpose, The ANN-based SDSM method was used to determine the historical data estimation performances of 29 CMIP models. The most appropriate GCMs are selected based on five statistical performance criteria, NSE, nRMSE, KGE, and MD. Iraq's future precipitation projection between 2020 and 2100 was evaluated temporally and spatially based on two scenarios (RCP4.5 and RCP8.5).

2. STUDY AREA AND DATASETS

2.1. Study area and observed datasets

Iraq, situated in Southwest Asia, has geographical coordinates spanning from 29.25° N to 38.25° N in latitude and 38.75° E to 48.75° E in longitude. The Iraqi borderline is shared with Iran, Kuwait, Syria, Turkey, Jordan, and Saudi Arabia, as indicated in Figure 1a. The land area of Iraq is approximately 438,317 km2. Iraq is ranked 58th in the world in terms of land area. Geographically, Iraq is primarily lowland and tropical. There are deserts in the west, fertile plains in the east, and mountains in the northeast of Iraq. The minimum, maximum, and average annual precipitation were 63.18 millimeters, 1195.62 millimeters, and 216.1 millimeters, respectively. The mean, maximum, and minimum annual temperatures were 9.54 degrees Celsius, 26.79 degrees Celsius, and 22.61 degrees Celsius, respectively. As can be seen in Figure 1-b, the average yearly precipitation observed for all stations is shown. A dramatic decrease in precipitation is observed in Figure 1-b as it moves from north to south. A difference of up to 15 times between the region's lowest and highest precipitation indicates that precipitation is highly variable. Thus, a study that utilizes a small number of stations in Iraq, where precipitation varies, may not be reliable. In order to evaluate the projection, 102 stations in Iraq were uniformly distributed. Table 1 shows the number of stations and their provinces selected from Anbar province, which has the largest area, and Baghdad province, which has the smallest area. The data for the period 1979–2013 were obtained from the Global Weather Service (globalweather.tamu.edu).

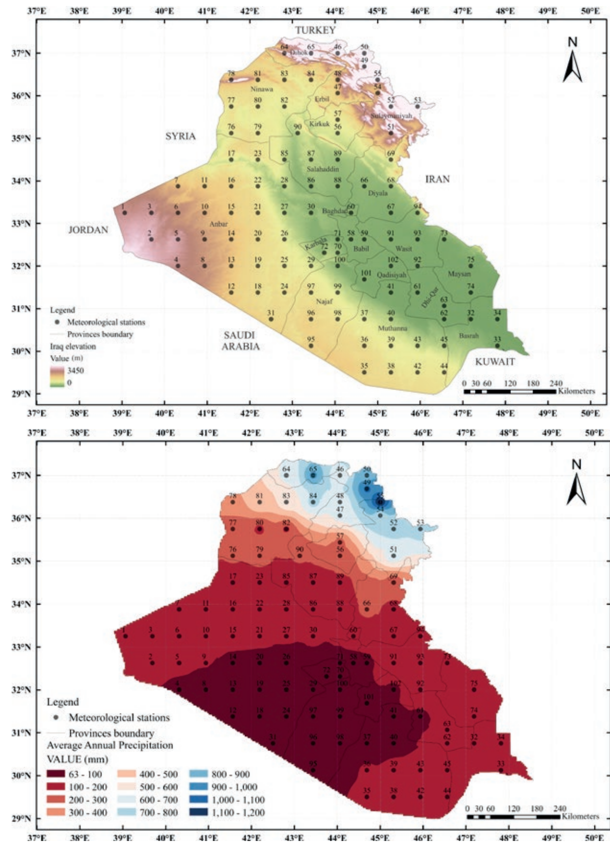

Figure 1. (a) Elevation map and location of the stations, (b) Spatial distribution of annual average precipitation (mm).

2.2. CMIP5 dataset

The GCMs are integral tools developed to simulate and predict large-scale climate dynamics for the past,

Table 1. The meteorological stations used in the study.

Province	No	Station ID	Province	No	Station ID	Province	No	Station ID
Anbar	1	333391	Muthanna	35	295447		69	345453
	2	326397		36	301447	Karbala	70	323441
	3	333397		37	308447		71	326441
	4	320403		38	295453		72	323438
	5	326403		39	301453	Maysan	73	326466
	6	333403		40	308453		74	314472
	7	339403		41	314453		75	320472
	8	320409		42	295459	Ninawa	76	351416
	9	326409		43	301459		77	358416
	10	333409		44	295466		78	364416
	11	339409		45	301466		79	351422
	12	314416	Erbil	46	370441		80	358422
	13	320416		47	361441		81	364422
	14	326416		48	364441		82	358428
	15	333416		49	367447		83	364428
	16	339416		50	370447		84	364434
	17	345416	Sulaymaniyah	51	351453	Salahaddin	85	345428
	18	314422		52	358453		86	339434
	19	320422		53	358459		87	345434
	20	326422		54	361450		88	339441
	21	333422		55	364450		89	345441
	22	339422	Kirkuk	56	351441		90	351431
	23	345422		57	354441	Wasit	91	326453
	24	314428	Babil	58	326444		92	320459
	25	320428		59	326447		93	326459
	26	326428	Baghdad	60	333444		94	333459
	27	333428	Dhi-Qar	61	314459	Najaf	95	301434
	28	339428		62	308466		96	308434
	29	320434		63	311466		97	314434
	30	333434	Dihok	64	370428		98	308441
	31	308425		65	370434		99	314441
Basrah	32	308472	Diyala	66	339447		100	320441
	33	301478		67	333453	Qadisiyah	101	317447
	34	308478		68	339453		102	320453

present, and future, providing an in-depth understanding of the Earth's complex climate system. However, their raw outputs are at a global scale. For local applications, these models need to be downscaled to capture regional climate variations. The effectiveness of these downscaled GCMs hinges on their ability to accurately reproduce the statistical characteristics of historical climate data on various timescales, from monthly to daily, in simulations of historical periods. Therefore, it's necessary to compare the downscaled simulated data with observational precipitation data during the historical period. This comparison allows us to evaluate the performance of the downscaled GCMs for analyzing and studying the impacts of climate change on local water resource systems.

A GCM data production server (www.dkrz.de) provided the climatic data required; the data obtained were for CMIP5. This first step involved extracting monthly data in NetCDF format for all climate variables obtained for 102 locations in the Iraq region. The process was carried out for 29 models of the CMIP5 (Table 2). CMIP5 models were used in this study for both single- and multiple-level data. In this study, monthly predicted time series of precipitation in the historical period of 1979-2005 have been used to compare with the corresponding historical time series at base stations. The inverse dis-

Table 2. The information of used CMIP5 models.

No	Model	Country	Resolution Lon° ×Lat°
1	ACCESS1.3	Australia	1.875° × 1.25°
2	BCC-CSM1.1	China	2.8125° × 2.7906°
3	BCC-CSM1.1(m)	China	2.8125° × 2.7906°
4	BNU-ESM	China	2.8125° × 2.7906°
5	CanESM2	Canada	2.8125° × 2.7906°
6	CCSM4	United States	1.25° × 0.9424°
7	CESM1-BGC	United States	1.25° × 0.9424°
8	CESM1-CAM5	United States	1.25° × 0.9424°
9	CESM1-WACCM	United States	2.5° × 1.8848°
10	CMCC-CM	Italy	0.75° × 0.7484°
11	CMCC-CMS	Italy	3.75° × 3.7111°
12	CNRM-CM5	United States	1.40625° × 1.4008°
13	CSIRO-Mk3-6-0	Australia	1.875° × 1.8653°
14	FGOALS-g2	China	2.8125° × 2.7906°
15	FIO-ESM	China	2.80° × 2.80°
16	GISS-E2-R	United States	2.5° × 2°
17	HadGEM2-AO	England	1.875° × 1.25°
18	INM-CM4	Russia	2° × 1.5°
19	IPSL-CM5A-LR	France	3.75° × 1.8947°
20	IPSL-CM5A-MR	France	2.5° × 1.2676°
21	IPSL-CM5B-LR	France	3.75° × 1.8947°
22	MIROC5	Japan	1.40625° × 1.4008°
23	MIROC-ESM	Japan	2.8125° × 2.7906°
24	MIROC-ESM-CHEM	Japan	2.8125° × 2.7906°
25	MPI-ESM-LR	Germany	1.875° × 1.8653°
26	MPI-ESM-MR	Germany	1.875° × 1.8653°
27	MRI-CGCM3	Japan	1.125° × 1.12148°
28	NorESM1-M	Norway	2.5° × 1.8947°
29	NorESM1-ME	Norway	2.5° × 1.8947°

tance weight averaging method was used to interpolate the predictors of GCMs with different resolutions from the four grid points closest to each station to bring them to the same resolution, and the obtained data were used as input in the ANN method.

3. METHOD

3.1. Procedure

The approach to this research is visualized in a sequence of steps detailed in Figure 2. It starts with data acquisition, where independent atmospheric variables from General Circulation Models (GCMs) are gathered for both a reference period (1979-2005) and a future period (December 2006-2100). The data is procured from the four closest GCM grid points to each station, utilizing the inverse distance interpolation method. Next in the process comes preprocessing and predictor selection. This step involves identifying the five GCM predictors that correlate most strongly with the historical temperature and precipitation data of each station. These predictors are subsequently defined as dominant. The dominant predictors serve as inputs in an ANN-based SDSM. Table 3 provides a list of all the predictors used in the study. This table outlines the predictors, all of which are aggregated on a monthly scale, along with their relevant units. The predictors include both multi-level variables such as relative humidity, and temperature for different geopotential height (200m, 300m, 500m and 850m), and single-level variables like sea level pressure, surface pressure, 2m temperature, and precipitation.

The aim of this model is to predict observed precipitation at each station. Performance evaluation follows, assessing the ability of the GCMs to simulate monthly total precipitation at the stations. This evaluation is based on five performance criteria: the Correlation Coefficient (CC), Nash-Sutcliffe Efficiency (NSE), normalized root mean square error (nRMSE), Kling-Gupta Efficiency (KGE), and Modified Agreement Index (md). In the model selection stage, the Comprehensive Rating Index (CRI) is used to identify the best-performing models based on the evaluation criteria. Finally, future projections for each station are made. These projections incorporate RCP4.5 and RCP8.5 scenarios for the period 2006-2100, using the top three best-performing GCMs.

The general procedure of this study is as follows:

1. First, the independent atmospheric variables of the GCM outputs (reference and future period) used in the ANN-based SDSM to generate for each station were obtained using the inverse distance interpolation method from the nearest four GCM grid points. The number of predictors was 16, including multi-level predictors such as geopotential height, relative humidity and temperature, as well as single-level predictors such as sea level pressure, surface pressure, 2m temperature and precipitation, with each multi-level predictor including five different levels: 200hpa, 300hpa, 500hpa and 850hpa. The data between 1979-2005 are evaluated as the reference period, and December 2006-2100 as the future period.
2. The first five GCMs predictors (out of 16) with the highest correlation with each station's historical temperature and precipitation data were selected as the dominant predictors.
3. The dominant predictors determined from the independent variables obtained from the GCMs were defined as inputs to the ANN-based model for pre-

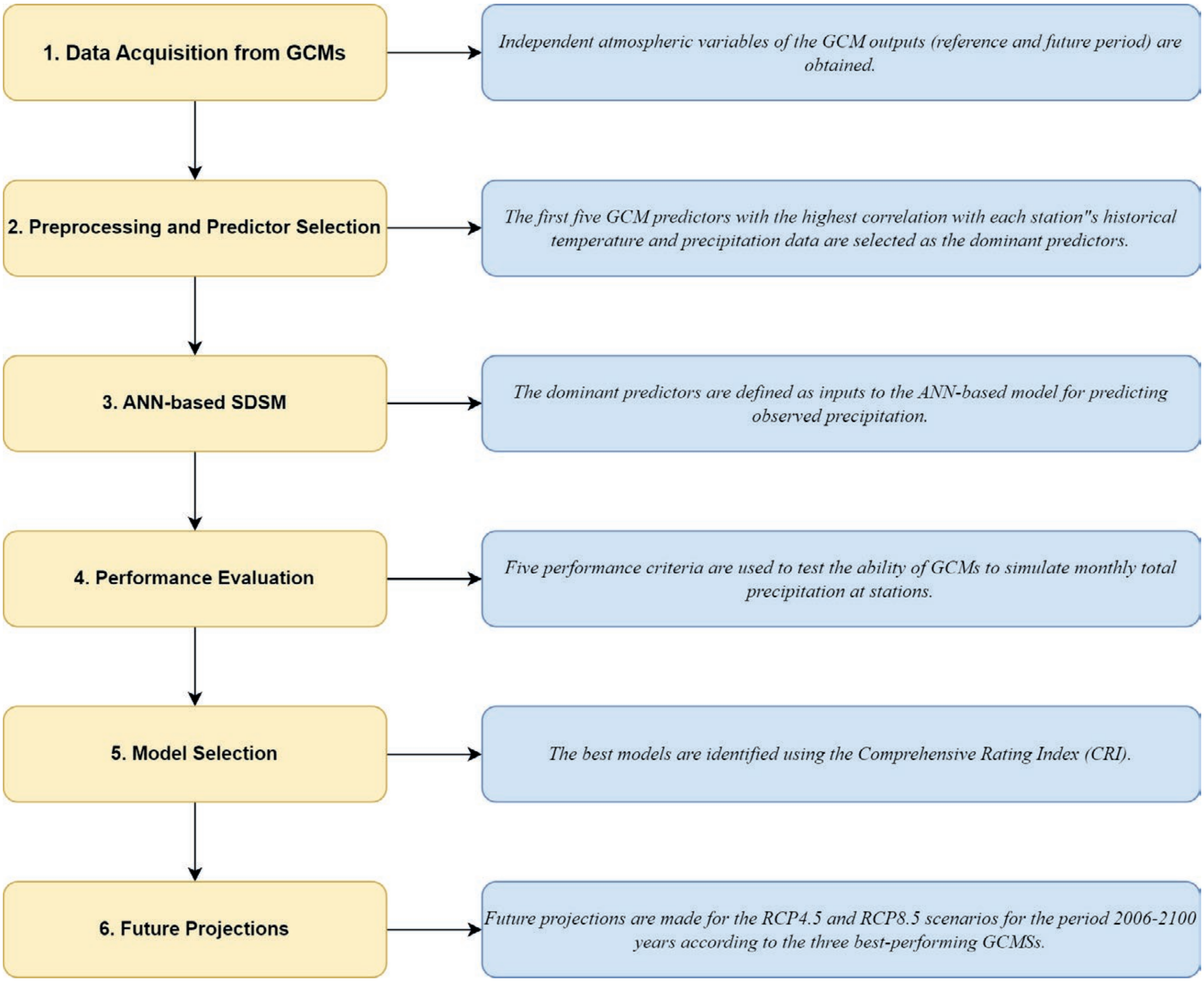

Figure 2. Flowchart of the study.

dicting observed precipitation. The observed precipitation data based on the station are defined as the model's output.

4. Five performance criteria are used to test the ability of GCMs to simulate monthly total precipitation at stations. These are Correlation Coefficient (CC), Nash-Sutcliffe Efficiency (NSE), normalized root mean square error (nRMSE), Kling-Gupta Efficiency (KGE) and Modified Agreement Index (md).
5. The best models in the study were identified using the Comprehensive Rating Index (CRI), which allows all performance criteria to be evaluated together.
6. Future projections from all regional synoptic stations for the RCP4.5 and RCP8.5 scenarios for the period 2006-2100 years were made according to the three best-performing GCMSs.

3.2. The artificial neural network method

The artificial neural network (ANN) method, particularly the feed-forward error backpropagation artificial neural network technique, is popular in hydrometeorology for modeling problems lacking analytical relationships (Seker and Gumus 2022). This study applies this technique to examine precipitation in Iraq, using 29 CMIP5 models across 102 stations. The ANN model consists of input, hidden, and output layers, with the model selecting five highly correlated independent variables with precipitation for each GCM model and station as an input. The output layer has a single value, and this is precipitation. The number of hidden layers is determined through a trial-and-error method, ranging from 1 to 10, with the optimal number yielding the low-

Table 3. List of used predictors.

Predictor variables	Units	Pressure level	Number of Variable
Air temperature	K	200,300,500 ,850	4
Air pressure at sea level	Pa	Sea level	1
Relative humidity	%	200,300,500 ,850	4
Jeopatential height	M	200,300,500 ,850	4
Near-surface temperature	K	Surface	1
Precipitation	Kg m^{-2} s^{-1}	Surface	1
Air pressure	Pa	Surface	1

est normalized root mean square error (nRMSE). Consequently, the study evaluates the performance of the GCMs in predicting precipitation and temperature in the Iraq region by generating 2958 models, derived from the 29 models, 102 stations. The detail of the method can be found in Keskin and Terzi (2006)

3.3. Assessment of the GCM models

In order to determine the success of the downscaled GCMs in predicting precipitation observed with ANN-based models, four quantitative performance evaluation criteria were applied. As explained in Equations 1-4, these are Nash coefficients (NSE), normalized root mean square errors (nRMSE), Kling-Gupta efficiency (KGE), and The Modified Index of Agreement (md) (McMahon et al. 2015). As a result, the most successful method of model determination has been The Comprehensive Rating Index (CRI) method (Equation 5), which allows for ranking among the models by making a joint evaluation of all methods involved. Among these coefficients, NSE, KGE, and md are close to 1, and md to zero indicates that the model's success has increased. A CRI value of 1 indicates that a model is most successful.

$$\mathrm{NSE} = 1 - \left(\frac{\sum_{i=1}^{N}(P_{sml,i} - P_{obs,i})^2}{\sum_{i=1}^{N}(P_{obs,i} - \bar{P}_{obs})^2}\right) \tag{1}$$

$$NRMSE = \frac{\sqrt{\frac{1}{N}\sum_{i=1}^{N}(P_{sml,i} - o_{obs,i})^2}}{P_{obs(\max)} - P_{obs(\min)}} \tag{2}$$

$$KGE = 1 - \sqrt{(CC-1)^2 + \left(\frac{\overline{P_{sml}}}{P_{obs}} - 1\right)^2 + \left(\frac{\sigma_{model} / \overline{P_{sml}}}{\sigma_{obs} / \overline{P_{obs}}} - 1\right)^2} \tag{3}$$

$$md = 1 - \frac{\sum_{i=1}^{N}\left|P_{obs,i} - P_{sml,i}\right|}{\sum_{i=1}^{N}\left(\left|P_{sml,i} - \overline{P_{obs}}\right| + \left|P_{obs,i} - \overline{P_{obs}}\right|\right)} \tag{4}$$

$$CRI = 1 - \frac{1}{nm}\sum_{i=1}^{n} Rank_i \tag{5}$$

Where, $P_{obs,i}$ and are the observed and simulated values, respectively, $\overline{P_{obs}}$ and $\overline{P_{sml}}$ are the average observed and simulated values, respectively, and N is the number of data

4. RESULTS

4.1. Performance evaluation of GCMs

A compatibility analysis is conducted between the observed total precipitation data from 1979-2005 in the Iraq region and the predicted precipitation data derived from the CMIP5 model. Based on four statistical performance criteria, Figure 3 evaluates the predicted and observed precipitation values using 29 different GCMs of the CMIP5 model. These results indicate that the success of the models varies depending on the criteria. For example, a successful model is found to be FGOALS-g2 based on the NSE, KGE, and nRMSE values, whereas NorESM1-ME is successful based on the MD value. Due to this, it would be more realistic to determine the most successful models based on the CRI value, which evaluates the model performance by considering all criteria. The distribution of the calculated CRI values for each of the models used is shown in Figure 4. Further, Figure 5 shows the ranking of each model based on the CRI values. Therefore, nine GCM models have an acceptable CRI value (CRI>0.5). Furthermore, two of these models have an average CRI value above 0.6. These models are NorESM1-ME and FGOALS-g2.

The numbers in the heat map represent the rank of models. For example, the most successful model rank value in this is 1, while the worst is 29. The CRI results show that the NorESM1-ME, FGOALS-g2, and NorESM1-M models generally perform well in estimating the historical precipitation of the region. Figure 5 shows that NorESM1-ME is the most accurate model according to average ranks. This model was the most successful at 15 stations and among the top five most successful models at 57 stations.

On the other hand, the FGOALS-g2 model was the most accurate at more stations (17 stations) than the NorESM1-ME model. However, this model was among the top five most successful models at 44 stations. In addition, the third-best model, NorESM1-M, was the most successful model at only four stations and was among the list of the five most successful models at 29 stations. While the NorESM1-ME model can be considered the best-representing model for Iraq in general, it

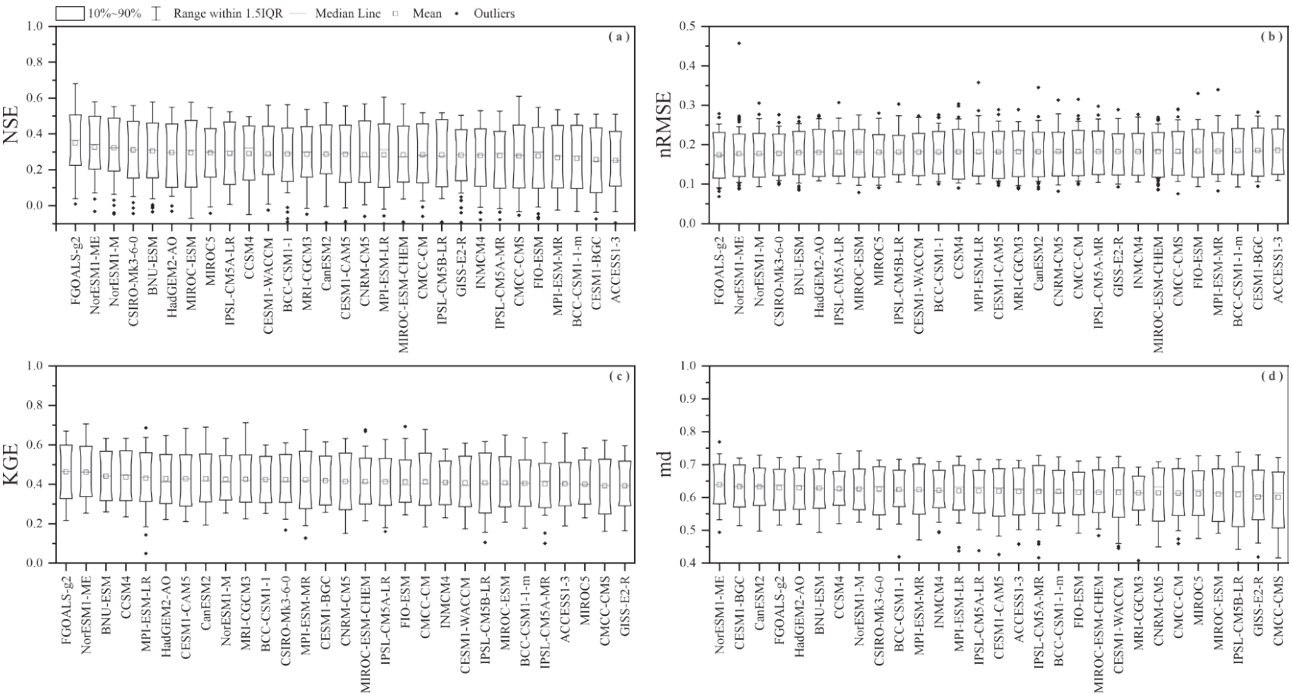

Figure 3. The distribution of statistics parameters (a) Nash coefficient, (b) nRMSE, (c) KGE, (d) md.

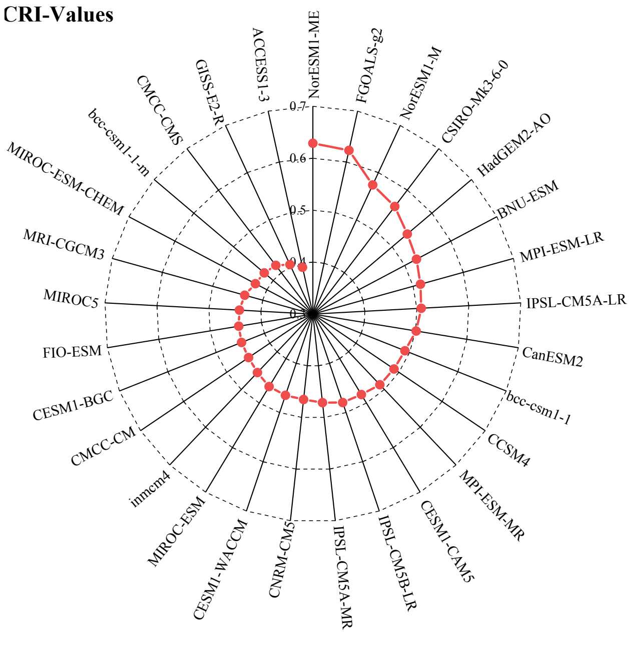

Figure 4. The radar graph of CRI values for all used CMIP5 models.

has been observed to be ineffective only at the stations located in the mountainous regions in the north. Mostly, the FGOALS-g2 and NorESM1-M models performed well at these stations. Therefore, the future projection of the region for two scenarios (RCP4.5 and RCP8.5) was evaluated with these three models.

4.2. Projection of precipitations for RCP4.5 scenario

In this part of the study, future precipitation projections for the Iraq region are based on the outputs of the best-performing GCMs in simulating historical precipitation. According to Figure 6, the average monthly precipitation in the future period (2006-2100) is different from the observation period (1979-2005) for the NorESM1-ME, FGOALS-g2, and NorESM1-M models with the RCP4.5 scenarios. According to RCP4.5, the seasonal precipitation for Iraq stations will decrease in all seasons. According to NorESM1-ME, FGOaLS-g2, and NOrESM1-M, the average seasonal decrease in spring was 20.37%, 20.49%, and 18%, respectively. 22.5%, 11.66%, and 16.67% were recorded for the autumn. However, the winter season was 5.56%, 6.33% and 5.68%. According to all models, the maximum decrease occurs during the spring season.

Based on historical precipitation, Figure 7 illustrates the spatial distribution of station-based changes in Iraq for the three most appropriate CMIP5 models. According to the results of the NorESM1-ME model, which gave successful results in the southern regions, the maximum decreases were -63%, -84.93%, -64.01%

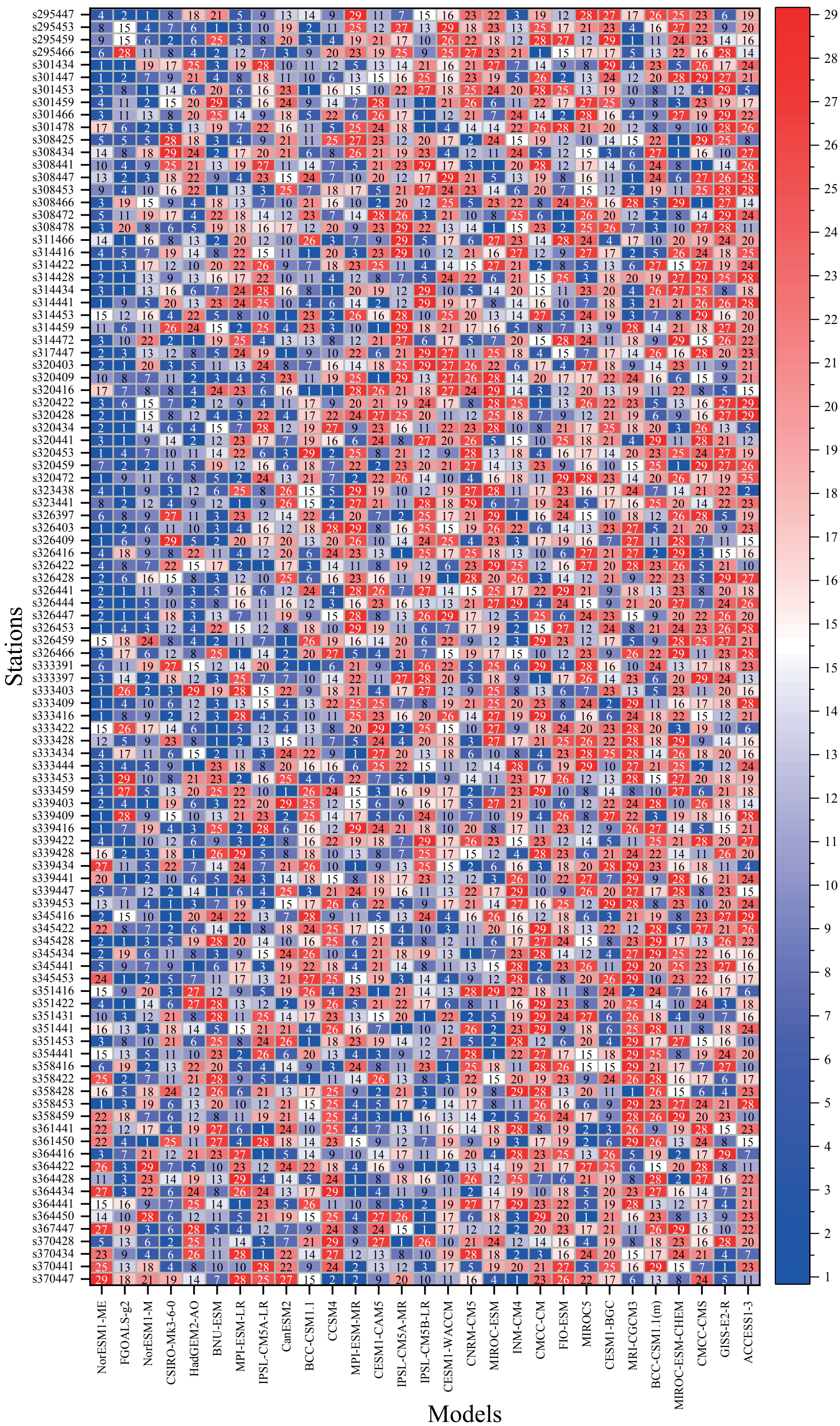

Figure 5. The heat map of 29 CMIP models based on the CRI ranking.

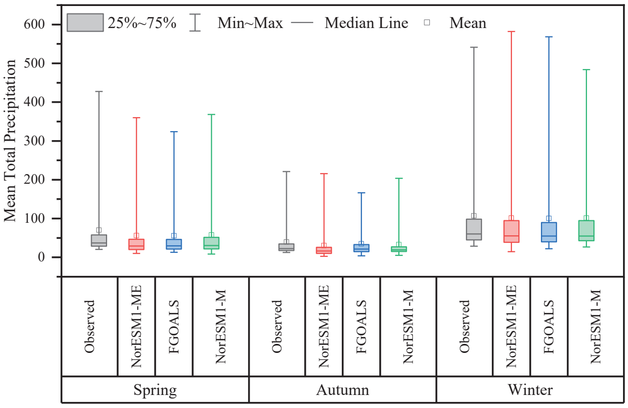

Figure 6. The box plot of observed and future precipitation for seasons according to the RCP4.5 scenario.

for spring, autumn, and winter, respectively. While the highest percentage of the decrease occurred in the autumn in the southern region, it is noteworthy that an increase occurred in the spring and winter in the mountainous northern regions. Additionally, spring precipitation was slightly increased in the eastern partially desert region. However, in the previous section, it was stated that NorESM1-ME did not produce successful results in northern regions. Therefore, to evaluate the future projections for the northern regions, spatial maps of the changes based on FGOALS-g2 and NorESM1-M, two successful models, are shown in Figures 7 (b) and (c). This map indicates that precipitation will increase significantly in the northern region during the spring and winter but decrease in the autumn months.

4.3. Projection of precipitations for RCP8.5 scenario

Based on the RCP8.5 scenario, future seasonal precipitation for Iraq stations will decrease in all seasons' average precipitation (Figure 8). According to NorESM1-ME, FGOaLS-g2 and NOrESM1-M, the average seasonal decreases were 33.52%, 36.69%, and 28.06%, respectively, in the spring season. The autumn season represented 29.93%, 29.41%, and 24.30%, whereas the winter season represented 11.76%, 15.16%, and 12.06%. Therefore, the maximum decrease is observed to be associated with the spring season, as indicated by all models. In this scenario, precipitation decreased more than in RCP4.5, as expected.

Based on the RCP8.5 scenario, Figure 9 shows the spatial distributions of the station-based changes in Iraq according to historical precipitation using the three most accurate CMIP5 models. The spatial distribution of precipitation changes for the most accurate model, NorESM1-ME, is shown in Figure 9 (a). This model determined that the maximum decreases could be as high as -71.39% in spring, -84.54% in autumn, and -77.57% in winter, respectively. Precipitation increases in the region's east relative to RCP4.5 in spring were not observed in this scenario. On the contrary, the decrease in precipitation is seen at almost all stations except the northern region in spring. In autumn and winter, all regions except a few stations in the middle and south regions follow this. Therefore, when the FGOALS-g2 and NorESM1-M model results for the northern regions are evaluated, it is understood that there is an increase in the north only in spring, but a decrease in precipitation will occur in the northern regions in other seasons.

5. DISCUSSION

Climate change projections for historical (1979-2005) and future (2006-2100) time periods were made for 102 stations with 29 GCM outputs published in CMIP5 for the Iraq region. In the study, the ability of the models to simulate historical data was evaluated, and future projections were made based on the three most successful GCMs. According to the results of the present study, NorESM1-ME, FGOALS-g2, and NorESM-M ranked the first three based on the CRI value, a common evaluation criterion for the ability of GCMs to simulate historical data. It is observed that the models have an acceptable ability to predict precipitation in the region with moderate to low accuracy. It was also found that although the models provide reliable precipitation predictions, they have weak prediction capabilities in some cases. In the study conducted by Abbas et al. (2022) to simulate the historical precipitation data of CMIP5 models with bias correction method over the Iraqi region, it is seen that the success of NorESM1-ME and NorESM1-M models is not parallel. In the studies conducted by Homsi et al. (2019) in Syria and Abbasian et al. (2018) in Iran, which are neighbouring border countries with similar climatic conditions, the ability of the NorESM1-M model to simulate historical precipitation data is at a good level, which supports the findings of the present study.

Although the precipitation in the region in this study changes partially from model to model, it is seen that, on average, there is a general decrease in all models. It is noted that the change in precipitation is greater in the RCP8.5 scenario compared to the RCP4.5 scenario. It can be seen that the decreases in the southern parts of the region are more pronounced than in the northern parts. For example, in the projection study carried out by Mohammed and Hassan (2022) in a local region

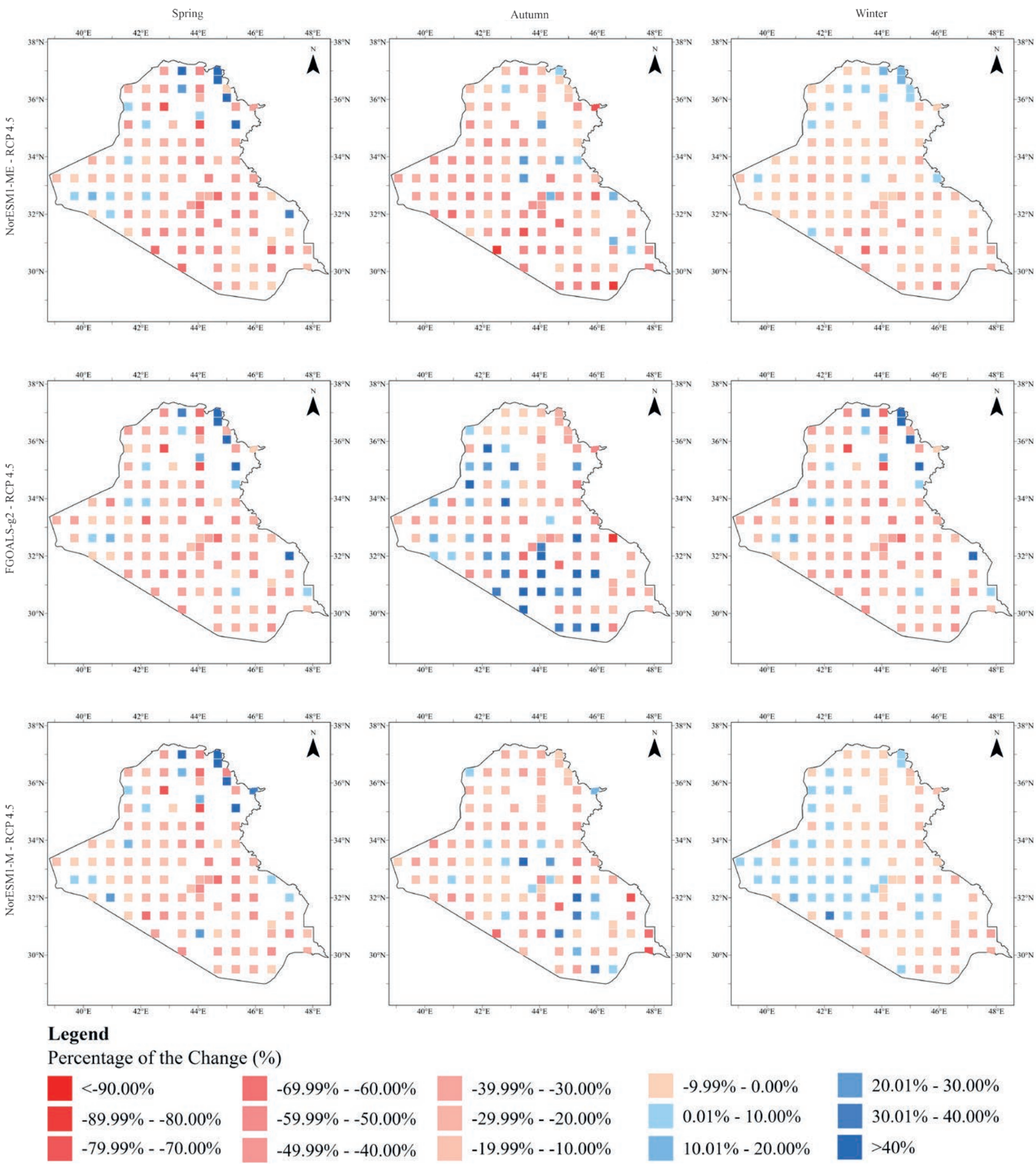

Figure 7. Spatial distribution of percentage change of the precipitation according to the RCP4.5 scenario for NorESM1-ME, FGOALS-g2 and NorESM1-M.

in south-eastern Iraq using the LARS-WG6.0 statistical scale reduction method, it was found that precipitation during the rainy seasons (autumn, winter, and spring) will increase in the future. In another study conducted by Al-Mukhtar and Qasim (2019), it was stated that precipitation in the region would decrease more in the

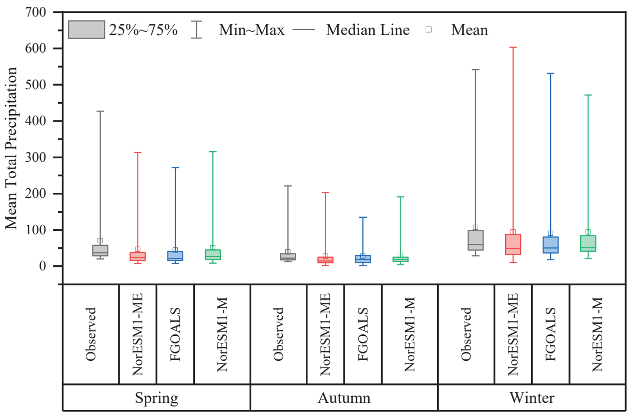

Figure 8. The box plot of observed and future precipitation for seasons according to the RCP8.5 scenario.

northern than in the southern parts using the statistical scale reduction method. In another study, Hamed et al. (2022) stated that precipitation will decrease in the northern parts of the region and increase in the southern regions. The results of this study are not in parallel with the above study. In addition, the results obtained in the study conducted in the southern parts of Khuzestan province (Rahimi et al. 2019), which is located in the southern parts of Khuzestan province within the borders of Iran, a regional neighbour, show that precipitation will decrease in the rainy seasons in the future; this result is in line with this study.

The assessment of the future seasonal precipitation change in the region shows an increase, especially in winter and spring months and a decrease in autumn months in the southern regions according to the RCP4.5 scenario. Considering the precipitation change in the region, the decreases in the spring months are significant. Considering the RCP8.5 scenario assessment, although it is more significant than the RCP4.5 scenario, the decrease in spring precipitation is also generally significant. In the study conducted by Ozturk et al. (2018), there is a decrease in precipitation in all seasons in the region in general. In another study conducted by Evans (2008), it is observed that there is an increase in precipitation in all seasons, and the increases are significant, especially in the autumn months.

6. CONCLUSION

In this study, the most successful CMIP5 model for the future projection of precipitation values of 102 stations in Iraq was determined using five different statistical parameters. While the model that best represents the country, in general, was the NorESM1-ME model, this model was insufficient to represent the country's northern region. Therefore, the most successful 2nd and 3rd Models in the country's northern region were FGOALS-g2 and NorESM1-M. In addition, the future projection of the country was evaluated according to two different scenarios using the most successful models. As a result of the projection study carried out according to RCP4.5, it was determined that the precipitation would decrease in the majority of the country, and there is a potential for a decrease in precipitation only in the northern region of the country in some seasons. On the other hand, according to RCP8.5, it has been seen that there will be a severe decrease in precipitation in almost the whole country.

Precipitation may decrease in regions sensitive to climate change, such as Iraq, and regions already suffering from drought will experience more problems. For this reason, it is considered that it will be helpful to examine the change in precipitation by the projection of precipitation and temperature with CMIP6 in addition to CMIP5 in Iraq by using soft computing techniques in downscaling.

REFERENCES

Abbas SA, Xuan Y, Al-Rammahi AH, Addab HF. 2022. A Comparison Study of Observed and the CMIP5 Modelled Precipitation over Iraq 1941–2005. Atmosphere. 13(11).

Abbasian M, Moghim S, Abrishamchi A. 2018. Performance of the general circulation models in simulating temperature and precipitation over Iran. Theoretical and Applied Climatology. 135(3-4): 1465-1483.

Afzali-Gorouh Z, Bakhtiari B, Qaderi K. 2018. Probable maximum precipitation estimation in a humid climate. Natural Hazards and Earth System Sciences. 18(11): 3109-3119.

Al-Mukhtar M, Qasim M. 2019. Future predictions of precipitation and temperature in Iraq using the statistical downscaling model. Arabian Journal of Geosciences. 12(2).

Andrews T, Andrews MB, Bodas-Salcedo A, Jones GS, Kuhlbrodt T, Manners J, Menary MB, Ridley J, Ringer MA, Sellar AA et al. 2019. Forcings, Feedbacks, and Climate Sensitivity in HadGEM3-GC3.1 and UKESM1. Journal of Advances in Modeling Earth Systems. 11(12): 4377-4394.

Chen H, Sun J. 2013. Projected change in East Asian summer monsoon precipitation under RCP scenario. Meteorology and Atmospheric Physics. 121(1-2): 55-77.

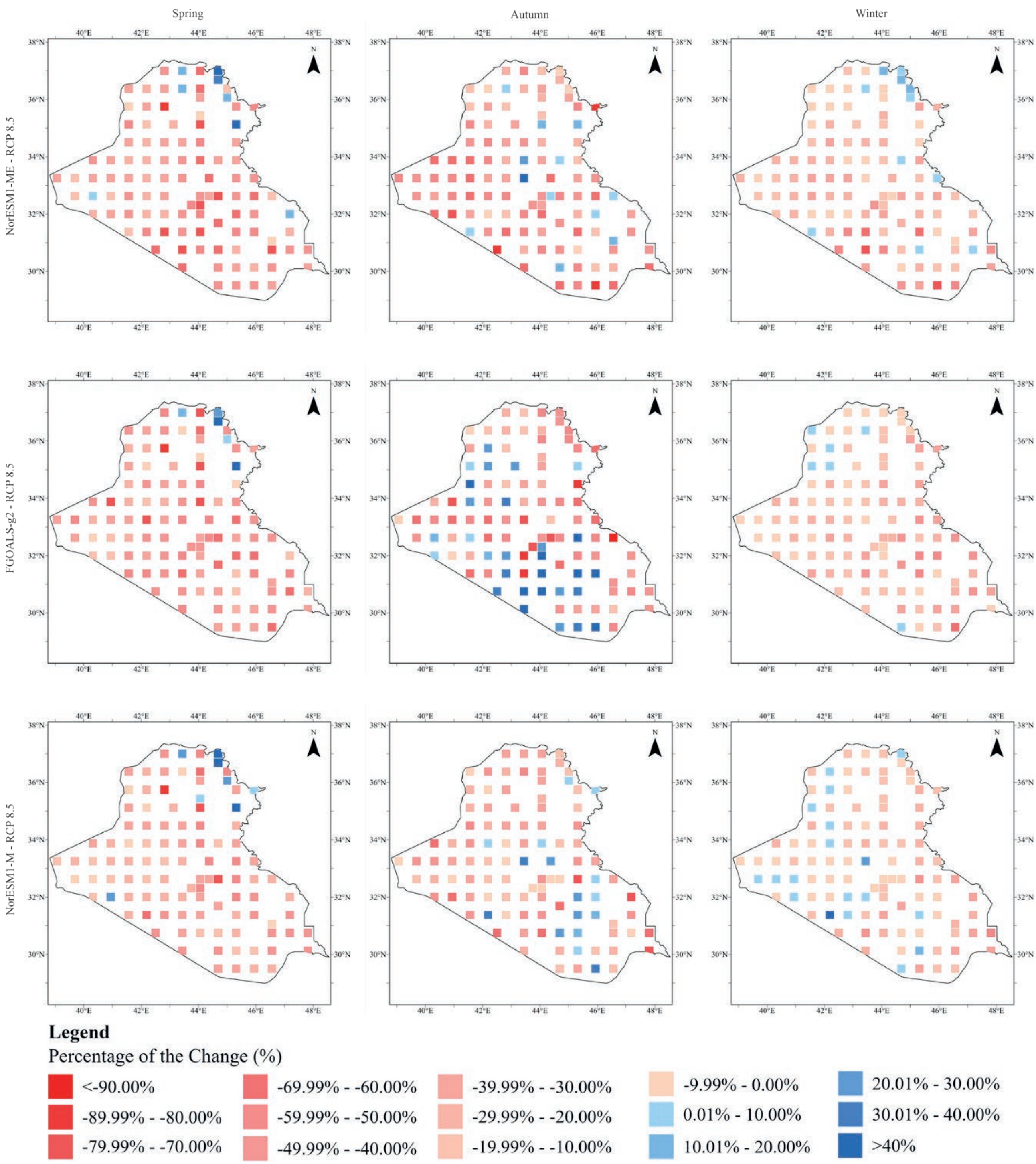

Figure 9. Spatial distribution of percentage change of the precipitation according to the RCP8.5 scenario for NorESM1-ME, FGOALS-g2 and NorESM1-M.

Danandeh Mehr A, Kahya E. 2016. Grid-based performance evaluation of GCM-RCM combinations for rainfall reproduction. Theoretical and Applied Climatology. 129(1-2): 47-57.

Demirel MC, Moradkhani H. 2015. Assessing the impact of CMIP5 climate multi-modeling on estimating the precipitation seasonality and timing. Climatic Change. 135(2): 357-372.

Elsaeed GH, Kheireldin K, AL-Sheer MT, Elzahry EF. 2021. Long Term Impact of Climate Change on Precipitation of Greater Zab River Basin, Iraq. Engineering Research Journal. 1(47): 130-138.

Evans JP. 2008. 21st century climate change in the Middle East. Climatic Change. 92(3-4): 417-432.

Eyring V, Bony S, Meehl GA, Senior CA, Stevens B, Stouffer RJ, Taylor KE. 2016. Overview of the Coupled Model Intercomparison Project Phase 6 (CMIP6) experimental design and organization. Geoscientific Model Development. 9(5): 1937-1958.

Feng J, Wang L, Chen W, Fong SK, Leong KC. 2010. Different impacts of two types of Pacific Ocean warming on Southeast Asian rainfall during boreal winter. Journal of Geophysical Research: Atmospheres. 115(D24).

Hamed MM, Nashwan MS, Shiru MS, Shahid S. 2022. Comparison between CMIP5 and CMIP6 Models over MENA Region Using Historical Simulations and Future Projections. Sustainability. 14(16).

Hashim BM, Al Maliki A, Alraheem EA, Al-Janabi AMS, Halder B, Yaseen ZM. 2022. Temperature and precipitation trend analysis of the Iraq Region under SRES scenarios during the twenty-first century. Theoretical and Applied Climatology. 148(3-4): 881-898.

Her Y, Yoo S-H, Cho J, Hwang S, Jeong J, Seong C. 2019. Uncertainty in hydrological analysis of climate change: multi-parameter vs. multi-GCM ensemble predictions. Scientific Reports. 9(1).

Homsi R, Shiru MS, Shahid S, Ismail T, Harun SB, Al-Ansari N, Chau K-W, Yaseen ZM. 2019. Precipitation projection using a CMIP5 GCM ensemble model: a regional investigation of Syria. Engineering Applications of Computational Fluid Mechanics. 14(1): 90-106.

IPCC A. 2013. Climate change 2013: the physical science basis. Contribution of working group I to the fifth assessment report of the intergovernmental panel on climate change. 1535.

Iqbal Z, Shahid S, Ahmed K, Ismail T, Khan N, Virk ZT, Johar W. 2020. Evaluation of global climate models for precipitation projection in sub-Himalaya region of Pakistan. Atmospheric Research. 245.

Keskin ME, Terzi Ö. 2006. Artificial Neural Network Models of Daily Pan Evaporation. Journal of Hydrologic Engineering. 11(1): 65-70.

Khan JU, Islam A, Das MK, Mohammed K, Bala SK, Islam G. 2020. Future changes in meteorological drought characteristics over Bangladesh projected by the CMIP5 multi-model ensemble. Climatic Change. 162(2): 667-685.

Khayyun TS, Alwan IA, Hayder AM. 2020. Selection of Suitable Precipitation CMIP-5 Sets of GCMs for Iraq Using a Symmetrical Uncertainty Filter. IOP Conference Series: Materials Science and Engineering. 671(1).

Maraun D. 2016. Bias Correcting Climate Change Simulations - a Critical Review. Current Climate Change Reports. 2(4): 211-220.

McMahon TA, Peel MC, Karoly DJ. 2015. Assessment of precipitation and temperature data from CMIP3 global climate models for hydrologic simulation. Hydrology and Earth System Sciences. 19(1): 361-377.

Mohammed ZM, Hassan WH. 2022. Climate change and the projection of future temperature and precipitation in southern Iraq using a LARS-WG model. Modeling Earth Systems and Environment.

Noor M, Ismail Tb, Ullah S, Iqbal Z, Nawaz N, Ahmed K. 2020. A non-local model output statistics approach for the downscaling of CMIP5 GCMs for the projection of rainfall in Peninsular Malaysia. Journal of Water and Climate Change. 11(4): 944-955.

Nourani V, Baghanam AH, Adamowski J, Gebremichael M. 2013. Using self-organizing maps and wavelet transforms for space–time pre-processing of satellite precipitation and runoff data in neural network based rainfall–runoff modeling. Journal of Hydrology. 476: 228-243.

Ostad-Ali-Askari K, Ghorbanizadeh Kharazi H, Shayannejad M, Zareian MJ. 2020. Effect of climate change on precipitation patterns in an arid region using GCM models: case study of Isfahan-Borkhar Plain. Natural Hazards Review. 21(2): 04020006.

Ozturk T, Turp MT, Türkeş M, Kurnaz ML. 2018. Future projections of temperature and precipitation climatology for CORDEX-MENA domain using RegCM4.4. Atmospheric Research. 206: 87-107.

Rabezanahary Tanteliniaina MF, Rahaman MH, Zhai J. 2021. Assessment of the Future Impact of Climate Change on the Hydrology of the Mangoky River, Madagascar Using ANN and SWAT. Water. 13(9).

Rahimi A, Borna R, Morshedi J, Ghorbanian J. 2019. The Vulnerability of Infrastructure of the Southern Regions of Khuzestan Province in Climate Change Conditions. Environmental Management Hazards. 6(4): 361-376.

Salman SA, Shahid S, Ismail T, Ahmed K, Wang X-J. 2018. Selection of climate models for projection of spatiotemporal changes in temperature of Iraq with uncertainties. Atmospheric Research. 213: 509-522.

Saraf VR, Regulwar DG. 2016. Assessment of Climate Change for Precipitation and Temperature Using Statistical Downscaling Methods in Upper Godavari River Basin, India. Journal of Water Resource and Protection. 8(1): 31-45.

Seker M, Gumus V. 2022. Projection of temperature and precipitation in the Mediterranean region through multi-model ensemble from CMIP6. Atmospheric Research. 280.

Shiravand H, Dostkamiyan M. 2019. Analysis of Temperature Fluctuations in the South West of Iran Based on General Circulation Model and Neural Network (Case Study: Plain and Mountainous Stations). Iran-Water Resources Research. 15(3): 206-217.

Shiru MS, Shahid S, Chung E-S, Alias N, Scherer L. 2019. A MCDM-based framework for selection of general circulation models and projection of spatio-temporal rainfall changes: A case study of Nigeria. Atmospheric Research. 225: 1-16.

Sreelatha K, Anand Raj P. 2019. Ranking of CMIP5-based global climate models using standard performance metrics for Telangana region in the southern part of India. ISH Journal of Hydraulic Engineering. 27(supl): 556-565.

Srinivasa Raju K, Sonali P, Nagesh Kumar D. 2016. Ranking of CMIP5-based global climate models for India using compromise programming. Theoretical and Applied Climatology. 128(3-4): 563-574.

Su B, Huang J, Gemmer M, Jian D, Tao H, Jiang T, Zhao C. 2016. Statistical downscaling of CMIP5 multi-model ensemble for projected changes of climate in the Indus River Basin. Atmospheric Research. 178-179: 138-149.

Taylor KE, Stouffer RJ, Meehl GA. 2012. An Overview of CMIP5 and the Experiment Design. Bulletin of the American Meteorological Society. 93(4): 485-498.

Wang X, Yang T, Li X, Shi P, Zhou X. 2016. Spatio-temporal changes of precipitation and temperature over the Pearl River basin based on CMIP5 multi-model ensemble. Stochastic Environmental Research and Risk Assessment. 31(5): 1077-1089.

Wilby RL, Wigley TM. 1997. Downscaling general circulation model output: a review of methods and limitations. Progress in physical geography. 21(4):530-548.

WMO. 2019. Greenhouse gas concentrations, in atmosphere reach yet another high. Geneva, Switzerland: World Meteorological Organization (WMO).

Wright DB, Knutson TR, Smith JA. 2015. Regional climate model projections of rainfall from U.S. landfalling tropical cyclones. Climate Dynamics. 45(11-12): 3365-3379.

Xu R, Chen N, Chen Y, Chen Z. 2020. Downscaling and Projection of Multi-CMIP5 Precipitation Using Machine Learning Methods in the Upper Han River Basin. Advances in Meteorology. 2020: 1-17.

Zarenistanak M. 2018. Historical trend analysis and future projections of precipitation from CMIP5 models in the Alborz mountain area, Iran. Meteorology and Atmospheric Physics. 131(5): 1259-1280.

Finito di stampare da
Logo s.r.l. – Borgoricco (PD) – Italia

RIGOROUS PEER REVIEW

Each submission to IJAm is subject to a rigorous quality control and peer-review evaluation process before receiving a decision. The initial in-house quality control check deals with issues such as competing interests; ethical requirements for studies involving human participants or animals; financial disclosures; full compliance with IJAm's data availability policy, etc.

Submissions may be returned to authors for queries, and will not be seen by our Editorial Board or peer reviewers until they pass this quality control check.

Each paper is subjected to critical evaluation and review by Field Editors with specific expertise in the different areas of interest and by the members of the international Editorial Board.

OPEN ACCESS POLICY

The Italian Journal of Agrometeorology provides immediate open access to its content. Our publisher, Firenze University Press at the University of Florence, complies with the Budapest Open Access Initiative definition of Open Access: By "open access", we mean the free availability on the public internet, the permission for all users to read, download, copy, distribute, print, search, or link to the full text of the articles, crawl them for indexing, pass them as data to software, or use them for any other lawful purpose, without financial, legal, or technical barriers other than those inseparable from gaining access to the internet itself. The only constraint on reproduction and distribution, and the only role for copyright in this domain is to guarantee the original authors with control over the integrity of their work and the right to be properly acknowledged and cited. We support a greater global exchange of knowledge by making the research published in our journal open to the public and reusable under the terms of a Creative Commons Attribution 4.0 International Public License (CC-BY-4.0). Furthermore, we encourage authors to post their pre-publication manuscript in institutional repositories or on their websites prior to and during the submission process and to post the Publisher's final formatted PDF version after publication without embargo. These practices benefit authors with productive exchanges as well as earlier and greater citation of published work.

COPYRIGHT NOTICE

Authors who publish with IJAm agree to the following terms:

Authors retain the copyright and grant the journal right of first publication with the work simultaneously licensed under a Creative Commons Attribution 4.0 International Public License (CC-BY-4.0) that allows others to share the work with an acknowledgment of the work's authorship and initial publication in IJAm.

Authors are able to enter into separate, additional contractual arrangements for the non-exclusive distribution of the journal's published version of the work (e.g., post it to an institutional repository or publish it in a book), with an acknowledgment of its initial publication in this journal.

Authors are allowed and encouraged to post their work online (e.g., in institutional repositories or on their website) prior to and during the submission process, as it can lead to productive exchanges, as well as earlier and greater citation of published work (See The Effect of Open Access).

PUBLICATION FEES

Unlike many open-access journals, the Italian Journal of Agrometeorology does not charge any publication fee.

WAIVER INFORMATION

Fee waivers do not apply at Firenze University Press because our funding does not rely on author charges.

PUBLICATION ETHICS

Responsibilities of IJAm's editors, reviewers, and authors concerning publication ethics and publication malpractice are described in IJAm's Guidelines on Publication Ethics.

CORRECTIONS AND RETRACTIONS

In accordance with the generally accepted standards of scholarly publishing, IJAm does not alter articles after publication: "Articles that have been published should remain extant, exact and unaltered to the maximum extent possible". In cases of serious errors or (suspected) misconduct IJAm publishes corrections and retractions (expressions of concern).

Corrections

In cases of serious errors that affect or significantly impair the reader's understanding or evaluation of the article, IJAm publishes a correction note that is linked to the published article. The published article will be left unchanged.

Retractions

In accordance with the "Retraction Guidelines" by the Committee on Publication Ethics (COPE) IJAm will retract a published article if:

- there is clear evidence that the findings are unreliable, either as a result of misconduct (e.g. data fabrication) or honest error (e.g. miscalculation)
- the findings have previously been published elsewhere without proper crossreferencing, permission or justification (i.e. cases of redundant publication)
- it turns out to be an act of plagiarism
- it reports unethical research.
- An article is retracted by publishing a retraction notice that is linked to or replaces the retracted article. IJAm will make any effort to clearly identify a retracted article as such.

If an investigation is underway that might result in the retraction of an article IJAm may choose to alert readers by publishing an expression of concern.

ARCHIVING

IJAm and Firenze University Press are experimenting a National legal deposition and long-term digital preservation service.

SUBMITTING TO IJAm

Submissions to IJAm are made using FUP website. Registration and access are available at: https://riviste.fupress.net/index.php/IJAm/submission

For more information about the journal and guidance on how to submit, please see https://riviste.fupress.net/index.php/IJAm/index

Principal Contact

Simone Orlandini, University of Florence

simone.orlandini@unifi.it

Support Contact

Alessandro Pierno, Firenze University Press

alessandro.pierno@unifi.it

GUIDE FOR AUTHORS

1. Manuscript should refer to original researches, not yet published except in strictly preliminary form.
2. Articles of original researches findings are published in Italian Journal of Agrometeorology (IJAm), subsequent to critical review and approval by the Editorial Board. External referees could be engaged for particular topics.
3. Three types of paper can be submitted: original paper, review, technical note. Manuscript must be written in English. All pages and lines of the manuscript should be numbered.
4. First Name, Last Name, position, affiliation, mail address, telephone and fax number of all the Co-Authors are required. Corresponding Authors should be clearly identified.
5. The abstract should be no longer than 12 typed lines.
6. Full stop, not comma, must be used as decimal mark (e.g. 4.33 and not 4,33).
7. Figures, tables, graphs, photos and relative captions should be attached in separate files. All images must be vector or at least 300 effective ppi/dpi to ensure quality reproduction.
8. Captions should be written as: Fig. x – Caption title, Tab. x – Caption title. Images should be referred to in the text as (Fig. x), (Tab. x).
9. Proof of the paper (formatted according to the Journal style) will be sent to the Corresponding Author for proof reading just one time. Corrections can be made only to typographical errors.
10. All the references in the text must be reported in the "References" section and vice-versa. In the text, only the Author(s) last name must be present, without the name or the first letter of the name (e.g. "Rossi, 2003" and not "Federico Rossi, 2003" or "F. Rossi, 2003"). If two authors are present, refer to them as: "Bianchi and Rossi, 2003" in the text (do not use "&" between the surnames). If more than two Authors are present, refer to them as: "Bianchi et al., 2003" in the text.

For journals, references must be in the following form:

Bianchi R., Colombo B., Ferretti N., 2003. Title. Journal name, number: pages.

For books:

Bianchi R., Colombo B., Ferretti N., 2003. Book title. Publisher, publishing location, total number of pages pp.

Manuscripts "in press" can be cited.

BECOME A REVIEWER

Peer review is an integral part of the scholarly publishing process. By registering as a reviewer, you are supporting the academic community by providing constructive feedback on new research, helping to ensure both the quality and integrity of published work in your field. Once registered, you may be asked to undertake reviews of scholarly articles that match your research interests. Reviewers always have the option to decline an invitation to review and we take care not to overburden our reviewers with excessive requests.

You must login before you can become a reviewer.

If you don't want to be a reviewer anymore, you can change your roles by editing your profile.

COMPETING INTERESTS

You should not accept a review assignment if you have a potential competing interest, including the following:

- Prior or current collaborations with the author(s)
- You are a direct competitor
- You may have a known history of antipathy with the author(s)
- You might profit financially from the work

Please inform the editors or journal staff and recuse yourself if you feel that you are unable to offer an impartial review.

When submitting your review, you must indicate whether or not you have any competing interests.

Italian Journal of Agrometeorology

Rivista Italiana di Agrometeorologia

n. 2 – 2023

Table of contents